

A MULTIWAVELENGTH INVESTIGATION OF BE/X-RAY BINARIES IN THE
GALAXY

A THESIS SUBMITTED TO
THE GRADUATE SCHOOL OF NATURAL AND APPLIED SCIENCES
OF
MIDDLE EAST TECHNICAL UNIVERSITY

BY

MEHTAP ÖZBEY ARABACI

IN PARTIAL FULFILLMENT OF THE REQUIREMENTS
FOR
THE DEGREE OF DOCTOR OF PHILOSOPHY
IN
PHYSICS

AUGUST 2014

Approval of the thesis:

A MULTIWAVELENGTH INVESTIGATION OF BE/X-RAY BINARIES IN THE GALAXY

submitted by **MEHTAP ÖZBEY ARABACI** in partial fulfillment of the requirements for the degree of **Doctor of Philosophy in Physics Department, Middle East Technical University** by,

Prof. Dr. Canan Özgen
Dean, Graduate School of **Natural and Applied Sciences** _____

Prof. Dr. Mehmet T. Zeyrek
Head of Department, **Physics** _____

Prof. Dr. Ümit Kızıloğlu
Supervisor, **Physics Department, METU** _____

Assoc. Prof. Dr. Ünal Ertan
Co-supervisor, **Faculty of Engineering and Natural Sciences, Sabancı University** _____

Examining Committee Members:

Prof. Dr. Ethem Derman
Astronomy and Space Sciences Department, Ankara University _____

Prof. Dr. Ümit Kızıloğlu
Physics Department, METU _____

Prof. Dr. Altan Baykal
Physics Department, METU _____

Assoc. Prof. Dr. Sinan Kaan Yerli
Physics Department, METU _____

Assoc. Prof. Dr. S. Çağdaş İnam
Electrical Engineering Department, Başkent University _____

Date: _____

I hereby declare that all information in this document has been obtained and presented in accordance with academic rules and ethical conduct. I also declare that, as required by these rules and conduct, I have fully cited and referenced all material and results that are not original to this work.

Name, Last Name: MEHTAP ÖZBEY ARABACI

Signature :

ABSTRACT

A MULTIWAVELENGTH INVESTIGATION OF BE/X-RAY BINARIES IN THE GALAXY

Arabacı, Mehtap Özbey

Ph.D., Department of Physics

Supervisor : Prof. Dr. Ümit Kızıloğlu

Co-Supervisor : Assoc. Prof. Dr. Ünal Ertan

August 2014, 164 pages

As displaying different transient optical and X-ray behaviors both among themselves and individually, Be/X-ray binaries (BeXRBs) have been one of the most interesting populations of High Mass X-ray Binaries (HMXBs) since their discovery. Although their standard observational properties can be put together in distinct classes, there still have been several Be/X-ray systems showing unique features beyond these classifications. In this thesis, we first present a new and comprehensive catalog of Be/X-ray binaries and potential candidates in the Galaxy. With this new list, we review the most important properties of all sources and check the evidences leading them to be classified as BeXRBs. Next, we investigate the long-term optical/IR and X-ray properties of three BeXRBs selected from the catalog, EXO 0331+530, XTE J1946+274 and SAX J2103.5+4545. We showed that each source has their own characteristics despite their common X-ray outburst types. We also searched for the short-term variations, attributed to the non-radial pulsations (NRP), in the photometric data of the Be stars. Our sample includes IGR J01363+6610, IGR J01583+6713, RX J0440.9+4431, SWIFT J2000.6+3210 and GS 2138+56. Although we did not find any periodic variations, the results are still preliminary since it is an ongoing project.

Keywords: Be stars, Decretion Disk, Emission lines, Non-Radial Pulsation, X-ray outbursts, V/R variations

ÖZ

GALAKSİDEKİ BE/X-IŞIN ÇİFTLERİNİN ÇOKLU DALGABOYU İNCELEMESİ

Arabacı, Mehtap Özbey

Doktora, Fizik Bölümü

Tez Yöneticisi : Prof. Dr. Ümit Kızıloğlu

Ortak Tez Yöneticisi : Doç. Dr. Ünal Ertan

Ağustos 2014 , 164 sayfa

Geçici optik ve X-ışını davranışlarının sistemden sisteme ve kendi içinde farklılıklar göstermeleri nedeniyle, Be/X-ışın çiftleri keşfedildiklerinden bu yana Yüksek Kütleli X-ışın çiftlerinin en ilginç popülasyonlarından biridir. Gözlemsel özellikleri temel başlıklar altında toplanabiliyor olsa da, halen birçok Be/X-ışın sistemi bu sınıflamanın dışında kendine özgü davranışlar gösterebilmektedir. Bu tezde, öncelikle Galaksideki Be/X-ışın çiftleri ve adaylarının yeni ve kapsamlı bir kataloğunu sunmaktayız. Bu yeni katalogla birlikte, tüm kaynakların Be/X-ışın çifti olarak sınıflandırılmalarına neden olan en önemli özellikleri gözden geçirilmektedir. Daha sonra bu katalogdan seçilmiş 3 sistemin, EXO 0331+530, XTE J1946+274 ve SAX J2103.5+4545, uzun dönemli optik/kızıl ötesi ve X-ışın karakterleri incelenmektedir. Benzer X-ışın parlama tiplerine rağmen, bu sistemlerin kendilerine özgü karakterleri olduğu gösterilmiştir. Ayrıca Be yıldızlarının fotometrik verilerindeki radyal olmayan salınımlardan kaynaklanan kısa dönemli değişimler araştırılmıştır. Örneklemimiz IGR J01363+6610, IGR J01583+6713, RX J0440.9+4431, SWIFT J2000.6+3210 ve GS 2138+56 kaynaklarını içermektedir. Bu incelemede herhangi periyodik bir değişim bulunmasa da, projenin halen devam etmekte olması sebebiyle sonuçlar henüz başlangıç aşamasındadır.

Anahtar Kelimeler: Be Yıldızları, Boşaltım Diski, Salma Çizgileri, Radyal-Olmayan Salınımlar, X-Işın Parlamaları, V/R değişimleri

To my baby girl Zeynep

ACKNOWLEDGMENTS

First and foremost, I would like to express my deep and sincere gratitude to my supervisor Prof. Dr. Ümit Kızılođlu for giving me a great chance and opportunity to work with him. Without his advices and guidance it would be harder to conclude this study. It has been an honour to be his student.

I am grateful to my co-supervisor Assoc. Prof. Dr. Ünal Ertan for his encouragement, fruitful discussions and valuable advices about this work.

I would like to thank Assoc. Prof. Dr. Emrah Kalemci for pushing me to the X-ray universe and giving me a chance to work with him. I will be forever indebted to him for providing financial support during the last year of my research through his projects.

I also would like to thank to my unofficial advisor, Assoc. Prof. Dr. Sinan Kaan Yerli for being a mentor, a colleague, and a friend of mine during my years at METU Physics Department. I express my sincere gratitudes to Prof Dr. Altan Baykal, Prof. Dr. Nilgün Kızılođlu and Prof. Dr. Şölen Balman for their valuable suggestions throughout this work.

Additionaly I am grateful to Dr. Ascension Camero Arranz for her collaboration through the project X-ray/optical connections in Be/X-ray systems.

My special thanks to Cemal Arabacı for his love, patience and understanding since I met him. I would have not completed this thesis without your support and encouragement.

My dearest friends and colleagues; Yakup Pekön, Kıvılcım B. Vural, Çađan Aksak, Ceren Sibel Sayın and Gül Çorbaciođlu, thank you guys so much for being such great friends.

I acknowledge support from TÜBİTAK , The Scientific and Technological Research Council of Turkey, through the projects 106T040, 109T736 and 111T222.

TABLE OF CONTENTS

ABSTRACT	v
ÖZ	vii
ACKNOWLEDGMENTS	x
TABLE OF CONTENTS	xi
LIST OF TABLES	xiv
LIST OF FIGURES	xvi
CHAPTERS	
1 INTRODUCTION	1
1.1 Be/X-Ray Binaries	1
1.1.1 Observational Characteristics of Decretion Disk	2
1.1.2 Decretion Disk Formation and Interaction with the Neutron Star	6
1.1.3 Be/X-ray Binaries in Corbet Diagram: P_{spin} vs P_{orb}	10
1.1.4 Non-Radial Pulsations in Be/X-ray Systems	14
1.2 Thesis Outline	16
2 CATALOG OF BE/X-RAY BINARIES AND CANDIDATES IN THE GALAXY	19

2.1	Description of The Tables	20
2.2	Sources	21
2.3	γ -Ray Binaries with Be Companions	53
2.4	γ Cas and its analogs	55
2.5	Distribution of Spectral Type and X-ray Activity	57
2.6	P_s and P_{orb} Relation	59
2.7	$H\alpha$ and $H\beta$ Strength vs P_{orb}	63
2.8	Summary	65
3	LONG-TERM MONITORING OF BE/X-RAY BINARIES	69
3.1	Observations and Data Reduction	70
3.1.1	Optical/IR Photometric Observations	70
3.1.2	Optical Spectroscopic Observations	71
3.2	EXO 0331+530	72
3.2.1	Results	74
3.2.1.1	Optical Photometric Observations	74
3.2.1.2	$H\alpha$ Observations	77
3.2.2	Discussion	81
3.3	XTE J1946+274	82
3.3.1	Results	85
3.3.1.1	Quiescent State I (MJD 52130–55350)	85
3.3.1.2	Active State (MJD 55350–55800)	87

	3.3.1.3	Quiescent State II (MJD 55800–up to now)	88
	3.3.2	Summary and Discussion	95
3.4		SAX J2103.5+4545	97
	3.4.1	Results	98
		3.4.1.1 Optical/IR Photometry	98
		3.4.1.2 H α Line Variations and Decretion Disk of Be Star	102
	3.4.2	Summary	106
4		SEARCHING OF PERIODIC SHORT-TERM VARIATIONS IN BE/X-RAY BINARIES	109
	4.1	T100 Observations and Data Reduction	110
	4.2	Results and Discussion	112
5		CONCLUSIONS	119
		CURRICULUM VITAE	161

LIST OF TABLES

TABLES

Table 1.1	List of Galactic Be/X-ray systems having NRPs.	15
Table 2.1	Catalogue of Be/X-ray binaries and Candidates in the Galaxy.	45
Table 2.2	Be/X-ray binaries and Candidates in the Galaxy.	49
Table 2.3	General properties of γ -ray binaries.	55
Table 2.4	Galactic high mass X-ray binaries with known orbital and spin periods.	60
Table 3.1	Selected photometric reference stars in the neighborhood of the optical counterpart of EXO 0331+530 (BQ Cam) and SAX J2103.5+4545 (GSC 03588-00834) with the ROTSEIIIId telescope.	71
Table 3.2	H α line EW and FWHM measurements for EXO 0331+530. Negative values of EW indicate that the line is in emission.	79
Table 3.3	H α equivalent width (EW) measurements of optical counterpart to XTE J1946+274.	88
Table 3.4	Optical and IR magnitudes of XTE J1946+274 observed with IAC80 and TCS telescopes respectively.	92
Table 3.5	Optical photometric observations of the optical counterpart to SAX J2103.5+4545 performed with the IAC80 telescope.	100
Table 3.6	IR observations of the optical counterpart to SAX J2103.5+4545 taken with the TCS telescope.	101
Table 3.7	H α line width measurements of the optical counterpart to SAX J2103.5+4545. Positive values indicate that the line is in absorption.	104
Table 4.1	Log of the T100 observations.	110

Table 4.2 Photometric reference stars used to find the differential magnitudes of the observed sources with T100. The reference star names and magnitudes denotes the USNO-B1.0 catalog ID and R_1 magnitudes respectively. 112

LIST OF FIGURES

FIGURES

<p>Figure 1.1 Top panel: Optical/IR emission of X Persei system for different states: with and without (lower curve) the decretion disk (taken from Teltzing et al. (1998)). Bottom panel: $H\alpha$ and HeI lines both with disk and without disk conditions (taken from Reig (2011)).</p>	4
<p>Figure 1.2 Relation between EW of $H\alpha$ emission and IR color index of $J - K$ for several Be/X-ray systems confirming the idea that both optical and IR emission arise from the decretion disk (taken from Reig (2011)).</p>	5
<p>Figure 1.3 Critical values of α at $n:1$ resonance radii for different Be/X-ray systems (taken from Okazaki & Negueruela (2001a)). Numbers on the top give the locations of $n:1$ commensurabilities of disk and mean binary orbital frequencies.</p>	8
<p>Figure 1.4 P_{orb}-EW($H\alpha$) diagram for the Be/X-ray binaries updated by Reig (2007). Galactic Be/X-ray systems represented by circles whereas SMC sources by squares. Open symbols indicate systems whose orbital periods have been estimated from Corbet diagram (see Chap. 1.1.3).</p>	9
<p>Figure 1.5 Three distinct locations of HMXBs in the Corbet Diagram (taken from Corbet (1986)). Be/X-ray systems are presented by circles (a-i) whereas the squares (j-n) indicate Supergiant HMXBs (sgHMXBs). Roche-Lobe filled systems are shown with crosses (o-q). The solid line corresponds to $P_{spin} \propto P_{orb}$.</p>	11
<p>Figure 2.1 The spectral distribution of Be stars in Be/X-ray systems. The red boxes represent confirmed systems while the candidates are seen in blue-colored boxes.</p>	57
<p>Figure 2.2 The distribution of X-ray activities for a sample of 37 BeXRBs. The abbreviations in the chart stand for: I, Type I outburst; II, Type II outbursts; F, flare; P, persistent. Note that two of these persistent BeXRBs systems are not confirmed.</p>	58

Figure 2.3	The updated Corbet diagram for BeXRBs and candidates in Tables 2.2 and for the galactic HMXBs. The green-filled circles represent the HMXBs with supergiant/giant companions. Majority of this group is located at a distinct region called 'wind-fed HMXBs'. The confirmed BeXRBs are seen in blue-filled triangles, whereas the red ones indicate the candidate BeXRBs. The SFXTs (gold-squares) are placed between the wind-fed HMXBs and BeXRBs. The two radio pulsars are placed at the bottom right of the diagram.	61
Figure 2.4	Corbet diagram for BeXRBs and candidates	62
Figure 2.5	Orbital period against eccentricity for the BeXRBs in.. . . .	63
Figure 2.6	Variation of maximum $H\alpha$ EW with respect to the orbital period. Red squares are updated values of the systems given Table 2.2. The linear regression fit to the values given in Reig et al. (1997a) is shown with a dashed-line which is not compatible with our measurements since most of the values have changed. Four of these systems, corresponding to a) 4U 0115+634, b) GRO J1008-57 c) 1A118-616 and d) EXO 2030+275, with the values out of date from Reig et al. (1997a), are also indicated with the black-circles.	64
Figure 2.7	Variation of maximum $H\beta$ EW with respect to the orbital period. There is not a clear relation between these two parameters.	66
Figure 2.8	Maximum $H\beta$ emission as a function the maximum $H\alpha$ emission.	67
Figure 3.1	ROTSEIIIId daily averaged differential light curve (upper panel) and the <i>RXTE</i> /ASM light curve (1.3-12 keV) of EXO 0331+350 for the time interval MJD 53100-54205. The horizontal black-dashed line in the Rotse panel denotes quiescent differential magnitude (~ 0.73) of the source.	74
Figure 3.2	Comparison of <i>Swift</i> /BAT light-curve (15-50 keV) with a bin size equal to 2 days with the ROTSEIIIId magnitudes of EXO 0331+350, for the time interval MJD 54275-56300. The horizontal black-dashed line in the Rotse panel denotes quiescent differential magnitude (~ 0.73) of BQ Cam whereas the vertical red-dashed line in the X-ray panel represents the time of the periastron passages of the NS.	76
Figure 3.3	$H\alpha$ line profiles of EXO 0331+530 observed between 2006-2014. The single-peaked emission of the line does not change on a long-term basis.	78

Figure 3.4 Evolution of the EW and FWHM measurements of the $H\alpha$ emission line. The red-dashed vertical line denotes the beginning and ending of the optical outburst seen in ROTSEIIIId light curve (see also Fig.3.2) whereas black-dashed line shows the time of the turning point from decreasing to increasing trend just after (~ 10 d) the strong X-ray outburst around MJD ~ 54850	80
Figure 3.5 <i>Swift</i> /BAT light-curve (15–50 keV) with a bin size equal to 10 d. Tick marks on the segments located above the light-curve denote the times of the optical/IR photometric data from the ground-based telescopes ROTSEIIIId (green), IAC80 (blue) and TCS (red) and the optical spectroscopic observations come from OSN (purple), NOT (magenta) and RTT150 (orange) (see also Table 3.3).	84
Figure 3.6 ROTSEIIIId light curves of the optical counterpart to XTE J1946+274 for the quiescent phase I	86
Figure 3.7 Power spectra of ROTSEIIIId data of XTE J1946+274 obtained with Lomb-Scargle (upper) and Clean algorithms (below). The red-dashed lines in each panel represent the $P=99\%$ confidence levels above which only observational windows are seen.	87
Figure 3.8 $H\alpha$ line emission observed in the spectrum of 2007 Jul 18. The EW and FWHM measurements of the line is compatible with the values detected by Wilson et al. (2003a).	89
Figure 3.9 Comparison of ROTSEIIIId magnitudes (upper) with the <i>Swift</i> /BAT (middle) and <i>RXTE</i> /ASM (lower) light curves of XTE J1946+274 during the X-ray activity. The black-dashed line in ROTSEIIIId panel shows the average of 53 data points. The time of the periastron and apastron passages of the NS is marked with diamonds and corresponding letters (A and P) in the middle panel.	90
Figure 3.10 Optical/IR light curves of XTE J1946+274 for the quiescent state2.	91
Figure 3.11 $H\alpha$ line profiles of XTE J1946+274 observed between 2012 March–2014 August. The single-peaked emission of the line does not change on a long-term basis.	94
Figure 3.12 The variation of EW and FWHM measurements of $H\alpha$ emission line during the observations. An inverse relation between the two measurements is seen until end of 2013. Note that during the observations both the lowest and the highest values of $H\alpha$ emission for XTE J1946+274 were detected.	95

Figure 3.13 <i>Swift</i> /BAT light-curve of SAX J2103.5+4545 in 15–50 keV energy band with a bin size equal to the orbital period of 12.68 d. The time span of the optical/IR photometric data from the ground-based telescopes ROTSEIIIId (orange), IAC80 (blue) and TCS (red) are represented by the tickmarks on the segments located above the light-curve. The optical spectroscopic observations performed with OSN (purple), NOT (yellow) and RTT150 (light red) are also denoted in the plot (see also Table 3.7).	98
Figure 3.14 Comparison of optical/IR and X-ray light curves of SAX J2103.5+4545	99
Figure 3.15 Evolution of the H α line profile for SAX J2103.5+4545.	102
Figure 3.16 Variations V/R ratios (open squares) of the H α emission line during the observations. The peak separation ΔV between the peaks is also indicated with stars.	105
Figure 4.1 Light-curves of a) IGR J01363+6610, b) RX J0440.9+4431 and c) GS 2138+56 for the observation runs 6 August , 2 September and 5 July 2013 respectively.	113
Figure 4.2 R magnitudes of IGR J01583+6713 for the different observing runs (see Table 4.1).	115
Figure 4.3 Light-curves of SWIFT J2000.6+3210 for the four different observation nights (see Table 4.1).	116
Figure 4.4 (Upper Panel) Power spectra of IGR J01583+6713 obtained from Clean (a) and Lomb-Scargle (b) algorithms. The two highest frequencies of 0.482 and 1.801 d ⁻¹ are also shown in LS periodogram. (Bottom Panel) Power spectra of SWIFT J2000.6+3210 obtained from Clean (a) and Lomb-Scargle (b) algorithms. The two highest frequencies of 1.06 and 2.74 d ⁻¹ are also shown in LS periodogram.	117

CHAPTER 1

INTRODUCTION

1.1 Be/X-Ray Binaries

With improving knowledge about the X-ray sources, the questions regarding the high energy universe have still been increasing, even nearly ~ 50 years had passed after the discovery of the first X-ray binary outside the solar system, Sco X-1 (Giacconi et al. 1962). However, assuming that having a compact object orbiting around its optical companion is a necessary requirement, there has been a firm consensus on the classification scheme of the X-ray binaries. They are divided into two classes according to the mass of their optical companion; Low Mass X-ray Binaries (LMXBs) with a mass donor $\leq 1M_{\odot}$ and High Mass X-ray Binaries (HMXBs) $\gtrsim 10M_{\odot}$. In addition to these two main groups, they have subclasses depending on the evolutionary status of the companion.

Being the most-populated subclass of HMXBs, Be/X-ray binaries (BeXRBs) are attractive sources both for observational and for theoretical aspects since the physical mechanisms behind their several distinguishing features among the other systems have not been completely explained. Nevertheless, the main properties of BeXRBs that have been well accepted as yet can be summarized as follows:

- They consist of a Be type star, a non-supergiant early type star which shows or has shown (at a time in the past) emission lines (Balmer series and several metallic lines) in its spectrum (Be-phenomenon), and a neutron star (NS) revealing itself as an X-ray pulsar.

- The orbits are relatively wide and mostly eccentric ($e \gtrsim 0.3$). Their orbital periods (P_{orb}) are substantially confined in the range of ~ 20 – 300 days.
- The Be star in the system is surrounded by a circumstellar material at its equator (so called decretion disk) stem from the stellar mass loss, whereas the NS might have an accretion disk formed by the gas captured from the decretion disk.
 - Both disks are temporary, depending upon the physical processes controlled by the optical companion and the NS, respectively.
 - The decretion disks disperse and refill on time scales of \sim years, while the time-span for the accretion disks is much shorter (\sim weeks to months).
- Due to the transient nature of the mass transfer between the decretion disk and the NS, two types of X-ray activities are seen with respect to the luminosity:
 - Type I (normal) outbursts ($L_X \sim 10^{36-37}$ erg s $^{-1}$): They are short-lived (0.2 – $0.3 P_{orb}$), and usually regular outbursts. They either begin or peaked at/near the periastron passage of the NS.
 - Type II (giant) outbursts ($L_X \gtrsim 10^{37}$ erg s $^{-1}$): These are least frequent, relatively long outbursts without showing any orbital modulation and related to the major disruptions in the decretion disk.
- There are also BeXRBs which are always detectable in low-luminosity X-ray domain. ($L_{2-20 keV} \gtrsim 10^{34-35}$ erg s $^{-1}$), called persistent Be/X-ray binaries.

Although this dissertation includes only BeXRBs in the Milky Way, it should be also noted that they are exceptionally abundant in Small Magellanic Cloud (SMC) interpreted as a result of bursts of star formation about 60 Myr ago in regions where the HMXBs are located in addition to the low metallicity of SMC (Antoniou et al. 2009; Harris & Zaritsky 2004, and references therein).

1.1.1 Observational Characteristics of Decretion Disk

What makes Be/X-ray systems unique among the High Mass X-ray binaries is obviously the existence of their circumstellar envelopes that give rise to the transient

outbursts of the compact companion by making them most powerful sources in the X-ray sky. Therefore, it is not surprising to see that the majority of the studies in the literature try to clarify the physical picture of these systems by putting the disk structure of the Be star to the centre of context. Indeed, it is the point of origin for both observational and theoretical works.

From an observational point of view, there are two main observables arising due to the presence of the decretion disk: Emission lines and strong infrared (IR) excess. The line emission, an essential indicator for distinguishing an ordinary B type star from a Be one, is caused by the recombination of ionized Hydrogen while bound-free and free-free transitions from the ionized and dense gas in the disk (e.g. thermal Bremsstrahlung) produce an excess of photons at IR and longer wavelengths (Riquelme et al. 2012). Spectroscopic observations of Be stars both in optical and in near-IR/IR wavelengths reveal emission of Hydrogen Balmer lines (particularly $H\alpha$ and $H\beta$) when the decretion disk is present. In Fig. 1.1 these two observational evidences of decretion disk are represented for the Be/X-ray binary system X-Per. Furthermore, the correlation between IR color index and emission line strengths supports the idea that both properties have a common origin (see Fig. 1.2). On the other hand, using combined near-IR interferometric and optical spectroscopic observations of several Be stars, Gies et al. (2007) showed that K -band emission area was smaller than the $H\alpha$ emitting region. In other words, these two main observational characteristics of Be stars are certainly produced in the decretion disk but at different parts of it: close to Be star emission is dominated in the near-IR while optical emission occurs farther than this region.

The profile variations of emission lines seen in the spectra of the Be stars are also important since they are directly related to the changing conditions in the decretion disk. As a prime indicator of circumstellar material around a Be star, $H\alpha$ line can reveal itself in different types of emission profiles through long-term observations. Although there are wide range of emission line shapes (single/double or triple-peaked, wine-bottle shaped, shell profile etc.), they can be divided into two main categories (Hummel & Hanuschik 1997; Negueruela et al. 1998);

i) Symmetric profiles: They are identified as double-peaked emissions with each

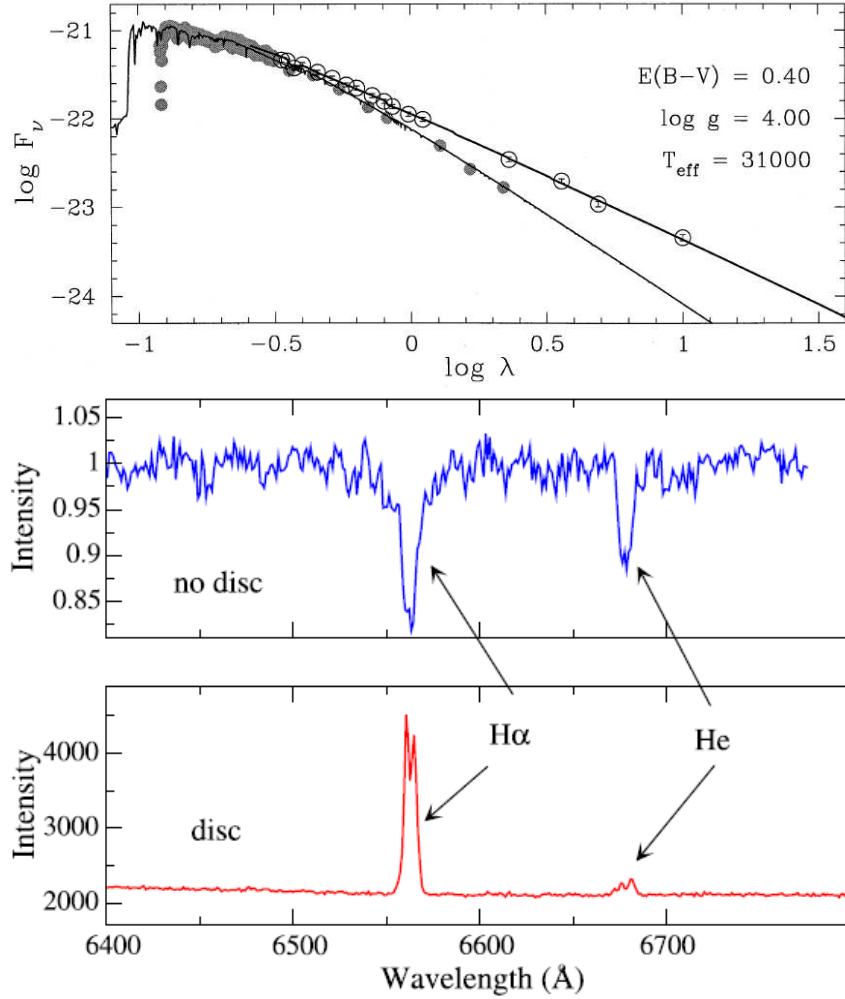


Figure 1.1: Top panel: Optical/IR emission of X Persei system for different states: with and without (lower curve) the decretion disk (taken from Telting et al. (1998)). Bottom panel: $H\alpha$ and HeI lines both with disk and without disk conditions (taken from Reig (2011)).

peak having the same intensity/flux and they are believed to be produced in a stable quasi-Keplerian disks with a time-scale of few years.

- ii) Asymmetric profiles: They are associated with the quasi-cyclic variations of both peaks of the emission profile, so called **Violet to Red ratio (V/R)**. Periods of V/R change from decades to years and they do not depend on spectral type of the Be star. In addition to this, the profiles are seen blueward (redward) shifted when the red (blue) peak is stronger (Rivinius et al. 2013).

The abovementioned time-scales of the profile variations are generally relevant for

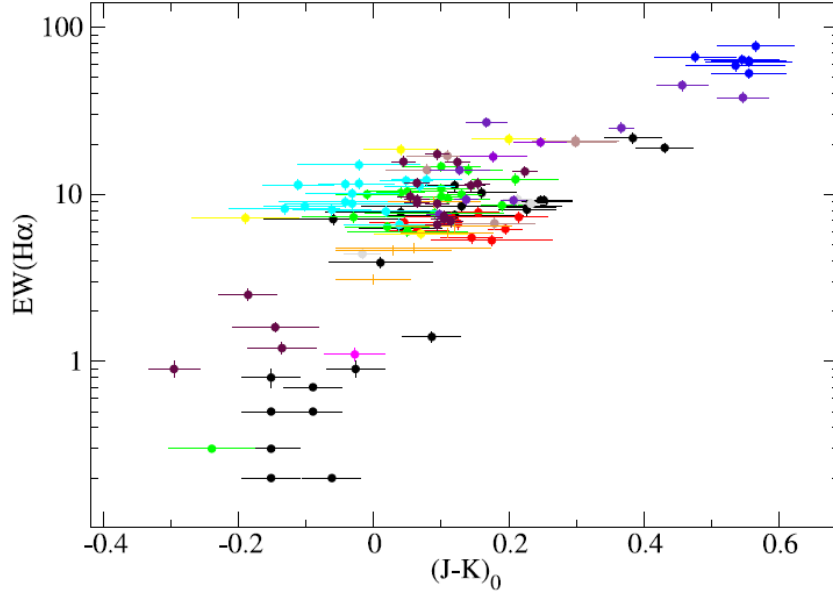


Figure 1.2: Relation between EW of $H\alpha$ emission and IR color index of $J - K$ for several Be/X-ray systems confirming the idea that both optical and IR emission arise from the decretion disk (taken from Reig (2011)).

isolated Be stars whereas for Be/X-ray binaries they are much shorter (Reig & Zezas 2014a). The responsible physical mechanism for the V/R variations is due to global oscillations caused by the perturbed non-uniform density distributions in the disk (Okazaki 1991). It was Okazaki (1991) who proposed existence of global one-armed oscillations ($m=1$ modes), confined in the decretion disk, similar to global waves explained by Kato (1983) for accretion disks. Although suggested mechanism of Okazaki (1991) was initially built just for retrograde mode variations in the disk, later Papaloizou et al. (1992) showed that inclusion of a quadrupole-term in gravitational potential of rotationally flattened Be star explained the V/R variations, matching up with the observational results (Telting et al. 1994). Yet, in literature theoretical attempts modelling the problem diverge due to lack of repeating cycles of the variation where a correct decision cannot be made easily (Okazaki 1997; Papaloizou & Savonije 2006; Vakili et al. 1998, and references therein). It is commonly assumed that propagation of non-axisymmetrical density perturbations (a high density zone with a spiral shape, see Carciofi et al. (2009)) in the disk produces variations seen in the emission profiles attributed to the global one-armed oscillation model (Okazaki 2000). Basically double-peaked symmetric profiles are seen when the high density

region is behind or in front of the Be star while the asymmetric profile of $V > R$ ($V < R$) is produced by the motion of the high-density part toward (away from) the observer. Note, however, that this explains both observed periodicities and profile shifts of the V/R variations, and the global one-armed oscillation model puts a constraint on the mode ($m=1$) that it occurs only in the region where the radial outflow is highly subsonic (Okazaki 2007).

1.1.2 Decretion Disk Formation and Interaction with the Neutron Star

For the last twenty years, several decretion disk formation models have been put forward, with scenarios suggesting different responsible mechanisms, to explain the observational facts. However, there has been an agreement between models regarding to morphology of a Be star disk being geometrically thin and rotating at/near Keplerian velocities. Among these models only the viscous decretion disk model of Lee et al. (1991) can naturally yield near-Keplerian disks with highly subsonic outflows and can explain observed V/R variations. In this model, matter (i.e. angular momentum), supplied from the equatorial surface of a Be star to an inner boundary of its disk by an uncertain mechanism, is drifted outward by an action of viscous torques and forms the disk. Actually the model is not interested in why or how the matter is ejected from the central star (see Chapter 1.1.4), instead it assumes that the material is somehow brought to the inner disk. The basic equations of a viscous decretion disk is similar to a viscous accretion disk except that sign of mass accretion rate, \dot{M} , is opposite (Pringle 1981; Shakura & Sunyaev 1973). In addition, similar to accretion disks, the disks are truncated by tidal/resonant torques exerted by the companion. Therefore, the decretion disks never experience steady states; they either grow or decay (Okazaki 2001). As a result, assuming that the disk is governed by pressure and viscosity, the angular momentum is added to the disk by the viscous torques (T_{vis}) while it is removed by the tidal/resonant torques (T_{res}) of the NS (Negueruela & Okazaki 2001). The disk truncation occurs at a certain radii where ratio between the angular frequency of disk rotation and the angular frequency of mean binary motion is a rational number. The condition for the disk truncation is defined as,

$$T_{vis} + T_{res} \leq 0. \quad (1.1)$$

The viscous torque is given by,

$$\mathbf{T}_{vis} = 3\pi\alpha GM_*\sigma r \left(\frac{H}{r}\right)^2. \quad (1.2)$$

Here α is the Shakura-Sunyaev viscosity parameter, σ is the surface density and H is the vertical-scale height of the isothermal disk,

$$\frac{H}{r} = \frac{c_s}{V_K(R_*)} \left(\frac{r}{R_*}\right)^{1/2}, \quad (1.3)$$

where c_s ¹ is the isothermal sound speed and $V_K(R_*)$ is the Keplerian velocity at the stellar surface.

From their numerical calculations Okazaki & Negueruela (2001a) found that truncation of the disk happened when α is smaller than a critical value, α_{crit} (see Fig. 1.3). Unlike the conventional view (Okazaki & Negueruela 2001b), this result has an important meaning that there should be a gap between the disk and the companion. Explicitly, the gap is located between truncation radius and radius at which gravitational attraction of the neutron star begins to dominate where it is determined by the gap size, $\Delta(r)$. Thus the efficiency of the truncation mainly depends on $\Delta(r)$, and α . For typical values of $\alpha < 1$, the truncation is dominant when time, τ_{drift} , needed for a particle to exceed the gap is longer than the orbital period, P_{orb} (Reig 2011). Thus, systems with narrow orbits and with moderate eccentricities will be forced to have a more efficient truncation than systems with wide orbits and large eccentricities.

Eventually, we can now determine a general frame of X-ray activity of Be/X-ray systems based on a viscous accretion disk model and the fact of its truncation by the companion. As stated above, eccentricity of a system has a crucial role on the truncation and has an indirect effect on adjusting mass transition between the disk and the NS. Following the results and predictions of Okazaki & Negueruela (2001a), X-ray outburst formations in the Be/X-ray systems can be generalized according to the eccentricity:

- i)** Systems with large eccentricity ($e \geq 0.3$): Assuming that viscosity is not very low ($\alpha \gtrsim 0.03$), the disk truncation is not efficient since the truncation radius is

¹ $c_s = [(kT)/\mu m_H]^{1/2}$, where μ is the mean molecular weight of the gas, T is the (isothermal) electron temperature and m_H is the hydrogen mass.

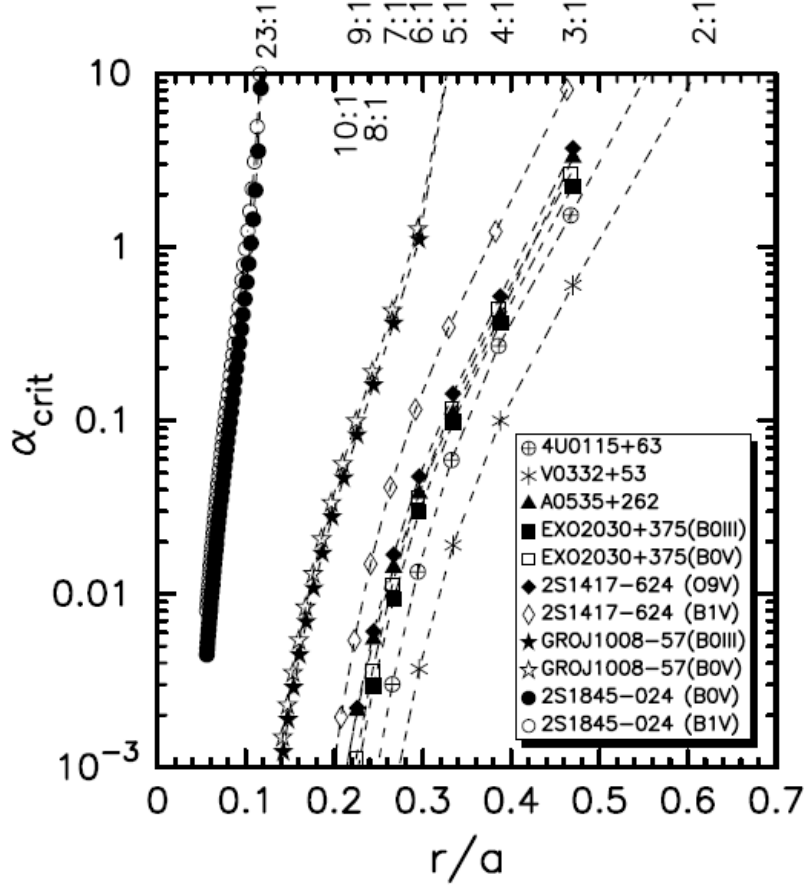


Figure 1.3: Critical values of α at $n:1$ resonance radii for different Be/X-ray systems (taken from Okazaki & Negueruela (2001a)). Numbers on the top give the locations of $n:1$ commensurabilities of disk and mean binary orbital frequencies.

close to critical lobe radius at periastron (or $\tau_{drift} \ll P_{orb}$). Resonant torque exerted on the disk is limited and outer disk radius can expand when the NS is far from the periastron (see Fig.2 in Okazaki & Negueruela (2001a)). Therefore the NS is able to accrete material at or close to the periastron passage resulting in regular Type I outbursts. For irregular/transient Type I outbursts, however, the decretion disk should be strongly elongated by global $m=1$ oscillations allowing overflowing of gas close to the periastron.

- ii) Systems with low/mid eccentricity ($e < 0.3$): In general, these type of systems are truncated at 3:1 resonance radius so that $\Delta(r)$ is much wider than those of large eccentric systems (or $\tau_{drift} > P_{orb}$). In other words, due to effective truncation the disk matter cannot pass the outer disk radius and produce Type I

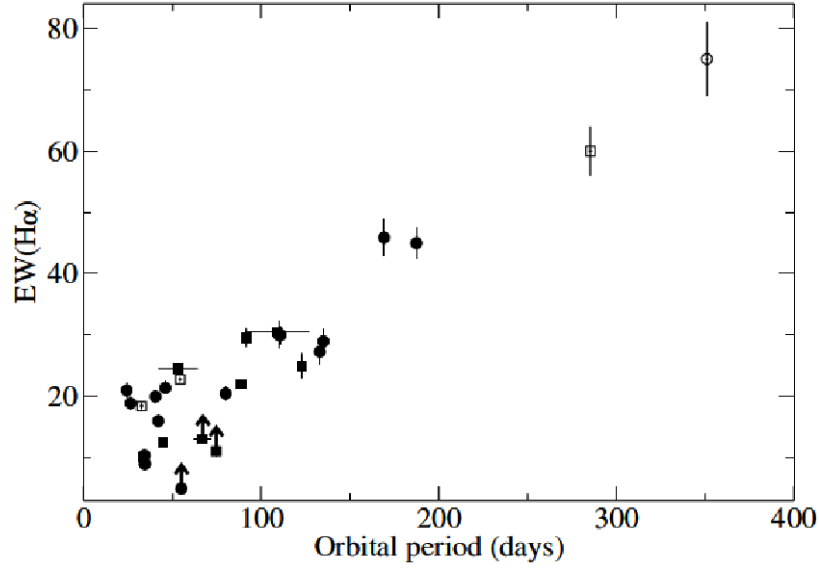


Figure 1.4: P_{orb} –EW($H\alpha$) diagram for the Be/X-ray binaries updated by Reig (2007). Galactic Be/X-ray systems represented by circles whereas SMC sources by squares. Open symbols indicate systems whose orbital periods have been estimated from Corbet diagram (see Chap. 1.1.3).

outbursts as seen in the case of large eccentric systems. Instead, it is blocked at the truncation radius by a resonant torque which leads to accumulation of gas in the outermost of the disk. As a result outer parts become optically thick and begins to warp and precess, because of the instability (Porter 1998). At this point, it is likely to see a change in emission line profile (affect of precession). As the disk precesses, interaction between stellar wind and stellar radiation can occur, leading the outer part of the disk to be deformed and elongated. Therefore a large amount of gas will be accreted by the NS causing a Type II outburst.

It should also be noted that abovementioned picture might not be applicable to all Be/X-ray binaries. Indeed, there are systems that cannot fit into this generalization. Particularly, physical mechanisms that trigger Type II outbursts have still been fuzzy. However there have been increasing observational evidences that systems showing giant outbursts have precessing warped disks which are misaligned with the binary orbital planes (Martin et al. 2014; Moritani et al. 2013).

To sum up, the interaction between the decretion disk and the NS works bidirectionally where the disk acts like a mass reservoir supplying required material to the NS for production of X-ray radiation, whereas the companion controls size of the disk by exerting resonant torques on it. As a matter of fact, it has been previously suggested by Reig et al. (1997a) that the NS should influence the size of the decretion disk depending on the correlation between the maximum equivalent width (EW) of $H\alpha$ ever observed and P_{orb} . According to this relation (see Fig. 1.4), the systems with long orbital periods (wide orbits) have larger disks since the NS has little/no effect on circumstellar envelope whereas for narrow orbits the NS acts as a barrier preventing formation of an extended disk. Although it is clear that $H\alpha$ EW measurements do not represent the disk size properly, the maximum EW ever observed value may provide a comparative estimate of the maximum disk size if the system has been monitored for a sufficiently long time, e.g. comparable with the time-scale of the changes in the disk (Negueruela & Okazaki 2001).

1.1.3 Be/X-ray Binaries in Corbet Diagram: P_{spin} vs P_{orb}

The existence of a relation between P_{orb} and P_{spin} periods for Be/X-ray binaries was first suggested by Corbet (1984) despite the inference based on the small number of sample systems (seven sources). However, with an increasing number of X-ray binaries with identified system parameters, the relation was confirmed not just for Be/X-ray binaries but also for other HMXBs with supergiant companions (Corbet 1986; Li & van den Heuvel 1996; Waters & van Kerkwijk 1989). According to this, the HMXBs are located at three distinct regions in the $\text{Log}(P_{orb})$ – $\text{Log}(P_{spin})$ plane, so called the Corbet Diagram, where at least two of them have certain correlations (Corbet 1986, see Fig. 1.5):

- i) Roche-Lobe overflowing systems with short spin periods (lower left part of the diagram),
- ii) Systems powered by the radially expanding winds with longer spin periods (upper left of the diagram),
- iii) BeXRBs having circumstellar disks from which amount of material for accretion

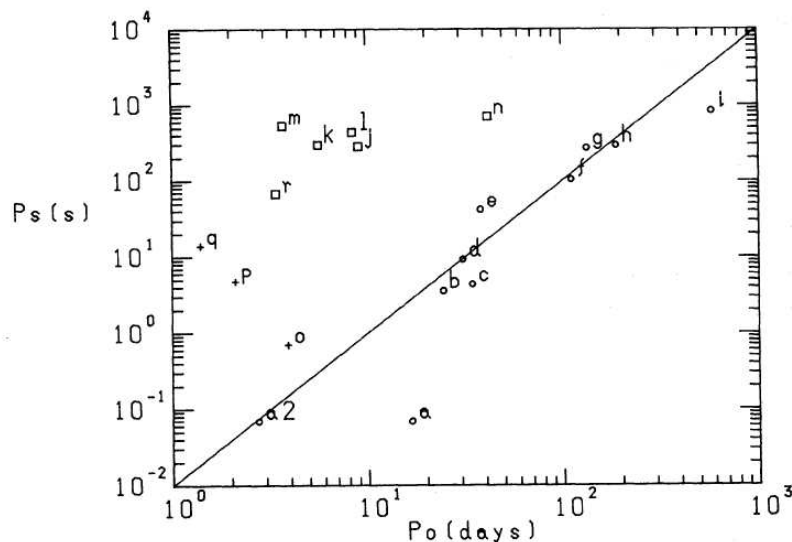


Figure 1.5: Three distinct locations of HMXBs in the Corbet Diagram (taken from Corbet (1986)). Be/X-ray systems are presented by circles (a–i) whereas the squares (j–n) indicate Supergiant HMXBs (sgHMXBs). Roche-Lobe filled systems are shown with crosses (o–q). The solid line corresponds to $P_{spin} \propto P_{orb}$.

is supplied.

The main idea behind this remarkable relation for HMXBs is basically relied on different mass-transfer mechanisms of accretion for different classes of objects. To understand the general physical picture of the accretion mechanism for the Be/X-ray binaries as well as the HMXBs, we should first introduce some fundamental parameters of stellar wind-accretion theory determined by Pringle & Rees (1972), Davidson & Ostriker (1973) and Lamb et al. (1973). Following the structure in Lamb et al. (1973), there are basically two radii definitions: Alfvén radius (r_A) and corotation radius (r_{co}).

For a spherical accretion, the Alfvén radius (r_A) is given as distance from the NS where energy density of stellar magnetic field equals to kinetic energy density of accreting matter,

$$\frac{B(r_A)^2}{8\pi} = \rho(r_A)v(r_A)^2, \quad (1.4)$$

where ρ is the inflowing plasma density and $B(r)$ is the magnetic field of the NS. Assuming a dipolar magnetic field,

$$B(r) \sim \frac{\mu}{r^3}, \quad (1.5)$$

where $\mu \equiv B_0 R^3$ is the magnetic moment in terms of the surface magnetic field B_0 . The typical radius of R and the surface magnetic field of B_0 values for a NS are assumed to be $\sim 10^6$ cm and $\sim 10^{12}$ G, respectively. Therefore the magnetic moment is found to be $\sim \mu^{30}$ G cm³. The density of spherically infalling matter, ρ , with free-fall velocity, v_{ff} , can be defined using continuity equation (steady-flow) as,

$$\rho \approx \left(\frac{dM}{dt} \right) \frac{1}{4\pi v_{ff} r^2} = \frac{\dot{M}}{4\pi v_{ff} r^2}, \quad (1.6)$$

where \dot{M} is the mass accretion rate. Combining Eq. 1.4 with Eqs. 1.5 and 1.6, the Alfvén radius is given as

$$r_A \simeq 2.9 \times 10^8 \left[\frac{\mu_{30}^{4/7}}{L_{37}^{2/7} R_6^{2/7}} \left(\frac{M}{M_\odot} \right)^{1/7} \right] \text{ cm}. \quad (1.7)$$

The quantity L_{37} is the total accretion luminosity in units of 10^{37} erg s⁻¹ and defined as follow:

$$L_{acc} \approx \dot{M} \left(\frac{GM}{R} \right). \quad (1.8)$$

Around NS, the region closer than the Alfvén radius (sometimes called as magnetospheric radius) known as the magnetosphere. For distances much farther than r_A , the magnetic field does not penetrate into the flowing matter (Shapiro & Teukolsky 1983). Although interaction between the accretion disk and the magnetic field is more complicated for disk accretion, the Alfvén radius is similar to that derived for the spherical case (Frank et al. 2002).

The second radius to be defined at this point is corotation radius (r_{co}). It is the radius at which the NS's rotational velocity is equal to the Kepler velocity of disk material and it is given by

$$r_{co} = \left(\frac{GM P_{spin}^2}{4\pi^2} \right)^{1/3}. \quad (1.9)$$

Using these two radii, we can give a rough generalization for the accretion on to a rotating magnetized NS in two conditions;

a) $r_A > r_{co}$: (Matter ejected) The matter cannot flow in the magnetospheric boundary. However if the corotation velocity exceeds the Keplerian velocity the matter will be spun away by centrifugal forces as soon as it enters into the magnetosphere (Illarionov & Sunyaev 1975, "propeller mechanism").

b) $r_A < r_{co}$: (Accretion occurs) The infalling matter with sufficient angular momentum enters into the magnetosphere and increases the angular velocity of the NS (spin up). The accretion of the material continues until condition of $r_A = r_{co}$ is satisfied. At this point the NS is known to rotate at its equilibrium spin period (so called "equilibrium period"), P_{eq} , which is given by

$$P_{eq} = 2.4(ms) B_9^{6/7} R_6^{16/7} M^{-5/7} \left(\frac{\dot{M}}{\dot{M}_{EDD}} \right)^{-3/7}. \quad (1.10)$$

where \dot{M}_{EDD} is the Eddington accretion rate (van den Heuvel 2001).

Indeed, Corbet (1984, 1986) interpreted the relation between Be/X-ray bineries in the Corbet Diagram in terms of the P_{eq} ; i.e. it is directly related to interaction between the neutron stars's magnetosphere and the material located in Be star's equatorial wind, as can be seen from Eq. 1.10. They defined this relation for Be/X-ray bineries as,

$$P_{spin} = \frac{1}{A^2} (1 - e)^3 P_{orb}^2, \quad (1.11)$$

where e is the eccentricity of the orbit and $A \sim 10$. Assuming that Be/X-ray bineries rotates at P_{eq} and using the assumptions of Waters & van Kerkwijk (1989), the above equation can be written as,

$$P_{eq} \propto P_{orb}^{2/7(4n-6)}. \quad (1.12)$$

The distribution observed in Corbet Diagram can be well fitted with $n=3.25$. Since observational results indicate that NSs in Be/X-ray bineries are rotating at their equilibrium periods (Rappaport & Joss 1983; Ziolkowski 2002, and references therein), the accretion mechanism for Be/X-ray bineries can be interpreted in terms of P_{eq} and P_{spin} which increases the importance of P_{eq} . It is obvious that through its eccentric orbit, instantaneous P_{eq} of the NS changes owing to the changing mass rate. So that one can expect to see much smaller P_{eq} near/close to periastron than that of the NS. In other words, at periastron passage, $P_{eq} < P_{spin}$, the matter can approach to the neutron star and get accreted since the velocity of outer part of the magnetosphere is smaller

than the Keplerian velocity. This process leads to a significant angular momentum transfer to the neutron star followed by a decrease in spin period (rapid spin up). For $P_{eq} > P_{spin}$, the circumstellar matter would be expelled by the magnetosphere acting like a propeller due to the centrifugal barrier (Davidson & Ostriker 1973; Illarionov & Sunyaev 1975). Therefore in a long-term time span, real rotation period of the NS adjusts itself with changing conditions, trying to reach an instantaneous P_{eq} which varies rapidly with time. Thus, there does not exist a stable P_{eq} for Be/X-ray binaries. Waters & van Kerkwijk (1989) suggested that observed distribution in the Corbet Diagram was strongly influenced by the observational selection effects. According to them we are more likely to observe the systems when they are in X-ray active phases.

1.1.4 Non-Radial Pulsations in Be/X-ray Systems

One of the unsolved issues regarding to the Be-phenomenon is certainly real mechanism causing mass ejection episodes from the central star. Although it is widely accepted that Viscous Decretion Disk Model well matches with observations, it does not explain how a Be star material is transported to inner boundary regions of the disk with a sufficient angular momentum, similar to several previously suggested models. Since Be stars are known to be fast-rotating stars, rotation has been thought to be the answer for mass ejection (Porter & Rivinius 2003). However, recent theoretical and observational studies show that their rotational velocity does not reach to the break-up velocity. Instead they rotate at 70-90% of their critical velocities (Frémat et al. 2005; Porter 1996). Therefore, need of an additional mechanism to provide the angular momentum for ejecting material into the circumstellar disk has been arisen to explain the phenomenon. There are basically two potential candidates for triggering the mass ejection: Magnetic Field (Balona 1995; Cassinelli et al. 2002) and non-radial pulsation (NRP) of the Be star (Rivinius et al. 1998). The former has not been accepted as a promising candidate for the additional mechanism since no clear detection of magnetic fields in Be stars has been reported so far (Neiner & Hubert 2009). Although it was initially suggested by Osaki (1986) as the only mechanism for the angular transport, NRP has been used to explain the Be-phenomenon accompanied with the rotation.

Table 1.1: List of Galactic Be/X-ray systems having NRPs.

Name	Spectral Type	M_V	P_{orb} (d)	Frequency (c d ⁻¹)	Amplitude (mmag)	Ref.*
4U 0115+634	B0.2 Ve	15.5	24.31	3.33	14	1
RX J0146.9+6121	B1–3 Ve	11.5	~330	2.92	6.5	2
GRO J2058+42	O9.5–B0 IV–Ve	14.9	55.03	2.40	13.4	3
SAX J2103+4545	B0 Ve	14.6	12.67	2.23	4	1

(*) References: (1) Gutiérrez-Soto et al. (2011b); (2) Sarty et al. (2009); (3) Kızıloğlu et al. (2007)

Spectroscopic and photometric observations reveal that Be type stars can show two main types of variabilities in their spectra and light curves;

- i) Long-term variations: They are related to the changes in the size and density of the decretion disk (see Chap. 1.1.1) with time-scales from weeks to years. They can be irregular or quasi-periodic.
- ii) Short-term variations: They are the variations on time-scales between 0.3 and 2 days and attributed to the NRPs of the Be star.

In the Hertzsprung-Russell (HR) diagram, Be stars are located between region of the Slowly Pulsating B stars (SPB) and the β Cephei stars. In fact, based on the results of Hipparcos observations, Hubert & Floquet (1998) found that short-term variations are present in almost all (86%) early Be type stars, in 40% of intermediate sub-spectral types (B4–B5e), and in only 18% of late-type Be stars. Recently, the number of Be stars showing NRPs has been increased significantly through space missions CoRoT², dedicated to stellar seismology and exoplanet searches, *KEPLER*³ and the ground-based observations (Gutiérrez-Soto et al. 2011a; Semaan et al. 2013).

The searches for NRPs in Be/X-binaries is relatively a new research topic, though it began to improve rapidly with discovery of systems with NRPs in the Magellanic Clouds (MC) (Fabrycky 2005; Schmidtke & Cowley 2005). Yet, there have been only four Galactic Be/X-ray binaries reported to show NRPs so far (see Table 1.1).

² <http://smc.cnes.fr/COROT/index.htm>

³ <http://kepler.nasa.gov/>

1.2 Thesis Outline

In Chapter 2 we present a new and a comprehensive catalog of Be/X-ray binaries and candidates in the Galaxy and provide brief comments on each source in the catalog. The updated properties of each source have been investigated in a general frame which allow us to revise the known characteristics of Be/X-ray systems. This new catalog includes 37 confirmed systems in addition to 26 candidates. We have updated the Corbet Diagram with 61 sources and confirmed that the Be/X-ray binaries have a distinct location in the plot supporting the relation of $P_{spin} \propto P_{orb}^2$. We show that the spectral distribution of Be/X-ray binary population in the Galaxy can be characterized by a narrow spectral range of B0–B2. Yet, we could not find any correlation between the maximum EW of $H\alpha$ emissions and the orbital periods of the sample sources as previously suggested by Reig et al. (1997a). From the distribution of the X-ray activities among the BeXRBs, we suggest that Type I (normal) are the most common types. Besides, Type II (giant) activities are always associated with flares or Type I outbursts.

Chapter 3 includes the long-term optical/IR analysis of EXO 0331+ 530, XTE J1946+274 and SAX J2103.5+4545, in addition to the comparisons with the archival X-ray data. In general, each source has their own characteristics despite the common X-ray outburst types. With the recent optical spectroscopic observations, we reveal that both EXO 0331+ 530 and XTE J1946+274 have narrow and single-peaked $H\alpha$ emissions in their spectra contradicting the previous works suggested V/R variations. EXO 0331+ 530 spends most of its time in optical brightening phases, lasted 2–4 years, which resulted in Type II outbursts followed by series of normal outbursts coinciding with time of the periastron passage of the Neutron Star. On the other hand, the long-term light-curves of XTE J1946+274 do not have any significant variations related to the X-ray activities. Indeed, the long X-ray quiescent states (\sim a decade) seem typical for this source. For SAX J2103.5+4545, we found a clear correlation between the optical/IR variability and the X-ray intensity. The optical/IR outbursts started about 3 months before the triggering of the X-ray activity. However, the optical/IR brightness and the $H\alpha$ EW values were anti-correlated; that is, the maximum of the EW of this line was reached during the decline of the brightness of the BVJHK_s magnitudes. For

this source, we confined the formation–disintegration time of the decretion disk to be ~ 10 months.

In Chapter 4, we present the preliminary results of an ongoing project aiming to search the periodic short-term variations in the photometric data of the Be stars attributed to the non-radial pulsations (NRPs). Our sample includes IGR J01363+6610, IGR J01583+6713, RX J0440.9+4431, SWIFT J2000.6+3210 and GS 2138+56. Although we did not find any periodic/quasi-periodic variations in their periodograms indicating the oscillations, we found that the brightness of the sources changed within 3–5 hours which could only be explained with the further observations.

Lastly, we give the conclusions of our studies in Chapter 5.

CHAPTER 2

CATALOG OF Be/X-RAY BINARIES AND CANDIDATES IN THE GALAXY

Owing to the X-ray space missions dedicated to the detection of X-ray/ γ -ray sources, family of Be/X-ray binaries has grown rapidly in the last decade. Particularly discoveries of *INTEGRAL* observatory through its deep Galactic Plane Surveys has made an exceptional contribution to number of BeXRBs. Together with this, several catalogs have been published including the results of these surveys. On the other hand, the first (and the last) catalog of Raguzova & Popov (2005) for the Be/X-ray binaries and candidates has not been updated although nearly nine years had passed after its publication. Therefore, need of an updated list of Be/X-ray binaries has emerged.

By making a thorough review of the literature for each system, we updated the catalog of Raguzova & Popov (2005) and created a new and comprehensive list of BeXRBs and potential candidates within the Milky Way. In addition to this, two different online databases of *INTEGRAL* (IGR) sources, maintained by J. Rodriguez & A. Bodaghee¹ and Nicola Masetti² were used to check the identification of both previously suggested IGR sources and newly discovered ones.

The first catalog of Be/X-ray binaries and candidates contained 69 systems of which 8 were labeled as γ -Cas like sources including the namesake γ -Cas. In our list, we have examined these sources in a different class, since their general properties are quite different from those seen in Be/X-ray binaries (Sect. 2.3). From remaining 61 sources, on the other hand, 12 sources were also removed, as BeXRB identification

¹ <http://irfu.cea.fr/Sap/IGR-Sources/>

² <http://www.iasfbo.inaf.it/masetti/IGR/main.html>

was not valid for these systems anymore either from the optical spectroscopic studies or from the X-ray observations. In total, our updated catalog includes 63 sources, 26 of which are potential BeXRB candidates. As a new class, γ -ray binaries with Be companions have been also investigated. The general optical, IR and X-ray properties of each system are given in Table 2.1 and Table 2.2. We also present the review of the most important features to each sources in Section 2.2. Lastly, the graphical representation of some of the parameters for the whole sample is given.

2.1 Description of The Tables

Table 2.1 lists general spectroscopic and photometric properties of 63 Be/X-ray systems that are ordered according to right ascension of the system. The columns have been arranged as follows;

Column Number	Description
1	ID – source sequence number in the catalog.
2-3	Name, Optical Companion – common name of the source usually defined by X-ray missions discovered the system, and name of the optical companion if it exists.
4-5	RA, DEC – equatorial coordinates (J2000) of the source. The format for the coordinates are HH:MM:SS.S and DD:MM:SS.S. The coordinates belong to the X-ray source unless its optical companion is identified spectroscopically.
6	Spectral Type – spectral and luminosity class of the optical companion
7-13	B, V, R, I, J, H, K – optical and IR magnitudes of the source for the given filters.
14	Ref. – references.

The orbital information of the systems in addition to the EW measurements of the emission lines are given in Table 2.2. The description of the columns are given as;

Column Number	Description
1	ID – source sequence number in the catalog.
2	Name – common name of the source.
3	E(B-V) – color excess of the source for the B and V magnitudes listed in Table 2.1.
4	A_V – total extinction of the source in V band.
5	e – eccentricity of the orbit.
6	d – distance to the source in kpc.
7-8	P_{orb} , P_{spin} – orbital and spin periods of the NS.
9-10	$H\alpha(\max)$, $H\beta(\max)$ – maximum $H\alpha$ and $H\beta$ emissions of the optical companion ever observed. Conventionally they are negative and given in Å units. The measurements found in this work are marked with (*).
11	F_{peak} – maximum observed X-ray flux of the source in units of milliCrab. Related energy bands are given in parentheses.
12	Note – additional notes regarding X-ray behavior and the most prominent features of the source. The following abbreviations have been used; I: type I outburst, II : type I outburst, F : flare, P : persistent V/R : V/R variation, NRP : non-radial pulsation, msP : millisecond pulsar.
13	Ref. – references.

2.2 Sources

4U 0115+634: Transient X-ray source 4U 0115+634 is one of the most active and best studied Be/X-ray binaries. It had been detected by *Vela* 5B satellite in 1969 during its giant outburst (Whitlock et al. 1989) although it was first mentioned in *UHURU* Catalog in 1972 (Giacconi et al. 1972). The system has a 3.6 second spinning neutron star (Clark & Cominsky 1978) orbiting around a B0.2 Ve type optical companion (V635 Cas) with a 24.3-day period (Negueruela & Okazaki 2001; Rappaport et al. 1978). In general, the system show both type II outbursts with a ~ 3 year quasi-periodicity (Whitlock et al. 1989) and type I outbursts in addition to the small

X-ray flares while the optical and infrared emissions related to these outbursts have a period of ~ 5 years (Negueruela & Okazaki 2001; Negueruela et al. 2001; Reig et al. 2007). The X-ray outbursts occur in pairs however sometimes the second one may be missing. Having photometrical variations with a frequency of 3.3 d^{-1} and amplitude of 18 mmag it is one of the four Be/X-ray binaries showing NRPs (Gutiérrez-Soto et al. 2011b). In addition 4U 0115+634 is the only Be/X-ray binary of which fundamental cyclotron line and related four harmonics have been studied in details (Boldin et al. 2013; Ferrigno et al. 2011; Nagase et al. 1991; Nakajima et al. 2006; Tsygankov et al. 2007; Wheaton et al. 1979; White et al. 1983). Revisiting the data of giant 2008 outburst taken with *RXTE* and *INTEGRAL*, Müller et al. (2013) found that previously suggested anti-correlation between the fundamental cyclotron energy and the X-ray flux is an artifact of the assumptions used to model the continuum. The source entered a new X-ray active phase with a weak outburst followed by a giant outburst in June 2011 after a ~ 3.2 year quiescence (Camero-Arranz et al. 2011b; Drave et al. 2011). Two small outbursts typically seen in series after a giant one were also detected during the recent X-ray activity of the system (Jenke et al. 2011; Nakajima et al. 2011).

IGR J01363+6610: It was discovered during its type I outburst in 2004 by the *INTEGRAL* imager IBIS/ISGRI. The average flux of the outburst was 17 mCrab ($\sim 2.6 \times 10^{-10} \text{ erg cm}^{-2} \text{ s}^{-1}$) in 17–45 keV energy band and 9 mCrab ($\sim 9.1 \times 10^{-11} \text{ erg cm}^{-2} \text{ s}^{-1}$) in 8–15 keV energy band (Grebenev et al. 2004b; Tomsick et al. 2011). The optical companion is a B1 IV-Ve type star with a cataloged name of [KW 97] 6-30 (Kohoutek & Wehmeyer 1999; Reig et al. 2005b). Corbet & Krimm (2010) found a modulation of 159 ± 2 day in the *Swift*/BAT light curve of the system. However it was noted that the given period cycles existed only in MJD 54500-55500. Although showing transient X-ray activity and having an emission line star as the optical companion make the system a potential Be/X-ray binary lowness of the quiescent X-ray luminosity ($< 1.4 \times 10^{31} \text{ erg s}^{-1}$) put the system into a unique place among the other Be/X-ray systems (Tomsick et al. 2011). The hard X-ray transient IGR J01363+6610 has been in a quiescent state since its discovery.

RX J0146.9+6121: This persistent low-luminosity X-ray source RX J0146.9+6121 (Haberl et al. 1998b) was identified as a Be/X-binary by Motch et al. (1991a) during the galactic plane survey of *ROSAT* satellite. It was initially detected by *EXOSAT*

when the system was in X-ray active phase in 1984 (White et al. 1987). The last detected outburst of the system which was a type I outburst with a peak flux of 3.2×10^{-10} erg cm⁻²s⁻¹ in 0.5–10 keV energy range was in 1997 (Haberl et al. 1998b). The system was also known to have a pulsar with the longest spin period of nearly 25 minutes (Haberl et al. 1998b; Hellier 1994; White et al. 1987). The optical companion LSI +61 235/V831 Cas is a B1 III-Ve star that shows V/R variations in its spectra with a quasi-period of ~ 1240 day (Reig et al. 1997b, 2000) and 3 strong periodicities in its V-band light curves at 0.34, 0.67 and 0.10 day (Sarty et al. 2009). The 0.34 day periodicity was attributed to the radial fundamental mode pulsation and 0.10 day as a higher order p-mode pulsation while the 0.67 day period was interpreted as the spin period of Be star.

IGR J01583+6713: The system has a a magnetic neutron star of $B \sim 4 \times 10^{12}$ G (Wang 2010) and a B2 type subgiant star having one of the strongest H α emission (~ 74.5 Å) among the galactic Be/X-ray binaries (Halpern & Tyagi 2005a; Masetti et al. 2006a). During its outburst leading to its discovery on 2005 December 6–7, the peak flux reached 14 mCrab in 20–40 keV (Steiner et al. 2005). After the outburst the flux of the source, found to be decreasing, could not be detected by ISGRI (Wang 2010). Kaur et al. (2008b) found a possible pulse detection of a 469.2 s using the *Swift* light curve of the source but it was not confirmed by Wang (2010) who searched the pulsation in *INTEGRAL*/IBIS data.

EXO 0331+530: The hard X-ray transient EXO 0331+530 (V 0332+53) was first detected during its giant outburst, reached a peak intensity of 1.6 Crab in 3–12 keV energy range, by *Vela* 5B satellite in 1973 (Terrell et al. 1983; Whitlock 1989). Subsequent X-ray and optical observations revealed that the system consists of a neutron star, exhibiting ~ 4.4 second pulsations which are dominated by the rapid random X-ray fluctuations (Makishima et al. 1990; Stella & White 1983; Stella et al. 1985; Terrell & Priedhorsky 1984), and an O8-9 Ve type optical companion at a distance of ~ 7 kpc (Negueruela et al. 1999). The system has showed both type II and type I outbursts since its discovery. It underwent a new X-ray activity in 2004 after a ~ 20 year quiescence (Swank et al. 2004). Analyses of 2004–2005 X-ray active phase led the discovery of three cyclotron resonant scattering features at 24.9 ± 0.1 , 50.5 ± 0.1

and 71.7 ± 0.8 keV (Kreykenbohm et al. 2005; Pottschmidt et al. 2005). The system showed weak type I outbursts in 2008, 2009 and 2010 (Krimm et al. 2009c, 2008a; Nakahira et al. 2010; Nakajima et al. 2010; Reig 2008).

4U 0352+309: The persistent low luminosity X-ray source 4U 0352+309 (Braes & Miley 1972; van den Bergh 1972), having average luminosity of $\simeq 10^{34}$ erg s $^{-1}$, is the brightest and one of the best studied systems among the Be/X-ray binaries (Di Salvo et al. 1998; Fabregat et al. 1992; Roche et al. 1993). The optical companion X Persei (X Per, HD 24534) is an O9.5 III–B0V type emission line star showing large scale variations, between minutes and years, in its optical/IR light curves (Fabregat et al. 1992; Lyubimkov et al. 1997; Slettebak 1982). The strength and the shape of Balmer emission lines are also highly variable indicating the disk loss and renewal phases (Clark et al. 2001; Mook et al. 1974; Roche et al. 1997). The system is known to have one of the slowest pulsars with a period of 837 s (Delgado-Martí et al. 2001; Haberl 1994; White et al. 1976). A cyclotron resonance scattering feature (CRSF) of ~ 29 keV was found in the *RXTE* spectrum of 4U 0352+309 (Coburn et al. 2001). Recently, by reanalyzing *RXTE*/PCA and *INTEGRAL*/ISGRI archival data of 1998–2010 Acuner et al. (2014) discovered a transient quasi-periodic oscillation (QPO) feature, peaking at ~ 0.2 Hz, suggesting the presence of the accretion disk.

RX J0440.9+4431: This persistent system was discovered during the *ROSAT* Galactic plane survey and associated with a B0.2 V type (Reig et al. 2005a) optical companion BSD 24-491/LS V +44 17 (Motch et al. 1997, 1996). Although it has typical characteristics of persistent Be/X-ray binaries such as showing persistent low X-ray luminosity $\sim 10^{34}$ erg s $^{-1}$ and having a relatively long spin period of 202.5 s (Reig & Roche 1999a). RX J0440.9+4431 is one of two systems (see RX J1037.5–5647) among the those of the same class due to its transient outburst behaviour (Ferrigno et al. 2013; Finger & Camero-Arranz 2010; Krivonos et al. 2010a; Morii et al. 2010; Tsygankov et al. 2011). Tsygankov et al. (2012) discovered a ~ 32 keV CRSF in *INTEGRAL* spectrum of the source obtained during its 2010 April outburst and they estimated the magnetic field strength of the pulsar as $\simeq 3.2 \times 10^{12}$ G. In addition recent *XMM*/Newton data indicate the spinning down of the source over 13 years (La Palombara et al. 2012).

A 0535+262: The recurrent hard X-ray transient A 0535+262 was discovered by *ARIEL V* satellite during its giant (~ 3 Crab) outburst and was found to show pulsations with a period of ~ 104 s (Rosenberg et al. 1975). The optical companion was subsequently identified as an O9.7–B0III type (Giovannelli & Graziati 1992; Janot-Pacheco et al. 1987; Steele et al. 1998) emission line star V725 Tau/HD 245770 (Liller 1975). The long-term $H\alpha$ line monitoring reveals that the decretion disk of Be star is subjected to global-one armed oscillations pertained to the V/R variations (Clark et al. 1998). The system which exhibits periodic outbursts usually centered at periastron passage of the neutron star in addition to the giant outburst and short flares that have been extensively studied in all energy ranges both in X-ray active and quiescent phases since its discovery (Caballero et al. 2007; Coe et al. 2006; Finger et al. 1996b; Grundstrom et al. 2007b; Ikhsanov 2001; Larionov et al. 2001; Motch et al. 1991b; Negueruela et al. 2000). A giant outburst with an X-ray flux of ~ 3.6 Crab in 2–100 keV energy band was detected on February 2011 by *INTEGRAL* (Caballero et al. 2011). After ~ 3 years silence in X-rays the system entered a new active phase on Feb 2014 (Camero-Arranz et al. 2014a; Takagi et al. 2014).

IGR J06074+2205: The X-ray activity of IGR J06074+2205 was detected during the public observations of the Crab region in 2003 (Chenevez et al. 2004). Having a remarkable difference between the X-ray active ($F_x \sim 1.3 \times 10^{-10}$ erg cm $^{-2}$ s $^{-1}$ in 3–10 keV) and quiescent phase ($F_x \sim 2.6 \times 10^{-12}$ erg cm $^{-2}$ s $^{-1}$ in 3–10 keV) in addition to the zero redshift made the system to be a potential Be/X-ray candidate (Halpern & Tyagi 2005b; Masetti et al. 2006a; Tomsick et al. 2006, 2008). Later Reig et al. (2010b) confirmed the nature of the optical counterpart as a B0.5 type main sequence emission line star which showed V/R variability in its spectra on timescales of months.

SAX J0635.2+0533: The system SAX J0635.2+0533, containing a millisecond pulsar (Cusumano et al. 2000) and a 12.8 magnitude emission line star, was first detected in the error box of the gamma ray source 2EG J0635+0521 by BeppoSAX with a flux of 1.2×10^{-11} erg cm $^{-2}$ s $^{-1}$ in 2–10 keV energy band (Kaaret et al. 1999). However subsequent High Energy Stereoscopic System (HESS) observations revealed that the

previously suggested gamma-ray source was not associated with SAX J0635.2+0533 due to the absence of the gamma-ray emission at its position (Aharonian et al. 2007). The nature of the system on the other hand has not been completely known since it has some peculiarities with respect to the typical accretion-powered pulsars (Mereghetti & La Palombara 2009).

XTE J0658–073: It was first detected by *SAS-3* during its ~ 80 mCrab (in 1.3–13 keV range) outburst in 1975 (Clark et al. 1975). Subsequent *ARIEL V* observations also detected two X-ray brightenings of the source with the peak flux of ~ 50 mCrab and ~ 70 mCrab respectively in 1976 (Kaluzienski 1976). The optical companion is a highly reddened O9.5 Ve type star at a distance of 3.9 kpc (McBride et al. 2006; Nespoli et al. 2012; Pakull et al. 2003). After approximately 27 years quiescence the source entered a new X-ray active phase of 4 months which led to the discovery of 160.7 s pulsations during this giant outburst (Morgan et al. 2003; Remillard & Marshall 2003). The last outburst of the system (Kreykenbohm et al. 2007), in 2007, led to discovery of a strong iron $K\alpha$ line with an equivalent width around 300 to 400 eV (Pottschmidt et al. 2007). Detailed X-ray and optical studies indicate that the system show type I and type II outbursts in X-rays. Besides the type II outburst behavior seems peculiar due to its flare-like appearance during its peak (Nespoli et al. 2012).

4U 0726–260: It was first mentioned in the fourth *UHURU* catalog (3A 0736–260) having a flux of $6.29 \pm 0.34 \times 10^{-11}$ erg cm $^{-2}$ s $^{-1}$ in 2–6 keV energy band (Forman et al. 1978). The source was also detected by the subsequent *ARIEL V*, *HEAO 1* and *ROSAT* experiments (Corbet & Mason 1984; Steiner et al. 1984; Wood et al. 1984). The pulsar in the system, having a spin period of 103.2 s, rotates at a orbit of a 34.5 days around its O8-9 Ve type optical companion (Corbet & Peele 1997b; Negueruela et al. 1996). Whilst the X-ray characteristics of the system have been poorly studied owing to the lack of detection of the significant activity since its discovery.

1H 0739–529: 1H 0739–529 was identified as a HMXB in HEAO 1 X-ray catalog with a flux of 1.77×10^{-11} erg cm $^{-2}$ s $^{-1}$ in 0.5–25 keV energy band (Wood et al. 1984). The optical counterpart HD 63666 is a B7 IV–Ve star listed in Hipparchos catalog (Perryman et al. 1997). Although the source was classified as an Be/X-ray bi-

nary both in Liu et al. (2006) and in Raguzova & Popov (2005), the X-ray behaviour and the observational characteristics of the system have not been studied in details since its discovery. Therefore we classify the source as a potential Be/X-ray binary candidate.

RX J0812.4–3114: RX J0812.4–3114 was found by cross-correlating in position of SIMBAD OB star catalog with the *ROSAT* Galactic all sky survey (Motch et al. 1997, 1996). During *ROSAT* observations the system was on X-ray outburst which led to the discovery of 31.89 s pulsations (Reig & Roche 1999b) and the orbital period of 80 days (Corbet & Peele 2000). The optical counterpart to the system, a B0.2 type III–IV star LS 992, shows emission and absorption profiles of H α line over the long-term spectroscopic observations indicating the formation and dissipation of the decretion disk (Reig et al. 2001).

GS 0834–430: The accretion-powered pulsar GS 0834–430 was discovered in 1990 with *WATCH* experiment on board GRANAT while it was in X-ray outburst that reached a flux of 1 Crab in the 5–15 keV energy range (Sunyaev 1990b). Since its discovery more than 10 X-ray outbursts which were separated by regular periods of 105–107 days including two irregular of them were detected by *ROSAT* (Belloni et al. 1993; Makino et al. 1990), *SIGMA* (Denis et al. 1993), *GINGA* (Makino & GINGA Team 1990; Makino et al. 1990) and *CGRO* (Wilson et al. 1997). The refined position and the optical counterpart of the system was found by Israel et al. (2000a). Recently the source entered an X-ray active phase which were detected by *INTEGRAL* and *FERMI* satellites (Drave et al. 2012b; Jenke et al. 2012a). Analyzing the *NuSTAR* high-energy X-ray telescope observations of the source, Miyasaka et al. (2013) detected a weak iron line (EW \sim 40 eV) anti-correlated with the 5–10 keV flux.

GRO J1008–57: The transient X-ray pulsar GRO J1008–57 was first detected by *CGRO/BATSE* in 1993 during its giant outburst that reached a peak flux of 1.4 Crab in the 20–50 keV energy band with a pulsation period of 93.59 s (Stollberg et al. 1993). The system has showed recurrent X-ray outbursts separated by \sim 248 days since 2005 (Camero-Arranz et al. 2011a; Evangelista et al. 2008; Grebenev et al. 2005; Krimm et al. 2007a; Kuehnel et al. 2011; Leyder et al. 2009a; Suzuki et al.

2010; Swank 2005). The recurrence time of the outbursts is attributed to orbital period of the binary (Coe et al. 2007). The system entered a new X-ray active period in November 2012 consisted of a one giant and normal outbursts (Krimm et al. 2012c; Kuehnel et al. 2012; Nakajima et al. 2012). Using *NuSTAR*, *SUZAKU* and *Swift* data both Bellm et al. (2014) and Yamamoto et al. (2014) confirmed the presence of the previously suggested CRSF feature at ~ 80 keV (Grove et al. 1995; Yamamoto et al. 2013) implying a magnetic field of 6.6×10^{12} G that is the highest among the X-ray binaries. The latest activity, ~ 10 days before the periastron passage of the neutron star, was detected by MAXI/GSC in December 2013 (Kawagoe et al. 2013b).

RX J1037.5–5647: The persistent low luminosity Be/X-ray system RX J1037.5–5647 (Li et al. 2012b) is identical to the previously identified *UHURU* source 4U 1036–56 (Forman et al. 1978). It consists of a BO III–V type emission line star LS 1698 (Motch et al. 1997, 1996) and a neutron star with a pulse period of 860 ± 2 s (Reig & Roche 1999a) whose X-ray spectrum is represented by a power law plus to an absolute black body model with a temperature of $kT \simeq 1.3$ keV (Ikhsanov & Beskrovnaya 2011; La Palombara et al. 2009). Using photometric observations of the optical companion Sarty et al. (2011) suggested an orbital period of 645 days derived from the long-term V-band variations. However Cusumano et al. (2013) showed that the *Swift*/BAT light curve of 100 months of the source had a periodic modulation of ~ 61 days which put the system to the place of Be binaries in the Corbet diagram (Corbet 1984). The system showed a transient X-ray outburst reaching a peak flux of 30 mcrab in 15–50 keV energy band in Feb, 2012 (Krimm et al. 2012d).

1A 1118–615: The hard X-ray transient source 1A 1118–615 was discovered by *ARIEL V* satellite during its giant outburst in 1974 (Eyles et al. 1975). Since then the system has been seen to exhibit two giant outbursts which were in 1992 (Coe et al. 1994b) and in 2009 (Leyder et al. 2009b; Mangano 2009). Analysis of the *RXTE* data taken during the last outburst of the system revealed a broad prominent CRSF at ~ 55 keV corresponding to a magnetic field of $B \sim 6-8 \times 10^{12}$ G was found by (Devasia et al. 2011a; Doroshenko et al. 2010; Nespoli & Reig 2011). The optical companion is a highly reddened Be type star (Chevalier & Ilovaisky 1975; Janot-Pacheco et al. 1981; Villada et al. 1999) whose spectrum shows extreme variations in the strength of

H α line equivalent width within short-time durations (Coe et al. 1994b; Motch et al. 1988; Villada et al. 1992). The system is also peculiar in terms of the relation between its spin (Doroshenko et al. 2010; Ives et al. 1975) and the orbital period (Staubert et al. 2011) which is not fitted in the Corbet diagram (Corbet 1984).

IGR J11305–6256: This source was first detected with an average flux of 8 mCrab in 20–60 keV energy band by IBIS/ISGRI instrument on board *INTEGRAL* during the Carina region observations in 2004 (Produit et al. 2004). Masetti et al. (2006e) identified the optical companion as the cataloged object HD 100199 (Ferne 1983), an emission line B0 IIIe type star (Garrison et al. 1977), at a distance of ~ 3 kpc. The system has been known to be a persistent Be/X-ray binary since it has always been detected with a weak X-ray luminosity (Bird et al. 2007; Masetti et al. 2006e; Negueruela & Schurch 2007; Tomsick et al. 2008). Recently using long-term *Swift*/BAT data La Parola et al. (2013b) found a modulation of 120.83 days in the light curve of the source which was interpreted as the orbital period of system.

IGR J11435–6109: The system has a pulsar that rotates with a 161.76 s spin period at a distance of ~ 8.6 kpc (Masetti et al. 2009) in its 52.46 day orbit (Corbet & Remillard 2005; in't Zand & Heise 2004). The faint emission line star USNO-B1.0 0288–0337502 was suggested as the counterpart of the system owing to the consistency with the Chandra position (Tomsick et al. 2007). Later Negueruela et al. (2007) confirmed the source as the correct counterpart of the system using their photometric and spectroscopic results. IGR J11435–6109 showed another X-ray activity in June 2005 with a peak flux of 15 mCrab in 17–60 keV (Revnivtsev et al. 2005) after the first outburst which led to its discovery in 2004 (Grebenev et al. 2004a). In addition we note that this source was also listed in previous catalogs with the designation of 2E 1141.6–6050 indicating a long X-ray history (in't Zand & Heise 2004; Thompson et al. 1998).

4U 1145–619: It was first mentioned in *UHURU* catalog of Giacconi et al. (1972) with the designation of 2U 1146–61. The intensity of the source was detected as 1.22×10^{-9} erg cm $^{-2}$ s $^{-1}$ in 2–10 keV energy band. The X-ray pulsar, a highly variable source, was associated with an emission line star Hen 715 (V801 Cen) after

ARIEL V observations (White et al. 1978). The source, located ~ 15 arcmin away from a supergiant HMXB 1E 1145.1–6141 (Lamb et al. 1980), shows recurrent X-ray outbursts with a period of 187.5 d (Priedhorsky & Terrell 1983; Warwick et al. 1981; Watson et al. 1981). 4U 1145–619 is one of the persistent Be/X-ray binaries that shows X-ray pulsations even at the low luminosities around $\approx 10^{34}$ erg s $^{-1}$ (Rutledge et al. 2007).

1ES 1210–646: Since its discovery in 1978 by *UHURU* satellite the peculiar source 1ES 1210–646 (4U 1210–64) has been observed several times by different satellites from high to low energy ranges (Bird et al. 2007; Elvis et al. 1992; Forman et al. 1978; Reynolds et al. 1999). Yet the presence of the strong iron emission line at 6.7 keV (EW ~ 400 eV) leads the source to be classified as an accreting WD (CV) initially it has been suggested that the source is a HMXB hosting a B5 type main sequence optical companion and a low magnetic field neutron star (Masetti et al. 2010a, 2009; Revnivtsev et al. 2007). Since its peculiarities that rarely seen in Be/X-ray binaries in the Galaxy such as having an optical companion with a spectral type beyond B2, we prefer to label the source as a potential Be/X-ray binary candidate.

1H 1255–567: This source was detected by HEAO A-1 and first mentioned in the X-ray source catalog of the satellite with a flux of 1.82×10^{-11} erg cm $^{-2}$ s $^{-1}$ in 2–10 keV energy band (Wood et al. 1984). It is associated with a 5.17 magnitude Be star HD 112091 (Maccarone et al. 2014; Percy et al. 1981; Slettebak 1982) which is located at 0.11 kpc (Chevalier & Ilovaisky 1998). The system parameters and the X-ray nature of the neutron star have not been known since no considerable X-ray emission of the source has been detected for ~ 28 years. Therefore we cataloged the source as a candidate Be/X-ray binary.

4U 1258–613: The ~ 272 s pulsar (McClintock et al. 1977) 4U 1258–613 (GX 304–1) was discovered during the X-ray balloon observations in 1967 (Lewin et al. 1968; McClintock et al. 1971). It was identified with a B2 type main sequence, emission line star V850 Cen, located at 2.4 kpc, showing photometric variabilities in the optical band (Bradt et al. 1977; Mason et al. 1978; Parkes et al. 1980). The system was highly active in X-rays between the years 1970 and 1980 exhibiting low luminosity

X-ray outbursts separated by ~ 132.5 d (Priedhorsky & Terrell 1983) and flares with 100 s durations (McClintock et al. 1977; Ricker et al. 1973). After 28 years quiescence the system was seen in brightening again with a flux level of 3–7 mCrab above 20 keV in 2008 (Manousakis et al. 2008). Since then, the system showed fourteen recurrent type I outbursts with a period of 132.5 d (Krimm et al. 2010b; Mihara et al. 2012; Yamamoto et al. 2011a, 2009, 2012) and a strong flaring activity (Klochkov et al. 2012a,b). The twelfth X-ray activity of GX 304–1, started 15 days earlier than that recurrent cycle, was on 21 September and followed by a giant outburst (Jenke et al. 2012b) reaching a peak flux of ~ 1700 mcrab in 12–50 keV as predicted (Mihara et al. 2012). The last outburst of the system was detected by MAXI/GSC on 9 July 2013 (Nakajima et al. 2013). The estimated magnetic field strength of the source is $\sim 4.7 \times 10^{12}$ G (Yamamoto et al. 2011b).

IGR J13020–6359: The first detection of this source was in the hard X-ray energy band with a peak flux of 11 mCrab (18–60 keV) in 2004 which gave rise to be identified as an accreting powered ~ 700 s pulsar whilst it has been already cataloged as a *ROSAT* source namely 2RXP 13059.6–635806 with an unknown nature (Chernyakova et al. 2005, 2004; Masetti et al. 2006e). Having an optical companion with a B0 type dwarf (Coleiro et al. 2013), it is one of the persistent X-ray binaries showing a typical luminosity at the order of $\sim 10^{34}$ – 10^{35} erg s $^{-1}$ (Bodaghee et al. 2007; Masetti et al. 2006e).

IGR J13186–6257: IGR J13186–6257 was first mentioned in Bird et al. (2007) as an unidentified hard X-ray source. The X-ray spectrum of the source was described by an unabsorbed flat power law fit with a flux of 5.8×10^{-11} erg cm $^{-2}$ s $^{-1}$ in 2–10 keV energy band (Landi et al. 2008). Due to the high and variable column density, Tomsick et al. (2009) suggested that the source was a HMXB. Analyzing the *Swift*/BAT light curves in 0.2–150 keV band D’Ài et al. (2011) showed that the source had a periodicity of 19.99 d which is typical for a Be/X-ray system. Since the optical spectrophotometric observations are needed to confirm the nature of the counterpart to IGR J13186–6257 we classified the source as a potential Be/X-ray binary.

SAX J1324–6200: This 170.84 s X-ray pulsar was discovered serendipitously dur-

ing the observation of the LMXB XB 1323–619 with *BeppoSAX* (Angelini et al. 1998). The X-ray spectrum of the source was described by a highly absorbed power law with a photon index ~ 1 . Although the X-ray nature of SAX J1324–6200 was poorly understood, it has been suggested that the system is one of the persistent Be/X-ray binaries due to its low X-ray luminosity and the absence of Fe emission lines in its spectrum (Kaur et al. 2009; Mereghetti et al. 2008). Due to the lack of information about the optical counterpart of the source we categorise SAX J1324–6200 as a potential persistent Be/X-ray binary.

4U 1416–62: It was first appeared in 4th *UHURU* catalog with a 2–10 keV flux of 1.82×10^{-10} erg cm $^{-2}$ s $^{-1}$ (Forman et al. 1978) and detected again by *SAS-3* satellite (2S 1417–624) with a ~ 3 times higher X-ray intensity than the previous *UHURU* observations Apparao et al. (1980). The only work in the literature related to the optical counterpart of this ~ 18 s pulsar (Kelley et al. 1981; Raichur & Paul 2010) belongs to Grindlay et al. (1984) who identified the source as a Be/X-ray binary. The renewed system parameters and the orbital period were determined by Raichur & Paul (2010) and Levine et al. (2011). The system was active in 2008 July (Manousakis et al. 2008) and in 2009 October (Beklen et al. 2009; Krimm et al. 2009b). After ~ 5 years quiescence 4U 1416–62 entered a new outburst phase detected by *INTEGRAL/IBIS* in January 2014 (Fiocchi et al. 2014).

IGR J14331–6112: The hard X-ray source IGR J14331–6112 was discovered by IBIS/ISGRI imager on board *INTEGRAL* during the observations of the Circinus X-1 region which was performed between 2003 and 2005 (Keek et al. 2006). Excluding the fact that the system is a HMXB with an early type BIIIe or BVe emission line star (Masetti et al. 2008a) and a compact companion that has a strong iron $K\alpha$ emission line (EW ~ 945 eV) in its spectra (Tomsick et al. 2009) any information about the system parameters has not been appeared in the literature.

IGR J14488–5942: The source IGR J14488–5942 is a Be/X-ray candidate due to its variable column density character and the longness of the orbital period (Corbet et al. 2010a). It was first mentioned in Bird et al. (2010) with a peak flux of 2.9 ± 0.5 mCrab in 20–40 keV energy band as an unidentified transient X-ray source. The follow-up

Swift/XRT observations showed that there were two possible IR counterparts to the source in IBIS error circle (Landi et al. 2009). The brighter X-ray source (N2) in the error circle was suggested to be the possible counterpart to IGR J14488–5942 by Landi et al. (2009) and Rodriguez et al. (2010) while Corbet et al. (2010a) found a 33.4 s marginal signal in *Swift*/XRT light curve of N1. Yet, the true counterpart of this X-ray source has not been identified so far.

XTE J1543–568: XTE J1543–568 was discovered by *RXTE*/PCA in 2000 (Marshall et al. 2000). It is classified as a Be/X-ray binary candidate since its 27.12 s spin period (Marshall et al. 2000) and 75.56 d orbital period (in’t Zand et al. 2001a) consistent with the position of the Be transients in Corbet diagram (Corbet 1984) which are optically confirmed. During the recent X-ray brightening of the system, detected by *Swift*/BAT monitor, Krimm et al. (2012a) found a possible 2MASS counterpart in the XRT circle.

2S 1553–542: Since its discovery in 1975 (Apparao et al. 1978) the only detected activity of the system was in 2007 with a flux of 170 mCrab (Krimm et al. 2007b). This flaring activity was studied by Pahari & Pal (2012) in details. The system has a pulsar with 9.3 s spin period orbiting at a circular orbit ($e < 0.09$) around its companion (Kelley et al. 1983). No optical counterpart has been proposed up to date.

1H 1555–552: It has been one of the poorly studied HMXBs although it was first mentioned in 1984 in *HEAO* A-1 X-ray catalog of Wood et al. (1984). Torrejón & Orr (2001) proposed an emission line star HD 141926/Hen 1110 (Grillo et al. 1992; Wackerling 1970) as the optical counterpart of 1H 1555–552 and using 1.8–10 keV *BeppoSAX* spectrum they suggested the source to be a low luminosity Be/X-ray binary. Since the system parameters and the detailed optical study of the companion have not been determined we categorize the source as a potential Be/X-ray candidate.

SWIFT J1626.6–5156: The hard X-ray transient SWIFT J1626.6–5156 was discovered in 2005 by *Swift*/BAT while it was showing series of short lived and intense flares (Krimm et al. 2005; Palmer et al. 2005). Since its discovery the system underwent type II and type I outbursts as well as the flares which are rare for among the

Be/X-ray transients (Belloni et al. 2006; Reig et al. 2008; Tarana et al. 2006). The neutron star in the system, revolving in an almost circular ($e=0.08$) and a 132.89 d orbit (Baykal et al. 2010, 2009) around its B0 Ve type companion (Reig et al. 2011) at a distance of ~ 15 kpc (Içdem et al. 2011), has a spin period of 15.38 s (Markwardt & Swank 2005). Using *RXTE*/PCA and HEXTE data, taken between 2005 December–2009 April, DeCesar et al. (2013) uncovered the presence of a CRSF at ~ 10 keV.

IGR J16327–4940: IGR J16327–4940 has listed in Bird et al. (2010) as an unidentified source with a peak flux of 1.59 ± 0.53 erg cm⁻² s⁻¹ in 20–40 keV energy band. Later, Masetti et al. (2010b) classified the source as a HMXB associated with an OB type emission line giant at a distance of ≈ 2 kpc. However due to the lack of the information about the system parameters we classified it as a candidate Be/X-ray binary.

AX J1700.2–4220: The X-ray source AX J1700.2–4220, discovered by *ASCA* satellite (Sugizaki et al. 2001), contains a 54.22 s pulsar (Markwardt et al. 2010) orbiting around its companion with a period of ~ 44 d (Corbet et al. 2010c). The emission line star HD 153295 was tentatively identified as the optical counterpart to the pulsar by Masetti et al. (2006d). However the refined position of AX J1700.2–4220 reveals that HD 153295 position is inconsistent with its coordinates (Markwardt et al. 2010). Although the nature of optical/IR counterpart to the system has not been realized yet the spin and orbital period measurements place the system among the Be/X-ray binaries in Corbet’s diagram (Corbet 1984).

IGR J17200–3116: The accretion powered 328.182 s pulsar (Nichelli et al. 2011) was first listed in *ROSAT* bright source catalog (Voges et al. 1996) then re-detected by *INTEGRAL*/IBIS during its Galactic-Center region survey with a flux of 1.6 ± 0.2 mCrab in 18–60 keV energy band (Revnivtsev et al. 2004). An emission line star was suggested as the optical counterpart to IGR J17200–3116 (Masetti et al. 2006c). Yet the system is known to be a persistent X-ray source neither the spectral class of the companion nor the orbital period of the system has been found yet (Krivonos et al. 2010b; Nichelli et al. 2011).

RX J1739.4–2942: It is suggested that this *ROSAT* source is identical with GRS

1736–297 (Motch et al. 1998), discovered by ART-P telescope aboard the *GRANAT* spacecraft in 1990 (Pavlinsky et al. 1992; Sunyaev 1990a), since it is located well within the 90° radius of the 90% confidence of GRANAT error circle. Although it has been previously classified as a LMXB (Wilson et al. 2003b, references therein), we categorize RX J1739.4–2942 as a candidate Be/X-ray binary owing to its identification with a Be star suggested by Motch et al. (1998). The last detected X-ray activity of the system of which average flux in 18–45 keV energy band was recorded as 4.4 mCrab was in 2006 (Grebenev et al. 2006).

IGR J17404–3655: This source was first mentioned in 3rd IBIS/ISGRI catalog of Bird et al. (2007) with an unidentified classification. Subsequent *Swift*/XRT and *CHANDRA* observations led the counterpart of IGR J17404–3655 to be discovered (Landi et al. 2008; Masetti et al. 2008b). An emission line star listed in USNO-A2.0 catalog (0525–28851523) was suggested as the optical companion (Masetti et al. 2009). Although Masetti et al. (2009) claims that IGR J17404–3655 is a LMXB it is likely a member of HMXB systems due to its hard X-ray spectrum (Tomsick et al. 2009).

AX J1749.1–2733: It was discovered during the Galactic survey of *ASCA* satellite between the years 1993 and 1999 (Sakano et al. 2002). Since its strong intrinsic absorption (Karasev et al. 2008) and the spectral properties which are similar to supergiant fast X-ray transient systems (Grebenev & Sunyaev 2007; Sguera et al. 2006) the classification of AX J1749.1–2733 has remained unclear until its spin and orbital periods have been determined. The system has a ~ 66 s pulsar which rotates around its B0-B3 type companion in a 185.5 d orbit (Heras et al. 2007; Zurita Heras & Chaty 2008) at a distance of 8-19.5 kpc (Karasev et al. 2010). The source is labeled as a candidate Be/X-ray system in the catalog since the spectral properties of the counterpart are still unclear.

AX J1749.2–2725: This highly absorbed, $N_H \approx 10^{23}$ cm $^{-2}$, ~ 220.4 s pulsar was discovered with *ASCA* in 1995 (Torii et al. 1998). The pulsation period of the source was also confirmed by the subsequent *ASCA* observations (Sakano et al. 2002). Kaur et al. (2010) and Karasev et al. (2010) individually suggested a high mass B-type star

as the optical counterpart to AX J1749.2–2725 using IR and optical data. However the system parameters and the spectral features of the companion have not been discovered yet.

GRO J1750–27: GRO J1750–27 was discovered by BATSE instrument on *CGRO* (Wilson et al. 1995b) during its ~ 30 mCrab outburst lasted ~ 60 days in 1995 (Scott et al. 1997). Due to its observed very large spin-up rate (38 pHz s^{-1} at peak) that is typically seen during type II outbursts of Be/X-ray systems and the correlation between the 4.45 s spin period and the 29.8 d orbital period, Scott et al. (1997) suggested the source to be a Be/X-ray binary. However no optical counterpart has been reported so far. The last X-ray outburst of the system, a giant outburst (Brandt et al. 2008; Kuulkers et al. 2008) with a total flux of $6.5 \times 10^{-9} \text{ erg cm}^{-2} \text{ s}^{-1}$ in 0.1–100 keV (Shaw et al. 2009), was detected by *Swift*/BAT in 2008 (Krimm et al. 2008b).

AX J1820.5–1434: This candidate Be/X-ray system was discovered during the ASCA Galactic plane survey in 1997. A coherent pulsation at a period of 152.26 s in the 2–10 keV energy band was reported by Kinugasa et al. (1998). They suggested the source to be a highly obscured accretion-driven X-ray pulsar on the Scutum arm due to its high N_H value and the X-ray spectral properties. A 17.33 mag (in R) emission line star was identified as the optical counterpart in the error circle of the pulsar by (Israel et al. 2000b, references therein). However it was not confirmed by the further investigations. In addition possible different 2MASS counterparts; a bright star in NIR and a B type star with $H\alpha$ absorption line were also suggested by Kaur et al. (2010) and Negueruela & Schurch (2007) respectively. Despite the nature of the optical companion has still been uncertain the study of Segreto et al. (2013), including all available *Swift*/BAT data related, revealed the orbital parameter to be 54 d that placed the system among the Be/X-ray systems in the Corbet diagram (Corbet 1984).

IGR J18219–1347: The source was first mentioned in *INTEGRAL*/IBIS 7-year All-Sky Hard X-Ray Survey as an unclassified source having a flux of $7.1 \pm 0.13 \times 10^{-12} \text{ erg cm}^{-2} \text{ s}^{-1}$ in 17–60 energy band (Krivonos et al. 2010b). Follow-up *Swift*/XRT observations revealed the association with an XMM Slew Survey source XMMSL1 J182155.0–134719 and a 2MASS source located in the XMM error box (Landi et al.

2011). A transient X-ray activity having ~ 25 times of the previously reported flux in (Krivonos et al. 2010b) was detected with *Swift*/BAT (Krimm et al. 2012e). No confirmed optical or IR counterpart has been found so far Karasev et al. (2012). On the other hand La Parola et al. (2013a) suggested a orbital period of 72.44 d using 88-month BAT survey data. Due to the longness of the orbital period and the transient X-ray nature the system classified as a candidate Be/X-ray binary.

IGR J18406–0539: This source was discovered during a hard X-ray survey of the Sagittarius arm tangent region by *INTEGRAL* in 2003 (Molkov et al. 2004a). The emission line B5 V type star SS 406 was suggested to be a probable counterpart to IGR J18406–0539 (Masetti et al. 2006b). However, Negueruela & Schurch (2007) reclassified this source as a chemically peculiar star and also claimed the possibility of a binary with two unevolved stars which made the Be/X-ray binary classification dubious. Likewise the suggestion of association with the previously suggested candidate radio counterpart NVSS J180437–05317 was also failed after the searching of *INTEGRAL* error box by Pandey et al. (2007). As the nature of the companion has not been classified yet we have placed the system as a candidate Be/X-ray in our catalog.

GS 1843+009: The hard X-ray source GS 1843+009 was discovered in 1988 near the Scutum region during the Galactic Plane Scan observations of *GINGA* satellite (Makino & *GINGA* Team 1988b,e). The system, consisting of a B0–2 IV–Ve type emission line star (Israel et al. 2001) and a 29.5 s pulsar (Koyama et al. 1990; Makino & *GINGA* Team 1988e), underwent several type I and type II outbursts since its discovery (Cherepashchuk et al. 2003; Krimm et al. 2006, 2009d; Piraino et al. 2000). Using the IBIS/ISGRI data, taken at different epochs during the hard X-ray outbursts of the system in 2004, Seifina (2007) found the orbital period of source to be 160 d.

2S 1845–024: The recurrent hard X-ray source 2S 1845–024 has been one of the poorly studied Be/X-ray systems although it was first detected by *ARIEL 5* satellite with a designation of in 1974 A 1845–02 in 1974 (Villa et al. 1976). Later using *CGRO*/BATSE and *RXTE*/ASM data Zhang et al. (1996) and Soffitta et al. (1998) showed that the system underwent regular outbursts separated by 241 days and lasted about 13 days. The association of the source with GRO 1849–03, A 1845–02 and

with GS 1843–02 than became clear. The system includes a 94.8 s pulsar (Makino & GINGA Team 1988a) rotating at a highly eccentric ($e=0.88$) binary orbit about a massive companion (Finger et al. 1999). The last outburst of the system, reached a peak flux of ~ 40 mcrab, was detected by *Swift*/BAT monitor in August, 2012 (Krimm et al. 2012b). Indeed the orbital parameters and the outburst behavior of the source suggest a Be type companion it has not been confirmed spectroscopically yet.

XTE J1858+034: The hard X-ray transient XTE J1858+034 was discovered with *RXTE*/ASM during its outburst in 1998 (Remillard et al. 1998). Subsequent observations with ASM showed that the system has a ~ 221 s pulsar (Takeshima et al. 1998) having a QPO feature at a frequency of 0.11 Hz in its light curve (Paul & Rao 1998). Since its discovery three more outbursts one of which reached a peak flux of 50 mCrab in 15–50 keV energy band were detected (Krimm et al. 2010c; Molkov et al. 2004b; Sootome et al. 2011a). Besides Mukherjee et al. (2006) detected additional QPOs in the frequency range of 0.14–0.185 Hz in *RXTE*/PCA observations during the second outburst of the system in May 2004. Indeed the pulsations and the transient nature of the outbursts suggest a Be/X-ray binary no detailed spectral confirmation related to the optical companion has been appeared yet although Reig et al. (2004a) proposed a 18 mag. emission line star consistent with the coordinates of IBIS/ISGRI.

XTE J1859+083: This transient 9.8 s X-ray source was first detected with *RXTE*/PCA in 1999 during its outburst with a peak flux of 2×10^{-10} erg cm $^{-2}$ s $^{-1}$ (Marshall et al. 1999). *Swift*/XRT observations of the field of XTE J1859+083 was reported by Romano et al. (2007) that no X-ray detection up to 5×10^{-14} erg cm $^{-2}$ s $^{-1}$ was detected. Using *RXTE*/ASM data cover 12 year time interval Corbet et al. (2009) suggested that the system showed an extended type II outburst between 1996 June–1997 January and found a possible orbital modulation of 60.65 days. The transient nature of the source and the correlation between the orbital and spin period suggest a Be/X-ray binary even though its optical companion has not been discovered yet.

4U 1901+03: The X-ray source 4U 1901+03 which was located in Aquila-Serpens-Scutum region was first listed in 2nd *UHURU* catalog of Giacconi et al. (1972) with the designation of 2U 1907+02. The third catalog of the same satellite also included

the source having a peak intensity of 1.48×10^{-9} erg cm $^{-2}$ s $^{-1}$ in 2–6 keV band (Giaccconi et al. 1974). After a ~ 40 year X-ray quiescence phase the system underwent a new outburst, reaching a peak flux of ~ 240 mCrab in 2.5–25 keV, was detected with both *RXTE* and *INTEGRAL* (Galloway et al. 2003a,b, 2005; Molkov et al. 2003). Using the archival *RXTE*/PCA data James et al. (2011) revealed the presence of several flares, a broadening of spin frequency peak and a QPO at ~ 0.135 Hz. The system has an X-ray pulsar with a spin period of 2.76 s rotating around its companion in a nearly circular ($e = 0.036$) 22.58 days orbit (Galloway et al. 2005). The last detected X-ray activity of 4U 1901+03 was in 2011 (Jenke & Finger 2011; Sootome et al. 2011b). Since no optical or IR counterpart has been found for this source we classify 4U 1901+03 as a candidate Be/X-ray binary.

IGR J19294+1816: The transient X-ray system IGR J19294+1816 was discovered with IBIS/ISGRI during the observations of the field around GRS 1915+10 while it was undergoing a giant outburst in 2009 (Turler et al. 2009). The analysis of archival *Swift*/XRT data gave its refined position with a name of SWIFT J1929.8+1821 (Rodriguez et al. 2009c). The archival *Swift*/BAT light curves also revealed that the source showed a bright outburst with a peak flux of 25 mCrab in 15–50 keV energy band in 2008 Krimm et al. (2009a). The spin period of the neutron star is 12.44 s (Rodriguez et al. 2009a; Strohmayer et al. 2009) and the orbital period of the system is 117 d (Corbet & Krimm 2009). Rodriguez et al. (2009c) suggested that the spin and the orbital period would well fit the system in the population of Be/X-ray binaries in the Corbet diagram (Corbet 1984) yet they also noticed the possibility of being a SFXT due to its short and intense X-ray flares. Analyzing the *INTEGRAL* and *Swift* observations of IGR J19294+1816 after the 2010 outburst Bozzo et al. (2011) confirmed the idea that the system should be a member of the Be/X-ray binaries rather than a SFXT. In addition periodicity of the last two X-ray activity in 2012 and 2013, consisting with the time of periastron passage of the neutron star, are also typical for the type I outbursts indicative of a Be/X-ray binary (Drave et al. 2013; Fiacchi et al. 2012, 2013; Sidoli et al. 2012a).

1H 1936+541: This source was first listed in *HEAO* A-1 X-ray source catalog of Wood et al. (1984). It has not been observed any X-ray telescopes since its discovery

(Torrejón & Orr 2001). The system parameters have not been known either. A 9.8 mag. Be star DM +53 2262 (Wackerling 1970) appears as the optical counterpart of 1H 1936+541 although no related references can be found in the literature. The suggested optical counterpart of the system was observed at TUG between 2008–2014. The spectra of the source shows significant $H\alpha$ and $H\beta$ emissions as seen in Be type stars. We therefore classify 1H 1936+541 as a Be/X-ray binary candidate due to the lack of the information of system parameters.

XTE J1946+274: The hard X-ray transient XTE J1946+274 was discovered by *RXTE*/ASM during a scan of the Vul-Cyg region in 1998 (Smith & Takeshima 1998). Subsequent observations of *CGRO*/BATSE detected the source showing a strong pulsation of 15.8 s (Wilson et al. 1998b). The system includes a B0-1 IV-V type emission line star (Verrecchia et al. 2002) at a distance of 8–10 kpc. Wilson et al. (2003a) showed that the system underwent 13 outbursts between 1998 September and 2001 June which were not locked in orbital phase and seen in two pairs per orbit (~ 169.2 days). Investigating the $H\alpha$ line profiles, they also revealed that a density perturbation occurred in the decretion disk of the mass donor star as the X-ray outbursts ceased. The existence of a CRSF near 35 keV was also reported by Heindl et al. (2001). After ~ 9 years quiescence, the system was again in X-ray active phase in 2010 June (Krimm et al. 2010d; Müller et al. 2012).

KS 1947+300: KS 1947+300 is a recurrent hard X-ray transient first detected with a peak flux of 70 ± 10 mCrab in 2–27 keV (Borozdin et al. 1990) in 1989 by TTM coded-mask X-ray spectrometer on board the Kvant module of the *Mir* Space Station during the observations of GS 2023+338 region. Later in 1994, it was shown that a newly discovered *CGRO* source designated as GRO J1948+32, detected with a strong pulsation of 18.7 s (Chakrabarty et al. 1995) was identical to KS 1947+300 (Swank & Morgan 2000). The system was active again in between 2000 and 2001 including one giant and several normal outbursts (Galloway et al. 2004; Levine & Corbet 2000). James et al. (2010) reported the presence of a low-frequency QPO at 0.02 Hz during the decline of 2001 outburst indicative of an accretion disk. In addition, for the first time evidence of a glitch in an accretion-powered pulsar was uncovered (Galloway et al. 2004). The optical companion was identified by Negueruela et al. (2003) as a

B0 type emission line star. The latest active state of the system started in September 2013 and continued till August 2014 which was observed by several X-ray satellites and ground-based telescopes (Kawagoe et al. 2013a; Kennea et al. 2013; Kuehnel et al. 2014; Ozbey-Arabaci et al. 2014)

SWIFT J2000.6+3210: SWIFT J2000.6+3210 is a transient X-ray pulsar with a 1056 s period discovered with *Swift*/BAT during its hard X-ray survey between December 2004–March 2005 (Morris et al. 2009; Tueller et al. 2005). The companion is an emission line B type star ($EW \sim -10.2 \text{ \AA}$) at a distance of ≈ 8 kpc (Halpern 2006; Masetti et al. 2008a). The source has also existed in 4th *INTEGRAL* Catalog (Bird et al. 2010) with a mean flux of 2.2 ± 0.2 mCrab and 2.0 ± 0.3 mCrab in 20–40 keV and 40–100 keV energy bands respectively. Analyzing *Suzaku* and *Swift*/XRT observations Pradhan et al. (2013) suggested that the system had the same properties as persistent Be/X-ray binaries and had the spin period of ~ 890 s rather than 1056 s suggested previously by Morris et al. (2009).

EXO 2030+375: EXO 2030+375 has been one of the best studied Be/X-ray binaries since its discovery with *EXOSAT* during its giant outburst ($L_x \gtrsim 10^{38} \text{ erg s}^{-1}$) in 1985 (Parmar et al. 1985, 1989b). Using *RXTE*/ASM and *CGRO*/BATSE observations Wilson et al. (2002) revealed the detections of 71 outbursts majority of which occurred near or close to the periastron passage of the neutron star. Detailed analysis of the first giant outburst of the source indicate that the pulse period change, energy spectrum and pulse profile are strongly related to the luminosity (Parmar et al. 1989a; Reynolds et al. 1993). The system shows X-ray active and inactive phases which are commonly seen in Be/X-ray binaries. The second giant outburst of the system occurred in 2006 and detected by several X-ray observatories (Corbet & Levine 2006; Klochkov et al. 2008; Wilson & Finger 2006). The system has a ~ 42 s X-ray pulsar and a BO Ve type highly reddened optical companion (Baykal et al. 2008; Janot-Pacheco et al. 1988; Motch & Janot-Pacheco 1987) at a distance of 7.1 kpc (Wilson et al. 2002).

GRO J2058+42: GRO J2058+42, a transient 198 s pulsar, was discovered during its giant outburst in 1995 by BATSE instrument on *CGRO* (Wilson et al. 1995a). Fol-

lowing the giant outburst five small outbursts separated by ~ 110 days were detected by BATSE while *RXTE*/ASM data detected these outbursts with ~ 55 day interval which was later attributed to the orbital period of the system (Corbet et al. 1997; Wilson et al. 2005). The optical companion is an 09.5–B0 IV–Ve type star showing double-peaked $H\alpha$ emission line profiles even before and after the X-ray active phase (Kiziloglu et al. 2008; Reig et al. 2005b). GRO J2058+42 is one of the four Be/X-ray binaries showing NRPs (Kızılođlu et al. 2007). The system has been in X-ray quiescent state since 2008.

SAX J2103.5+4545: Having a ~ 12.7 d orbital period (Baykal et al. 2000) and a 358.6 s spin period (Hulleman et al. 1998) SAX J2103.5+4545 is one of the unusual Be/X-ray binaries that falls in wind-fed supergiant region of Corbet’s diagram (Corbet 1984). It includes a B0V type emission line star (Reig & Mavromatakis 2003; Reig et al. 2004b) exhibiting disk-loss and disk-renewal phases which last $\lesssim 2$ yr. In addition the long-term optical and X-ray data analyses of the system indicate a correlation between the strength and shape of $H\alpha$ line profile and the X-ray outbursts as well as the IR magnitudes (Camero et al. 2014; Reig et al. 2010a). Since its discovery in 1997 with *BeppoSAX* X-ray observatory SAX J2103.5+4545 has been observed several times in X-ray outburst (Baykal et al. 2000; Blay et al. 2004; Galis et al. 2007; Kiziloglu et al. 2010; Krimm et al. 2010a). İnam et al. (2004) reported the existence of transient QPOs around 0.044 Hz in *RXTE* data taken between 2002 December–2003 January. The system was in X-ray and optical active phase in June 2012 and May 2014 (Camero-Arranz et al. 2012b, 2014b; Ducci et al. 2014; Sguera et al. 2012).

IGR J21347+4737: IGR J21347+4737 was first listed in the soft gamma-ray survey catalog of Bird et al. (2007) as an unidentified source. Subsequent observations both performed with *INTEGRAL* and *CHANDRA* satellites showed that the source had a transient nature (Bikmaev et al. 2008; Krivonos et al. 2007; Sazonov et al. 2008). The optical companion of the system is a B1Ve type shell line star, locating at a distance of 8.5 kpc, shows $H\alpha$ absorption and emission features in its spectra indicative of the decretion disk formation and dissipation (Masetti et al. 2009; Reig & Zezas 2014a). Recently Reig & Zezas (2014b) showed that the system has a 320.5 s pulsar.

GS 2138+56: Transient X-ray pulsar GS 2138+56 (Cep X-4) was first detected by UCSD on OSO-7 satellite in 1972 (Ulmer et al. 1973). It was in quiescence phase until a coherent pulsation of 66.25 s was discovered during its ~ 100 mCrab outburst in 1988 by *GINGA* (Makino & GINGA Team 1988c,d). A cyclotron resonance feature at about 30.5 keV was detected by Mihara et al. (1991) and confirmed by McBride et al. (2007) using the data of 2002 outburst performed with *RXTE*. The optical companion is a Be star at a distance of 3.8 kpc (Bonnet-Bidaud & Mouchet 1998). The last activity of the source was detected with *MAXI/GSC* and *Swift/BAT* in 2014 during which the optical companion showed strong $H\alpha$ emission in its spectrum (Evans et al. 2014; Nakajima et al. 2014; Ozbey-Arabaci et al. 2014).

1H 2202+501: This source has been identified as a Be/X-ray binary in 4th HMXB Catalog of Liu et al. (2006). It was also listed as an X-ray source in *HEAO A-1* catalog of Wood et al. (1984) with a flux of 1.48×10^{-11} erg cm $^{-2}$ s $^{-1}$ in the 2–10 keV energy band. 1H 2202+501 has been associated with an emission line star BD +49 3718 (Tuohy et al. 1988) though IR spectroscopy of the source reveals that it must be a peculiar K type star (Harlaftis et al. 2001). Yet it has not been detected or observed any X-ray satellite so far. Since the nature of the system has not been confirmed we classify this source as a candidate Be/X-ray binary.

SAX J2239.3+6116: It was discovered with *BeppoSAX/WFC* during its weak outburst in 1997 (in't Zand et al. 2000). Searching of archival *RXTE/ASM* data showed that the system underwent five type I outbursts separated by 262 days pretended as the orbital period. The system have an X-ray pulsar with a spin period of 1247 s, orbiting around it B0–2 III–Ve type massive companion. The distance to the system is known to be 4.4 kpc based on its photometrical observations (in't Zand et al. 2001b).

IGR J22534+6234: The source was first mentioned in *INTEGRAL/IBIS* 9-year Galactic Hard X-ray Survey of Krivonos et al. (2012). Subsequent follow-up observations with *Swift/XRT* revealed the association both with a low-luminosity hard X-ray ROSAT source 1RXS J225352.8+624352 and a USNO-B1/2MASS source (Landi et al. 2012; Suchkov & Hanisch 2004). The source has a B 0–1 III–V type emission line star and a ~ 47 s pulsar (Esposito et al. 2013). The optical companion has strong

emission of $H\alpha$ line showing variations in strength in a half year (Lutovinov et al. 2013). Due to lack of information on the orbital parameters and X-ray nature we cataloged the source as a candidate Be/X-ray binary.

Table 2.1: Catalogue of Be/X-ray binaries and Candidates in the Galaxy.

ID	Name	Optical Companion	RA (J2000)	DEC (J2000)	Spectral Type	<i>B</i>	<i>V</i>	<i>R</i>	<i>I</i>	<i>J</i>	<i>H</i>	<i>K</i>	Ref.**
1	4U 0115+634	V635 Cas	01:18:31.9	+63:44:24.0	B0.2 Ve	16.9	15.5	14.6	13.5	12.6	12.9	11.9	1,2
2	IGR J01363+6610	[KW 97] 6–30	01:35:50.0	+66:12:40.0	B1 IV–Ve	14.7	13.3	12.3	11.4	10.0	9.6	9.1	3, 4
3	RX J0146.9+6121	V831 Cas	01:47:00.2	+61:21:23.7	B1 III–Ve	12.1	11.5	11.0	10.4	9.8	9.6	9.4	5,6
4	IGR J01583+6713	—	01:58:18.4	+67:13:23.5	B2 IVe	15.0	14.4	13.2	12.1	11.5	—	—	7, 8, 9,10
5	EXO 0331+530	BQ Cam	03:34:59.9	+53:10:24.0	O8–9 Ve	17.3	15.7	14.2	13.0	11.4	11.2	10.8	10, 11, 12
6	4U 0352+309	HD 24534	03:55:23.1	+31:02:45.0	O9.5 IIIe–B0 Ve	6.8	6.1–6.8	6.5	6.4	5.2–6.2	5.0–6.1	4.8–6.7	13, 14, 15, 16, 17
7	RX J0440.9+4431	LS V +44 17	04:40:59.3	+44:31:49.3	B0.2 Ve	11.4	10.8	10.3	9.9	9.4	9.1	9.0	18, 19
8	A 0535+262	V725 Tau	05:38:54.6	+26:18:57.0	O9.7–B0 IIIe	9.5	8.9	8.4	7.9	8.4	8.3	8.2	10, 16, 20, 21, 22
9	IGR J06074+2205	—	06:07:26.6	+22:05:48.0	B0.5 Ve	12.7	12.3	11.3	10.2	10.5	10.2	10.0	23, 24
10	SAX J0635.2+0533	—	06:32:38.1	+05:35:34.3	B1–2 III–Ve	13.8	12.8	12.0	—	—	—	—	25
11	XTE J0658–073	S100221212	06:58:17.3	–07:12:35.3	O9.5 Ve	13.2	12.4	11.4	—	9.7	9.3	9.0	16, 26, 27, 28, 29
12	4U 0726–260	V441 Pup	07:28:53.6	–26:06:29.0	O8–9 Ve	11.9	11.6	11.1	10.7	10.4	10.1	9.8	10, 16, 30, 31
13	1H 0739–529	HD 63666	07:47:23.6	–53:19:56.9	B7 IV–Ve	7.6	7.6	—	—	7.5	7.4	7.4	32, 33, 34
14	RX J0812.4–3114	LS 992	08:12:28.4	–31:14:21.0	B0.2 III–Ve	12.9	12.5	12.2	11.7	11.5	11.3	11.0	10, 35, 36
15	GS 0834–430	—	08:35:55.4	–43:11:11.9	B0–2 III–Ve	—	20.4	18.2	—	13.3	12.3	11.4	37
16	GRO J1008–57	—	10:09:46.9	–58:17:35.5	B1-2e	17.0	15.3	14.2	12.9	11.3	10.5	9.9	38, 39, 40
17	RX J1037.5–5647	LS 1698	10:37:35.2	–56:47:59.0	B0 III–Ve	12.8	11.3	11.0	—	—	—	—	16, 35, 41
18	1A 1118–615	Hen 3–640	11:20:57.2	–61:55:00.0	O9.5 IV–Ve	13.1	12.1	—	—	9.6	9.1	8.6	10, 42, 43, 44
19	IGR J11305–6256	HD 100199	11:31:06.9	–62:56:48.9	B0 IIIe	8.2	8.2	8.2	8.2	8.0	8.1	8.0	24, 45, 46, 47, 48
20	IGR J11435–6109	—	11:44:00.3	–61:07:36.5	B0 Ve	17.7	16.4	15.4	14.8	12.9	12.2	11.8	49, 50, 51
21	4U 1145–619	V801 Cen	11:48:00.0	–62:12:24.9	B1 Ve	9.5	9.3	—	—	8.6	8.3	8.0	10, 52, 53, 54, 55
22	1ES 1210–646	—	12:13:14.8	–64:52:30.5	B5 V	18.1	—	13.9	—	—	—	—	56, 57
23	1H 1255–567	HD 112091	12:54:36.9	–57:10:07.0	B5 Ve	5.1	5.2	—	—	5.3	5.4	5.3	10, 16, 58, 59, 60

Table 2.1: continued.

ID	Name	Optical Companion	RA (J2000)	DEC (J2000)	Spectral Type	<i>B</i>	<i>V</i>	<i>R</i>	<i>I</i>	<i>J</i>	<i>H</i>	<i>K</i>	Ref.**
24	4U 1258–613	V850 Cen	13:01:17.1	–61:36:07.0	B2 Vne	15.5	13.7	12.6	11.4	9.8	9.3	9.0	10, 16, 61, 62
25	IGR J13020–6359	—	13:01:58.7	–63:58:09.0	B0.5 Ve	—	19.7	17.7	16.1	13.0	12.1	11.4	47, 60
26	IGR J13186–6257	—	13:18:36.0	–62:56:48.0	—	17.9	—	15.8	—	13.6	12.7	12.8	16, 63
27	SAX J1324–6200	—	13:24:26.3	–62:00:53.0	—	—	—	—	—	—	—	14.4	10, 64
28	4U 1416–62*	—	14:21:12.2	–62:41:56.1	B1 Ve	18.6–19.3	~16.9	—	—	13.3	12.7	12.3	10, 65
29	IGR J14331–6112*	—	14:33:08.3	–61:15:39.7	B IIIe/mid B Ve	—	—	18.1	—	14.7	14.0	13.8	60, 66
30	IGR J14488–5942	—	14:48:49.0	–59:42:06.0	—	—	—	—	—	—	—	—	67
31	XTE J1543–568	—	15:44:05.2	–56:45:42.6	—	—	—	—	—	14.3	13.3	12.8	68
32	2S 1553–542	—	15:57:49.0	–54:24:54.0	Be	—	—	—	—	—	—	—	69
33	1H 1555–552	HD 141926	15:54:21.8	–54:19:44.8	B2 nne	9.2	8.6	—	—	7.1	6.8	6.5	10, 16, 70, 71, 72
34	SWIFT J1626.6–5156	—	16:26:36.5	–51:56:30.5	B0 Ve	16.8	15.5	15.8	14.3	13.4	13.0	12.5	73
35	IGR J16327–4940	—	16:32:39.9	–49:42:13.8	OB IIIe	—	—	15.5	—	—	—	—	74
36	AX J1700.2–4220	—	17:00:19.3	–42:20:19.2	—	—	—	—	—	—	—	—	75
37	IGR J17200–3116	—	17:20:05.9	–31:16:59.7	—	~19	—	—	16.2	13.6	12.3	12.0	16, 76, 77
38	RX J1739.4–2942	—	17:39:30.0	–29:42:08.9	Be	—	—	—	—	—	—	—	78
39	IGR J17404–3655	—	17:40:26.9	–36:55:37.4	—	18.8	—	17.3	—	—	—	14.3	51, 56, 63
40	AX J1749.1–2733	—	17:49:06.9	–27:32:32.9	B1–3	—	—	21.9	20.9	17.4	16.7	15.8	79, 80
41	AX J1749.2–2725	—	17:49:12.4	–27:25:38.3	B3	—	—	—	—	18.6	16.6	15.0	79
42	GRO J1750–27	—	17:49:12.7	–26:38:36.0	—	—	—	—	—	—	—	—	10, 81
43	AX J1820.5–1434	—	18:20:29.5	–14:34:24.0	Be	—	—	—	—	—	—	—	82
44	IGR J18219–1357	—	18:21:54.8	–13:47:26.7	—	—	—	—	—	—	—	—	83, 84
45	IGR J18406–0539	—	18:40:47.0	–05:46:51.0	—	—	—	—	—	—	—	—	85
46	GS 1843+009	—	18:45:36.8	+00:51:48.3	B0–2 IV–Ve	>24.1	20.6	18.6	16.8	13.8	13.2	—	86
47	2S 1845–024	—	18:48:17.7	–02:25:13.0	—	—	—	—	—	—	—	—	87

Table 2.1: continued.

ID	Name	Optical Companion	RA (J2000)	DEC (J2000)	Spectral Type	<i>B</i>	<i>V</i>	<i>R</i>	<i>I</i>	<i>J</i>	<i>H</i>	<i>K</i>	Ref.**
48	XTE J1858+034	—	18:58:36.0	+03:26:09.0	—	19.6	18.0	16.9	15.4	—	—	—	3
49	XTE J1859+083	—	18:59:06.0	+04:15:00.0	—	—	—	—	—	—	—	—	88
50	4U 1901+03	—	19:03:33.0	+03:12:24.0	—	—	—	—	—	—	—	—	89
51	IGR J19294+1816	—	19:29:55.9	+18:18:39.0	—	—	—	—	—	—	—	—	90
52	1H 1936+541*	DM +53 2262	19:32:52.3	+53:52:45.0	—	10.4	9.8	—	—	10.2	10.2	10.0	91, 92
53	XTE J1946+274	—	19:45:39.3	+27:21:55.4	B0–1 IV–Ve	18.6	16.9	15.3	13.3	12.7	12.1	11.6	93, 94
54	KS 1947+300*	—	19:49:30.5	+30:12:24.0	B0 Ve	15.0	14.1	13.5	12.8	11.8	11.4	11.1	10, 95, 96, 97
55	SWIFT J2000.6+3210	—	20:00:21.9	+32:11:23.2	BVe/mid BIIIe	17.1	—	16.1	14.4	12.0	11.3	10.9	66, 98
56	EXO 2030+375	V2246 Cyg	20:32:15.2	+37:38:15.1	B0 Ve	23.0	19.7	17.6	14.0	11.9	10.6	9.8	99, 100, 101, 102
57	GRO J2058+42	—	20:58:47.5	+41:46:37.0	O9.5–B0 IV–Ve	16.1	14.9	14.2	13.4	11.7	11.3	10.9	10, 103, 104
58	SAX J2103.5+4545	—	21:03:35.7	+45:45:04.0	B0 Ve	15.6	14.6	13.7	12.9	11.8	11.5	11.3	105, 106, 107
59	IGR J21347+4737	—	21:34:20.4	+47:38:00.2	B1 IVe	14.7	14.1	13.8	13.4	—	—	—	56, 108
60	GS 2138+56	V490 Cep	21:39:30.6	+56:59:12.9	B1–2 Ve	15.7	14.3	14.5	—	11.8	11.4	10.9	10, 97, 109
61	1H 2202+501	DM +493718	22:01:38.2	+50:10:05.0	Be?	9.0	8.8	—	—	8.8	8.7	8.5	10, 110, 111
62	SAX J2239.3+6116*	—	22:39:20.9	+61:16:26.8	B0–2 III–Ve	16.5	15.1	14.1	—	11.5	11.0	10.6	112
63	IGR J22534+6234*	—	22:53:55.1	+62:43:36.8	B0–1 III–Ve	17.4	17.6	13.7	—	11.6	11.0	10.5	113, 114

(*) *J*, *H*, *K* magnitudes of these source are taken from the Two Micron All Sky Survey (Cutri et al. 2003, 2MASS) based on the information and the coordinates given in Grindlay et al. (1984), Masetti et al. (2008a), and/or in Zand et al. (2001b) respectively.

(**) References: (1) Kholopov et al. (1981); (2) Reig et al. (2007); (3) Reig et al. (2005b); (4) Tomsick et al. (2011); (5) Reig et al. (1997b); (6) Reig et al. (2000); (7) Halpern & Tyagi (2005a); (8) Kaur et al. (2008b); (9) Masetti et al. (2006a); (10) Liu et al. (2006); (11) Negueruela et al. (1999); (12) Kaur et al. (2008a); (13) Slettebak (1982); (14) Oja (1991); (15) Telting et al. (1998); (16) Cutri et al. (2003); (17) Mathew et al. (2013); (18) Motch et al. (1997); (19) Reig et al. (2005a); (20) Steele et al. (1998); (21) Giovannelli & Graziati (1992); (22) Janot-Pacheco et al. (1987); (23) Reig et al. (2010b); (24) Tomsick et al. (2008); (25) Kaaret et al. (1999); (26) MacConnell (1981); (27) Pakull et al. (2003); (28) Nespoli et al. (2012); (29) McBride et al. (2006); (30) Hardorp et al. (1959); (31) Negueruela et al. (1996); (32) MacConnell (1982); (33) Perryman et al. (1997); (34) Coe et al. (1997); (35) Motch et al. (1996); (36) Reig et al. (2001); (37) Israel et al. (2000a); (38) Coe et al. (1997); (39) Coe et al. (2007); (40) Coe et al. (1994a); (41) Sarty et al. (2011); (42) Chevalier & Ilovaisky (1975); (43) Janot-Pacheco et al. (1981); (44) Coe et al. (1994b); (45) Perryman et al. (1997); (46) Negueruela & Schurch (2007); (47) Masetti et al. (2006e); (48) Fernie (1983); (49) Tomsick et al. (2007); (50) Negueruela et al. (2007); (51) Coleiro et al. (2013); (52) Okazaki & Negueruela (2001a); (53) Dower et al. (1978); (54) Chevalier & Ilovaisky (1998); (55) Stevens et al. (1997); (56) Masetti et al. (2009); (57) Monet & et al. (1998); (58) Slettebak (1982); (59) Levenhagen & Leister (2006); (60) Maccarone et al. (2014); (61) Parkes et al. (1980); (62) Haefner (1988); (63) Tomsick et al. (2009); (64) Mereghetti et al. (2008); (65) Grindlay et al. (1984); (66) Masetti et al. (2008a); (67) Bird et al. (2010); (68) Krimm et al. (2012a); (69) Apparao et al. (1978); (70) Reed & Beatty (1995); (71) Grillo et al. (1992); (72) Torrejón & Orr (2001); (73) Reig (2011); (74) Masetti et al. (2010b); (75) Markwardt et al. (2010); (76) Masetti et al. (2006c); (77) Epchtein et al. (1994); (78) Motch et al. (1998); (79) Karasev et al. (2010); (80) Zurita Heras & Chaty (2008); (81) Wilson et al. (1995b); (82) Kinugasa et al. (1998); (83) Krivonos et al. (2010b); (84) Karasev et al. (2012); (85) Molkov et al. (2004a); (86) Israel et al. (2001); (87) Ebisawa et al. (2003); (88) Marshall et al. (1999); (89) Galloway et al. (2003a); (90) Rodriguez et al. (2009c); (91) Wackerling (1970); (92) Høg et al. (2000); (93) Wilson et al. (2003a); (94) Verrecchia et al. (2002); (95) Riquelme et al. (2012); (96) Negueruela et al. (2003); (97) Ozbey-Arabaci et al. (2014); (98) Halpern (2006); (99) Baykal et al. (2008); (100) Reig et al. (1998); (101) Motch & Janot-Pacheco (1987); (102) Janot-Pacheco et al. (1988); (103) Wilson et al. (2005); (104) Wilson et al. (1998a); (105) Camero et al. (2014); (106) Reig & Mavromatakis (2003); (107) Reig et al. (2004b); (108) Reig & Zezas (2014a); (109) Bonnet-Bidaud & Mouchet (1998); (110) Tuohy et al. (1988); (111) Wackerling (1970); (112) in't Zand et al. (2001b); (113) Esposito et al. (2013); (114) Masetti et al. (2013)

Table 2.2: Be/X-ray binaries and Candidates in the Galaxy.

ID	Name	E(B-V)	A_V	e	d (kpc)	P_{orb} (d)	P_{spin} (s)	H α (max.) (-Å)	H β (max.) (-Å)	F_X (peak) (mCrab)	Note	Ref.**
1	4U 0115+634	1.65	4.8	0.34	7–8	24.31	3.6	23	—	~1900 (6–12 keV)	I, II, F, V/R, NRP	1, 2, 3, 4, 5, 6
2	IGR J01363+6610	1.61	5.0	—	~2	159	—	54	—	17 (17–45 keV)	I	7, 8, 9, 10
3	RX J0146.9+6121	0.93	2.9	—	2.3	~330	1412	18.1	1.6	~100 (2–10 keV)	I, P, V/R, NRP	11, 12, 13
4	IGR J01583+6713	1.46	4.5	—	4.0	—	—	75	6.4	14 (20–40 keV)	I	14, 15, 16
5	EXO 0331+530	1.87	6.2	0.31	~7	34.25	4.4	10.4	3.9	1600 (3–12 keV)	I, II	17, 18, 19, 20, 21, 22
6	4U 0352+309	0.39	1.2	0.11	0.95	250.30	837	23.8	—	50 (2–10 keV)	F, P, V/R	13, 23, 24, 25, 26, 27
7	RX J0440.9+4431	0.65	~2.0	—	~3.3	~155	202.5	9.3	0.5	240 (4–10 keV)	I, P, V/R	28, 29, 30, 31
8	A 0535+262	0.75	2.33	0.47	2	110.2	~104	30	3.2	8000 (20–40 keV)	I, II, F, V/R	32, 33, 34, 35, 36, 37, 38, 39
9	IGR J06074+2205	0.84	2.6	—	~4.5	—	—	12.8*	—	~15 (10–20 keV)	V/R	40, 41
10	SAX J0635.2+0533	1.20	3.8	0.29	2.5–5	11.2	0.03	30.3	3.2	—	msP	42, 43
11	XTE J0658–073	1.14	3.7	—	3.9	101.50	160.7	25.41	3.8	200 (2–12 keV)	I, II, F	44, 45, 46, 47, 48
12	4U 0726–260	0.73	2.3	—	6.1	34.46	103.2	9.0	0.7	10 (2–60 keV)	F	49, 50, 51
13	1H 0739–529	0.10	0.3	—	0.5	—	—	—	—	—	C	52
14	RX J0812.4–3114	0.65	2.0	—	~8.8	~80	31.9	20.5	2.2	10 (2–60 keV)	I, V/R	53, 54, 55, 56
15	GS 0834–430	4.0	13.2	0.10–0.17	3–5	105.80	12.3	33	—	1000 (5–15 keV)	I, II	57, 58, 59, 60, 61
16	GRO J1008–57	2.00	6.2	0.68	5	247.8	93.6	26	1.7	1400 (20–50 keV)	I, II, F, V/R	11, 62, 63, 64, 65
17	RX J1037.5–5647	~0.75	2.3	—	5	61	860	1.5	—	30 (15–50 keV)	I, P	36, 66, 67, 68
18	1A 1118–615	0.90	2.8	—	5	24	405	~107.3	7.1	500 (15–50 keV)	II, F	69, 70, 71, 72, 73, 74, 74, 76
19	IGR J11305–6256	0.31	~1	—	~3	120.83	—	7.9	0.4	8 (20–60 keV)	P	77, 78, 79
20	IGR J11435–6109	~1.6	7.98	—	1.33	52.46	161.8	26	3.5	18 (18–45 keV)	I	80, 81, 82, 83, 84, 85
21	4U 1145–619	0.35	1.1	~0.6	~0.5	187.5	292	45	4.5	600 (3–12 keV)	I, II	52, 86, 87, 88, 89, 90
22	1ES 1210–646	—	3.3	—	~2.8	6.71	—	—	—	14 (2–12 keV)	C	81, 91
23	1H 1255–567	0.04	0.1	—	0.1	—	—	25.5	—	—	C	52, 92

Table 2.2: continued.

ID	Name	E(B-V)	A _V	e	d (kpc)	P _{orb} (d)	P _{spin} (s)	H α (max.) (-Å)	H β (max.) (-Å)	F _X (peak) (mCrab)	Note	Ref.**
24	4U 1258–613	1.9	6.1	0.47	2.4	132.5	~272	27.31	—	~1680 (12–50 keV)	I, II, V/R	89, 93, 94, 95, 96, 97, 98, 99, 100
25	IGR J13020–6359	—	~10	—	~7	—	700	21.7	—	11 (18–60 keV)	P	77, 100, 101, 102, 103
26	IGR J13186–6257	—	—	—	—	19.99	—	—	—	0.8 (20–40 keV)	C	104, 105, 106
27	SAX J1324–6200	—	~29	—	1.5–8	—	170.8	—	—	—	P, C	107, 108, 109
28	4U 1416–62	1.9–2.7	6.1–8.9	0.42	1.4–11.1	42.19	17.5	16	—	~85 (15–50 keV)	I, II	11, 110, 111, 112, 113, 114
29	IGR J14331–6112	—	~6.5	—	~10	—	—	4.6	—	0.8 (20–60 keV)	I	115, 116
30	IGR J14488–5942	—	—	—	—	49.51	—	—	—	0.8 (20–40 keV)	C	117, 118
31	XTE J1543–568	—	—	<0.03	>10	75.56	27.1	—	—	14.9 (20–40 keV)	II, F	56, 117, 119, 120
32	2S 1553–542	—	—	<0.09	—	30.6	9.3	—	—	170 (15–50 keV)	II, F	56, 121, 122
33	1H 1555–552	—	2.4	—	0.96	—	—	—	—	—	C	123, 124
34	SWIFT J1626.6–5156	1.52	4.7	0.08	~15	132.89	15.4	45	5.1	>1500 (15–50 keV)	I, II, F	125, 126, 127, 128, 129
35	IGR J16327–4940	—	11.2	—	~2	—	—	31.3	7.6	2.1 (20–40 keV)	C	117, 130
36	AX J1700.2–4220	—	—	—	—	44.12	54.2	—	—	2.1 (20–40 keV)	C	117, 131, 132
37	IGR J17200–3116	—	—	—	—	—	328.2	5.5	—	2.8 (20–40 keV)	P, C	104, 133, 134
38	RX J1739.4–2942	—	—	—	—	—	—	—	—	4.4 (18–45 keV)	C	135
39	IGR J17404–3655	—	3.1	—	~9.1	—	—	14.2	<9	1.1 (20–40 keV)	C	81, 117
40	AX J1749.1–2733	—	—	—	8–19.5	185.5	~66	—	—	68 (22–50 keV)	C	136, 137, 138
41	AX J1749.2–2725	—	—	—	14	—	220.4	—	—	—	C	136, 139
42	GRO J1750–27	—	—	0.36	12–22	29.82	4.5	—	—	319 (10–25 keV)	C	140, 141, 142, 143
43	AX J1820.5–1434	—	—	—	~4.7/11.7	54	152.3	—	—	11.4 (20–40 keV)	C	117, 144, 145
44	IGR J18219–1347	—	—	—	—	72.44	—	—	—	33.5 (15–50 keV)	C	146, 147

Table 2.2: continued.

ID	Name	E(B-V)	A_V	e	d (kpc)	P_{orb} (d)	P_{spin} (s)	H α (max.) (-Å)	H β (max.) (-Å)	F $_X$ (peak) (mCrab)	Note	Ref.**
45	IGR J18406–0539	—	—	—	—	—	—	—	—	2 (18–60 keV)	C	148
46	GS 1843+009	2.3–2.9	7–9	0.01–0.5	≥ 10	160	29.5	14	—	220 (15–50 keV)	I, II	149, 150, 151, 152, 153
47	2S 1845–024	—	—	0.88	10	242.18	94.8	—	—	75 (20–100 keV)	I	154, 155, 156, 157
48	XTE J1858+034	—	—	—	—	—	221	8.2	—	96.3 (20–40 keV)	C	7, 158, 159
49	XTE J1859+083	—	—	—	—	60.65	9.8	—	—	—	C	160, 161
50	4U 1901+03	—	—	0.036	—	22.58	2.76	—	—	~ 240 (2.5–25 keV)	C	162
51	IGR J19294+1816	—	—	—	—	117.2	12.44	—	—	25 (15–50 keV)	C	163, 164, 165
52	1H 1936+541	—	—	—	—	—	—	31.9*	1.7*	—	C	—
53	XTE J1946+274	~ 2.0	6.7	0.33	9.5	169.2	15.8	47.6*	6	300 (12–25 keV)	I, II, V/R	166, 167, 168, 169
54	KS 1947+300	1.06	3.0	0.03	10.4	40.42	18.7	16.8	—	120 (1.5–12 keV)	I, II	170, 171, 172
55	SWIFT J2000.6+3210	—	~ 4.0	—	≈ 8	—	890	10.2	—	2.2 (20–40 keV)	I	115, 117, 173, 174
56	EXO 2030+375	3.8	—	0.42	7.1	46.02	41.8	20.2	—	859.9 (20–40 keV)	I, II, F	117, 175, 176, 177, 178
57	GRO J2058+42	1.4	4.34	—	~ 9	55.03	198	10.68*	—	300 (20–50 keV)	I, II, V/R, NRP	179, 180, 181
58	SAX J2103.5+4545	1.35	4.19	0.41	6.8	12.68	358.6	5.2	—	138.5 (20–40 keV)	I, V/R, NRP	117, 182, 183, 184, 185, 186, 187
59	IGR J21347+4737	0.76	2.4	—	8.5	—	320.35	8.1	1.2	2.1 (20–40 keV)	P	81, 117, 188
60	GS 2138+56	1.3	—	—	3.8	20.85	66.3	53.38*	3.3	~ 100 (1–20 keV)	I	190, 191, 192
61	1H 2202+501	0.3	—	—	0.7	—	—	—	—	—	C	123, 193
62	SAX J2239.3+6116	1.4	4.4	—	4.4	262.6	1247	7.46*	—	80 (20–100 keV)	I	194, 195
63	IGR J22534+6234	1.72–1.93	~ 6.7	—	4.4	—	~ 47	38	5	0.42 (17–60 keV)	C	196, 197

(*) EW measurements of H α and H β are found in this work, see Chapter 3 for EXO 0331+530, XTE J1946+274, SAX J2103.5+4545.

(**) References: (1) Negueruela & Okazaki (2001); (2) Reig et al. (2007); (3) Rappaport et al. (1978); (4) Clark & Cominsky (1978); (5) Whitlock et al. (1989); (6) Gutiérrez-Soto et al. (2011b); (7) Reig et al. (2005b); (8) Corbet & Krimm (2010); (9) Tomsick et al. (2011); (10) Grebenev et al. (2004b); (11) Reig et al. (1997b); (12) Sarty et al. (2009); (13) Haberl et al. (1998a); (14) Kaur et al. (2008b); (15) Masetti et al. (2006a); (16) Steiner et al. (2005); (17) Negueruela et al. (1999); (18) Stella et al. (1985); (19) Kodaira et al. (1985); (20) Whitlock (1989); (21) Terrell et al. (1983); (22) Reig (2008); (23) Telting et al. (1998); (24) Roche et al. (1997); (25) Delgado-Martí et al. (2001); (26) Jones et al. (2011); (27) Lutovinov et al. (2012); (28) Reig et al. (2005a); (29) Tsygankov et al. (2011); (30) Reig & Roche (1999a); (31) Morii et al. (2010); (32) Steele et al. (1998); (33) Finger et al. (1994); (34) Janot-Pacheco et al. (1987); (35) Rosenberg et al. (1975); (36) Giovannelli & Graziati (1992); (37) Aab (1985); (38) Wilson et al. (1994b); (39) Camero-Arranz et al. (2012a); (40) Reig et al. (2010b); (41) Chenevez et al. (2004); (42) Kaaret et al. (1999); (43) Cusumano et al. (2000); (44) McBride et al. (2006); (45) Yan et al. (2012); (46) Morgan et al. (2003); (47) Remillard & Marshall (2003); (48) Nespoli et al. (2012); (49) Negueruela et al. (1996); (50) Corbet & Peele (1997b); (51) Corbet & Peele (1997a); (52) Chevalier & Ilovaisky (1998); (53) Reig et al. (2001); (54) Corbet & Peele (2000); (55) Reig & Roche (1999b); (56) Okazaki & Negueruela (2001a); (57) Israel et al. (2000a); (58) Wilson et al. (1997); (59) Makino et al. (1990); (60) Grebenev & Sunyaev (1991); (61) Sunyaev (1990b); (62) Coe et al. (1994a); (63) Coe et al. (2007); (64) Stollberg et al. (1993); (65) Krimm et al. (2007a); (66) Motch et al. (1997); (67) Cusumano et al. (2013); (68) Krimm et al. (2012d); (69) Coe & Payne (1985); (70) Janot-Pacheco et al. (1981); (71) Coe et al. (1994b); (72) Staubert et al. (2011); (73) Ives et al. (1975); (74) Doroshenko et al. (2010); (75) Leyder et al. (2009b); (76) Suchy et al. (2011); (77) Masetti et al. (2006e); (78) Negueruela & Schurch (2007); (79) La Parola et al. (2013b); (80) Negueruela et al. (2007); (81) Masetti et al. (2009); (82) Coleiro et al. (2013); (83) in't Zand & Heise (2004); (84) Corbet & Remillard (2005); (85) Grebenev et al. (2004a); (86) Cook & Warwick (1987); (87) Warwick et al. (1981); (88) Stevens et al. (1997); (89) Priedhorsky & Terrell (1983); (90) Wilson et al. (1994a); (91) Corbet & Mukai (2008); (92) Dachs et al. (1992); (93) Menzies (1981); (94) White (2002); (95) Parkes et al. (1980); (96) McClintock et al. (1977); (97) Corbet et al. (1986); (98) Jenke et al. (2012b); (99) Klochkov et al. (2012a); (100) Devasia et al. (2011b); (101) Chernyakova et al. (2005); (102) Chernyakova et al. (2004); (103) Rodriguez et al. (2009b); (104) Bird et al. (2007); (105) D'Ai et al. (2011); (106) Landi et al. (2008); (107) Mereghetti et al. (2008); (108) Kaur et al. (2009); (109) Angelini et al. (1998); (110) Grindlay et al. (1984); (111) Raichur & Paul (2010); (112) Levine et al. (2011); (113) Krimm et al. (2009b); (114) Finger et al. (1996a); (115) Masetti et al. (2008a); (116) Keek et al. (2006); (117) Bird et al. (2010); (118) Corbet et al. (2010a); (119) in't Zand et al. (2001a); (120) Marshall et al. (2000); (121) Kelley et al. (1983); (122) Pahari & Pal (2012); (123) Liu et al. (2006); (124) Grillo et al. (1992); (125) Reig et al. (2011); (126) Baykal et al. (2009); (127) İçdem et al. (2011); (128) Baykal et al. (2010); (129) Palmer et al. (2005); (130) Masetti et al. (2010b); (131) Corbet et al. (2010c); (132) Markwardt et al. (2010); (133) Masetti et al. (2006c); (134) Nichelli et al. (2011); (135) Grebenev et al. (2006); (136) Karasev et al. (2010); (137) Zurita Heras & Chaty (2008); (138) Heras et al. (2007); (139) Torii et al. (1998); (140) Scott et al. (1997); (141) Shaw et al. (2009); (142) Wilson et al. (1995b); (143) Brandt et al. (2008); (144) Kinugasa et al. (1998); (145) Segreto et al. (2013); (146) La Parola et al. (2013a); (147) Krimm et al. (2012e); (148) Molkov et al. (2004a); (149) Israel et al. (2001); (150) Seifina (2007); (151) Makino & GINGA Team (1988e); (152) Koyama et al. (1990); (153) Krimm et al. (2006); (154) Finger et al. (1999); (155) Soffitta et al. (1998); (156) Makino & GINGA Team (1988a); (157) Zhang et al. (1996); (158) Remillard et al. (1998); (159) Krimm et al. (2010c); (160) Corbet et al. (2009); (161) Marshall et al. (1999); (162) Galloway et al. (2005); (163) Corbet & Krimm (2009); (164) Rodriguez et al. (2009c); (165) Krimm et al. (2009a); (166) Verrecchia et al. (2002); (167) Smith & Takeshima (1998); (168) Wilson et al. (2003a); (169) Camero-Arranz et al. (2010); (170) Riquelme et al. (2012); (171) Galloway et al. (2004); (172) Chakrabarty et al. (1995); (173) Morris et al. (2009); (174) Pradhan et al. (2013); (175) Motch & Janot-Pacheco (1987); (176) Wilson et al. (2002); (177) Parmar et al. (1985); (178) Reig et al. (1998); (179) Wilson et al. (2005); (180) Wilson et al. (1998a); (181) Kiziloglu et al. (2008); (182) Reig & Mavromatakis (2003); (183) Reig et al. (2004b); (184) Reig et al. (2010a); (185) Baykal et al. (2007); (186) Hulleman et al. (1998); (187) Kızıloğlu et al. (2009); (188) Reig & Zezas (2014a); (189) Reig & Zezas (2014b); (190) Bonnet-Bidaud & Mouchet (1998); (191) McBride et al. (2007); (192) Makino & GINGA Team (1988d); (193) Chevalier & Ilovaisky (1998); (194) in't Zand et al. (2000); (195) in't Zand et al. (2001b); (196) Esposito et al. (2013); (197) Masetti et al. (2013)

2.3 γ -Ray Binaries with Be Companions

This small group of systems are the members of a recently growing class called γ -Ray Binaries. There have been 6 γ -Ray binaries detected to date: RX J0240.4+6112 (LS I +61303), HESS J0632+057 (MWC 148), PSR B1259–63, RX J1826.2–1450 (LS 5039), AGL J2241+4454 (MWC 656) and 1FGL J1018.6–5856. Among these systems only two of them have confirmed compact companions whereas for the rest of them the nature of the companions are unclear. PSR B1259–63 has a young neutron star while AGL J2241+4454 is the first and the only known black hole binary system with a Be companion (Casares et al. 2014; Munar-Adrover et al. 2014). In general they are composed of a massive optical companion (O or Be type) and a compact object. They exhibit non-thermal emissions in radio, X-rays and in very high energy (VHE) γ -rays which are modulated with the orbital period of the system. The detailed observational characteristics and theoretical studies of γ -ray binaries out of the scope of the present work. Therefore we give only the general properties which are updated with the recent studies see Table 2.3 and brief historical background of the related sources below (Dubus 2013, for recent review on γ -ray binaries).

RX J0240.4+6112: This system is a member of Be/ γ -ray binaries that emits radiation virtually at all energy ranges from radio to TeV (Apparao 2001; Bignami et al. 1981; Mendelson & Mazeh 1989). RX J0240.4+6112 was first identified as the radio counterpart (GT 0236+610) of the gamma ray source CG 135+1 (Gregory & Taylor 1978; Hermsen et al. 1977; Sanduleak 1978). It has been now known that the system consists of a B0 Ve type star (LSI +61°303/V615 Cas) having variable $H\alpha$ emission line profiles in its spectra and a compact companion with unknown nature associated with 3EG J0241+6103/GT 0236+610 or COS B 2CG 135+01 (Abdo et al. 2009a; Bosch-Ramon & Paredes 2004; Frail & Hjellming 1991; Hutchings & Crampton 1981; Paredes & Figueras 1986). It shows radio outbursts at every 26.5 days associated with the binary period of the system (Gregory 2002; Taylor & Gregory 1982). This periodicity is also seen in X-rays (Apparao 2001; Paredes et al. 1997), optical (Hutchings & Crampton 1981), IR (Paredes et al. 1994), in γ -rays (Abdo et al. 2009a) as well as in variation of the $H\alpha$ emission lines (Zamanov et al. 2014, 1999). In addition the system has a super-orbital period of ~ 4.5 yr which is

visible again in the $H\alpha$ lines, in X-rays and in γ -rays (Gregory 2002; Grundstrom et al. 2007c; Li et al. 2012a; Zamanov & Martí 2000; Zamanov et al. 1999). Due to detection of relativistic radio-jets from the system LSI +61°303 is thought to be a microquasar candidate (Grundstrom et al. 2007c; Massi et al. 2012).

HESS J0632+057: The source was discovered during the Monoceros Loop Supernova Remnant observations of HESS between 2004–2005 March (Aharonian et al. 2007). Follow-up *XMM-Newton* observations uncovered the association of the source with the early type massive star MWC 148 (=HD 259440, BD +05 1291) and the significant variation in the spectrum (Hinton et al. 2009). The variability both in γ -ray and in X-ray was also found in the long-term VERITAS and *Swift* XRT observations (Acciari et al. 2009; Falcone et al. 2010) which led the discovery of the orbital period of the system as 321 ± 5 d (Bongiorno et al. 2011). In addition it has a weak (≈ 0.2 – 0.7 mJy at 1–5 GHz) radio-counterpart reported by Moldón et al. (2011b).

1FGL 1018.6–5856: This source was first mentioned in *Fermi*/LAT First Source Catalog (Abdo et al. 2010). Later, Corbet et al. (2011) suggested the possible association of a variable X-ray source with a position consistent with the location of the source. They also revealed the presence of a modulation of 16.58 days in 100 MeV–200 GeV light curve which was attributed to the orbital period of the system. Subsequent *Swift*/XRT observations also showed the same modulation with the γ -rays is seen in X-rays (An et al. 2013). The optical/IR companion of the system which is a O6 type main sequence star (2MASS 10185560–5856459) displays strong HeII absorption accompanied by weak NIII emissions in its spectrum (Corbet et al. 2011).

PSR B1259–63: It is a unique system in the sense being the only known radio pulsar ($P_{spin}=47.76$ ms) having a massive B1 V type companion (SS 2883) rather than an evolved one (Johnston et al. 1992b; Negueruela et al. 2011). The physical mechanisms responsible for the radio, X-ray and TeV emissions (Chernyakova et al. 2009; Johnston et al. 2005; Kargaltsev et al. 2014; Moldón et al. 2011a; Okazaki et al. 2011) of the system have been studied in detail since its discovery (Johnston et al. 1992a). The system was also detected in GeV range with *Fermi*/LAT during the 2010 periastron passage (Mori et al. 2011; Tam et al. 2011). Due to the misalignment of the

Table 2.3: General properties of γ -ray binaries.

Name	Optical Companion	Spectral Type	E(B-V)	A_V	$H\alpha(\text{max.})$ (-Å)	P_{orb} (d)	e	d (kpc)	Ref.*
RX J0240.4+6112	V615 Cas	B0 Ve	1.13	3.39	18.9	26.50	0.54	2.3	1,2,3,4,5,6
HESS J0632+057	MWC 148	B0 Vpe	—	—	56	321	0.83	~ 1.4	7,8,9
1FGL 1018.6–5856		O6V((f))	1.3	4.15	—	16.58	—	5.4	10,11
PSR B1259–63	LS 2883	O9.5 Ve	0.85	2.63	80	1236.9	0.87	2.3	9,12,13
RX J1826.2+1450	LS 5039	O6.5 V((f))	1.26	3.91	—	3.91	0.35	2.5	14,15

(*) References: (1) Hutchings & Crampton (1981); (2) Paredes & Figueras (1986); (3) Zamanov et al. (1999); (4) Gregory (2002); (5) Aragona et al. (2009); (6) Maraschi & Treves (1981); (7) Hinton et al. (2009); (8) Aragona et al. (2010); (9) Casares et al. (2012); (10) Corbet et al. (2011); (11) Napoli et al. (2011); (12) Johnston et al. (1992b); (13) Negueruela et al. (2011); (14) Drilling (1975); (15) Casares et al. (2005)

orbital plane and the decretion disk of Be star it was previously suggested that the pulsar crossed the disk twice in each orbit (Aharonian et al. 2009; Chernyakova et al. 2009). However, using 3-D SPH simulations Okazaki et al. (2011) showed that the pulsar truncated the disk at a significantly smaller radius than the pulsar orbit stripping off the outer part of the decretion disk of Be star. Therefore conversely the theory what have been assumed before the pulsar does not pass through the disk around the periastron passage. Besides interaction point of the pulsar and the disk substantially depends on how the pulsar wind interacts with circumstellar matter.

RX J1826.2–1450: Since the discovery of its association with luminous $V \sim 11.2$ star LS 5039 through the cross-correlation of *ROSAT* Galactic all sky survey and the several OB catalogs (Motch et al. 1997) RX J1826.2–1450 has been one of the extensively studied sources in the literature. The system is a source of non-thermal, persistent, and periodic gamma-ray emission at energies above 250 GeV (Abdo et al. 2009b; Aharonian et al. 2005; Collmar & Zhang 2014; Paredes et al. 2000). The modulation of the source spectrum is consistent with the orbital period of ~ 3.9 days (Aharonian et al. 2006; Dubus et al. 2008; Hadasch et al. 2012).

2.4 γ Cas and its analogs

Since its discovery as the first detected Be type star (Secchi 1866), γ Cas has always been the most captivating source not only because of its unique properties but also

being prototype of a new X-ray emitting class among the known Be/X-ray binaries. Although recent studies reveal that this bright ($m_V=2.5$) B0.5 Ve type star is placed in a binary within a 204 day orbit, the nature of the companion has not been identified so far (Harmanec et al. 2000; Miroschnichenko et al. 2002). What makes γ Cas to be unique is its unusual X-ray spectrum that is dominated by a very hot ($kT \sim 10\text{--}12$ keV) thermal emission in 2–20 keV energy band with a variable luminosity of $\sim 10^{32\text{--}33}$ erg s $^{-1}$ (Lopes de Oliveira et al. 2010; Smith et al. 2004). These properties are quite unusual for a Be star, isolated or in a binary (Berghoefer et al. 1997; Reig 2011). In addition no significant X-ray outbursts which are prerequisites for being a transient Be/X-ray system have been observed for γ Cas.

Recently, through the *INTEGRAL* observations several γ Cas-like sources have been identified: HD 110432 (Lopes de Oliveira et al. 2007; Torrejón et al. 2012), HD 119682 (Rakowski et al. 2006; Safi-Harb et al. 2007), HD 161103, SAO 49725 (Lopes de Oliveira et al. 2006), USNO 0750-13549725 (Lopes de Oliveira 2007; Motch et al. 2003, 2007), SS 397, HD 157832 (Lopes de Oliveira & Motch 2011), XGPS-36 (Motch et al. 2010). The members of this class have similar properties both in X-ray and in optical wavelengths. In general, their optical spectra which show strong H α line emissions e.g, EW $\sim 30\text{--}50$; (Lopes de Oliveira et al. 2007) have the properties of B0.5–1.5 type stars.

In the X-ray domain they show hard X-ray spectra dominated by a hot thermal component ($kT > 8$ keV) with changing flux in the time range of seconds to several minutes (Lopes de Oliveira et al. 2006). They do not undergo X-ray outbursts or exhibit continuous X-ray emission as strong as persistent Be/X-ray binaries. However the mechanism producing the X-rays remains as a mystery. Two models have been put forward to explain the nature of this type of systems, accretion on to a compact companion (most likely a white dwarf), and the magnetic interaction between the interface of the accretion disk and surface of the Be star.

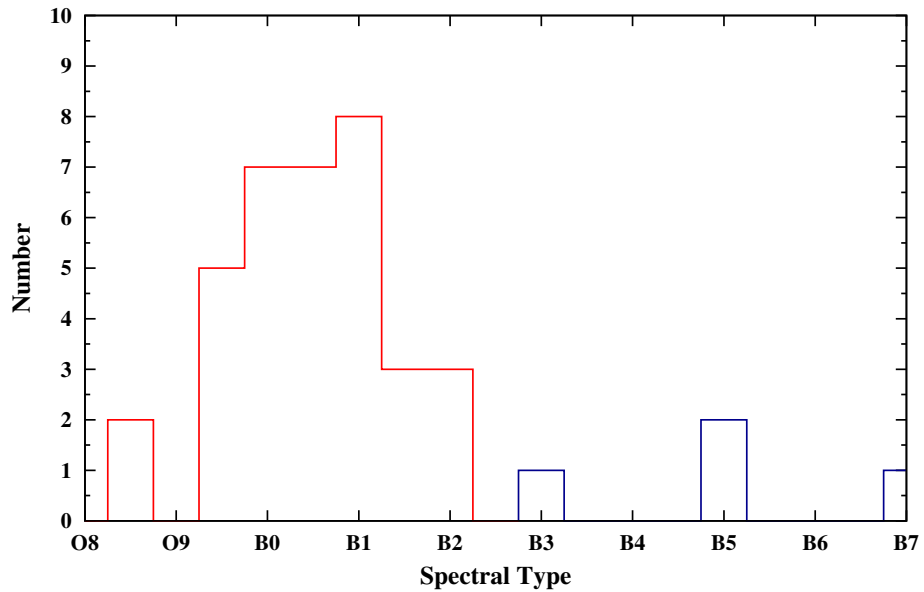


Figure 2.1: The spectral distribution of Be stars in Be/X-ray systems. The red boxes represent confirmed systems while the candidates are seen in blue-colored boxes.

2.5 Distribution of Spectral Type and X-ray Activity

Using sample of 39 sources from Table 2.1, including 9 candidates, with well known spectral types, we have generated an updated spectral distribution of BeXRBs in the Milky Way as seen in the Figure 2.1. The distribution is nearly same with the previous results that spectral class of optical companion in BeXRBs is confined in a very narrow range of B0–B2 peaking at B1. Although, there are also a few systems earlier than this group, it is clear that the Be phenomenon is not common beyond spectral class of B2.

Indeed, this result strongly supports the idea that early limit in the spectral range is the result of binary evolution of BeXRBs related to mass transfer (van Bever & Vanbeveren 1997). According to this, it is angular momentum loss per unit mass that directly determines the faith of the system during the evolution by restricting the mass of the companion to $>8M_{\odot}$, i.e. to earlier spectral types than B2 (Portegies Zwart 1995). Exposed to a spiral-in effect after the mass loss from L2 point, the systems with late-type stars are mostly affected by increasing amount of the angular momentum. In

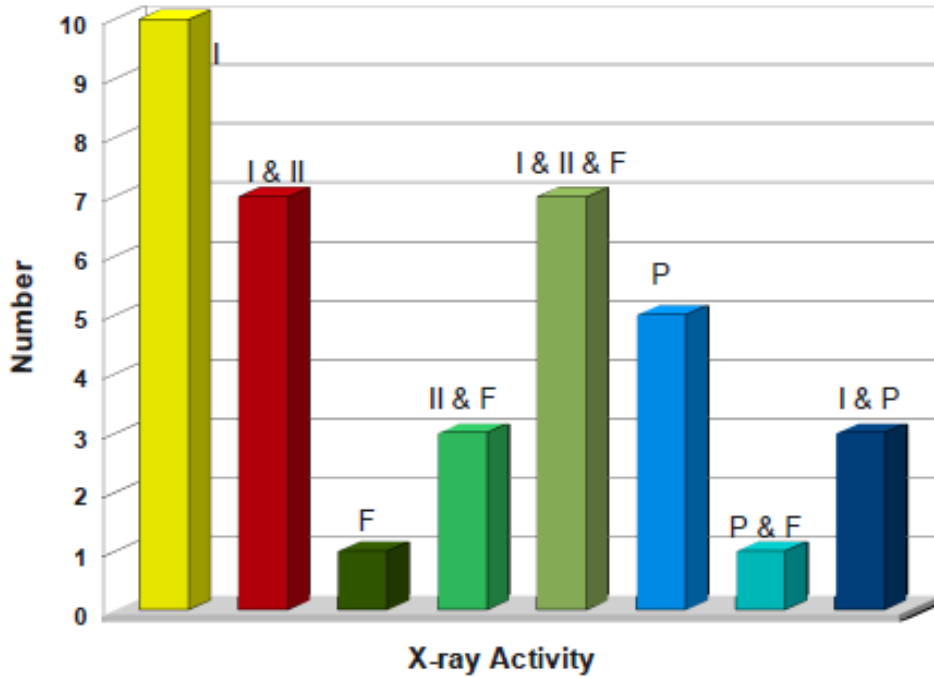


Figure 2.2: The distribution of X-ray activities for a sample of 37 BeXRBS. The abbreviations in the chart stand for: I, Type I outburst; II, Type II outbursts; F, flare; P, persistent. Note that two of these persistent BeXRBS systems are not confirmed.

other words, the number of systems with a late-type star and a NS do reduce with the increasing angular momentum loss (McBride et al. 2008). Therefore it is natural to see BeXRBS with early-type optical companions more likely. According to this, the candidates having late spectral classes in our catalog probably do not belong to BeXRBS if their classification is true.

As seen from the Table 2.2, BeXRBS can show variety of X-ray activities though characteristic outburst types are generalized in two classes (see Chap. 1.1). Figure 2.2 represents the number of BeXRBS for different X-ray behaviors reported so far. The notations used for each data point indicate a different activity type as: I, Type I outbursts; I & II, for systems showing both normal and giant outbursts; F, detected only with flare activity; II & F, for systems showing flares in addition to the Type II outbursts; I & II & F, systems with all types of activities; P, persistent systems; P & F, flare showing persistent systems; I & P, persistent systems with type I outbursts. It should be noted that, among 37 sources, only 2 candidates (IGR J17200–3116 and SAX J1324–6200) are included to the histogram which are cataloged as potential

persistent BeXRBs in Chapter 2.2.

From the distribution, it is interesting to see that BeXRBs do not show Type II outbursts alone; these outbursts are always accompanied with Type I outbursts and flares or both. On the other hand, we can safely state that Type I outbursts are the most common activities among BeXRBs which can be interpreted as a result of large number of systems with high eccentricities (see Chap. 1.1.2). There is only one system, 4U 0726–260, detected with only flaring activity. Similarly, X Per (4U 0352+309) is the only member of the class of persistent BeXRBs showing X-ray flares. Despite their detectable persistent X-ray emission, there are 3 systems with Type I outbursts, RX J0146.9+6121, RX J0440.9+4431 and RX J1037.5–5647. It is important to note that except RX J0440.9+4431, these two sources have the slowest pulsars among BeXRBs.

2.6 P_s and P_{orb} Relation

In Figure 2.3, an updated version of Corbet diagram for Galactic HMXBs including 61 systems is plotted. 19 of these systems have either giant or supergiant companions and 5 of them, represented by yellow-squares, are Supergiant Fast X-ray Transients (SFXTs) and potential candidates (Table 2.4). There exist 30 BeXRBs (blue triangles) and 7 candidate BeXRBs systems (red triangles) in the diagram, excluding the systems 1A 1118–615 and SAX J2103.5+4545 which appeared in the region of the wind-fed accreting SgXRBs (green circles). An explicit form of the diagram just for BeXRBs and candidates is also shown Fig.2.4. Despite the larger scatter of the data, BeXRBs clearly show a positive correlation between their P_{spin} and P_{orb} . Remembering that the NS tries to adjust its P_{spin} to P_{eq} , indeed, such a distribution is definitely expected as explained in Chapter. 1.1.3.

In addition to this we can examine this distribution in terms of the eccentricity (e) of the system together with the relation $P_{eq} \propto \dot{M}^{-3/7}$ (see Eq.1.10). According to this, in wide-orbit systems with long orbital periods the wind material would be less dense than the narrow-orbit systems. Therefore, due to the lower accretion rate, corresponding spin period would be longer. Excluding SAX J0635.2+033 (millisecond

Table 2.4: Galactic high mass X-ray binaries with known orbital and spin periods.

Source Name	$P_{orb}(d)$	$P_{spin}(s)$	Spectral Type	Ref.*
Giant and Supergiant X-ray Binaries				
IGR J00370+6122	15.663	359	BN0.7 Ib	1, 2
1A 0114+650	11.598	9720	B1Ia	3
Vela X-1	8.964	283.5	B0.5Ia	4
Cen X-3	2.1	4.8	O6-8Ia	5
1E 1145.14-6141	14.365	297	B2Iae	6, 7, 8
GX 301-2	41.498	685	B1.5Ia	9, 10
PSR B1259-63	1236.9	0.048	B2e	11
4U 1538-522	3.728	528.809	B0 Iab	12, 13, 14
IGR J16320-4751	8.96	1303	O8 I	15, 16, 17
AX J1639.0-4642	4.2	912	sgOB	18, 19
IGR J16493-4348	6.782	1069	B0.5 Ia-b	20, 21, 22
OAO 1657-415	10.444	38	B0-6 Ia-b	23, 24
EXO 1722-363	9.7403	413.9	O8.5 I/B0-1 Ia	25, 26, 27
PSR J1740-3052	231	0.57	B	28
IGR J18027-2016	4.57	139.612	B1 Ib	29, 30, 31
XTE J1855-026	6.072	361	B0 Iae	32, 33, 34
4U 1907+097	8.375	437.5	O8.5 Iab	35
X 1908+075	4.4	605	O7.5-9.5 I	36, 37, 38
4U 2206+54	19.25	5560	O9.5 VI	39, 40, 41
Supergiant Fast X-ray Transients and Candidates				
IGR J11215-5952	164.6	186.78	B1 I	40, 41
IGR J16418-4532 ^a	3.753	1212	sgOB	42, 43
IGR J16465-4507	30.243	227	B0.5 I/O9.5 Ia	44, 45
IGR J17544-2619	4.926	71.49	O9 Ib	45, 46, 47, 48
IGR J18483-0311	18.55	21.05	B0.5-1 Ia-b	29, 49, 50, 51

(*) References: (1) in't Zand et al. (2007); (2) González-Galán et al. (2014); (3) Grundstrom et al. (2007a); (4) Kreykenbohm et al. (2008); (5) Schreier et al. (1972); (6) Ray & Chakrabarty (2002); (7) White et al. (1978); (8) Densham & Charles (1982); (9) Sato et al. (1986); (10) Koh et al. (1997); (11) Wang et al. (2004); (12) Becker et al. (1977); (13) Clark (2000); (14) Reynolds et al. (1992); (15) Corbet et al. (2005); (16) Rodriguez et al. (2006); (17) Coleiro et al. (2013); (18) Corbet et al. (2010b); (19) Bodaghee et al. (2006); (20) Cusumano et al. (2010); (21) Corbet et al. (2010d); (22) Nespoli et al. (2010); (23) Chakrabarty et al. (1993); (24) Chakrabarty et al. (2002); (25) Thompson et al. (2007); (26) Rahoui et al. (2008); (27) Mason et al. (2009); (28) Stairs et al. (2001); (29) Hill et al. (2005); (30) Pandey et al. (2006); (31) Torrejón et al. (2010); (32) Corbet & Mukai (2002); (33) Corbet et al. (1999); (34) Negueruela et al. (2008); (35) Baykal et al. (2006); (36) Wen et al. (2000); (37) Levine et al. (2004); (38) Morel & Grosdidier (2005); (39) Reig et al. (2009); (40) Corbet et al. (2007); (41) Blay et al. (2006); (42) Romano et al. (2009); (43) Swank et al. (2007); (44) Corbet et al. (2006); (45) Sidoli et al. (2012b); (46) Clark et al. (2010); (47) Walter et al. (2006); (48) Drave et al. (2014); (49) Drave et al. (2012a); (50) Pellizza et al. (2006); (51) Sguera et al. (2007); (52) Giunta et al. (2009); (53) Rahoui & Chaty (2008)

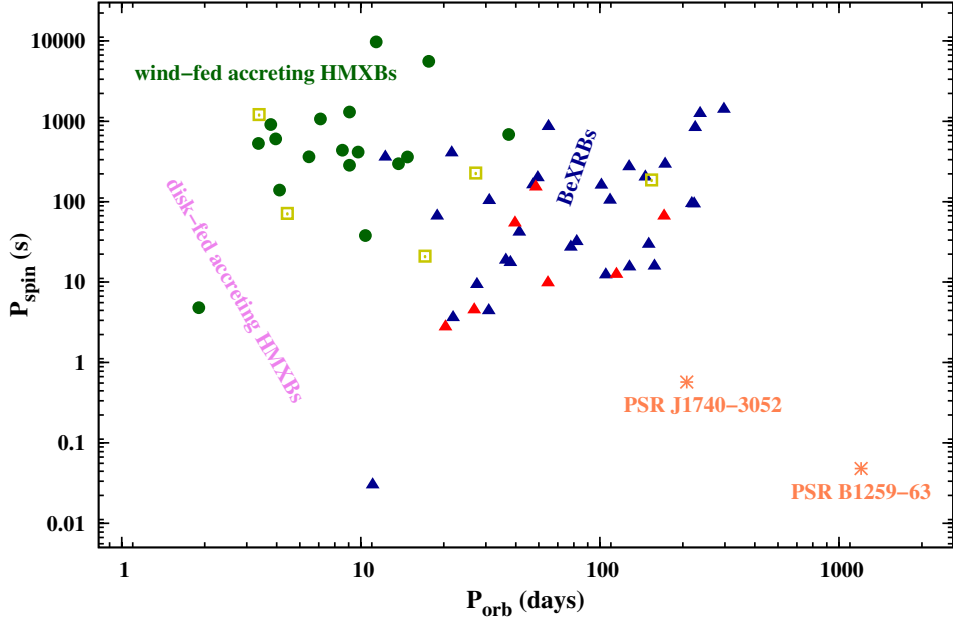


Figure 2.3: The updated Corbet diagram for BeXRBs and candidates in Tables 2.2 and for the galactic HMXBs. The green-filled circles represent the HMXBs with supergiant/giant companions. Majority of this group is located at a distinct region called 'wind-fed HMXBs'. The confirmed BeXRBs are seen in blue-filled triangles, whereas the red ones indicate the candidate BeXRBs. The SFXTs (gold-squares) are placed between the wind-fed HMXBs and BeXRBs. The two radio pulsars are placed at the bottom right of the diagram.

pulsar) and 4U 0352+309, orbital periods of BeXRBs confined in the region of ~ 20 –400 days. It can be inferred from Fig.2.4 that the persistent BeXRBs (green-filled triangles) contain slow pulsars ($P_{spin} > 200$ s) and reside in wider orbits ($P_{orb} \gtrsim 200$ d).

On the other hand we do not see a clear relation between e and P_{orb} for Be/X-ray binaries (see Fig. 2.5). To check whether there is a relation between these parameters or not we applied the Spearman rank correlation test for both original and log-linear data. Excluding Be/ γ -ray binaries, the rank correlation coefficient ρ is found to be 0.336 with two-tailed value of p as 0.203 for 12 data points (N), indicating the association between the two variables would not be considered statistically significant for 2σ confidence level (95%). Although adding 4 Be/ γ -ray binaries to the test improved

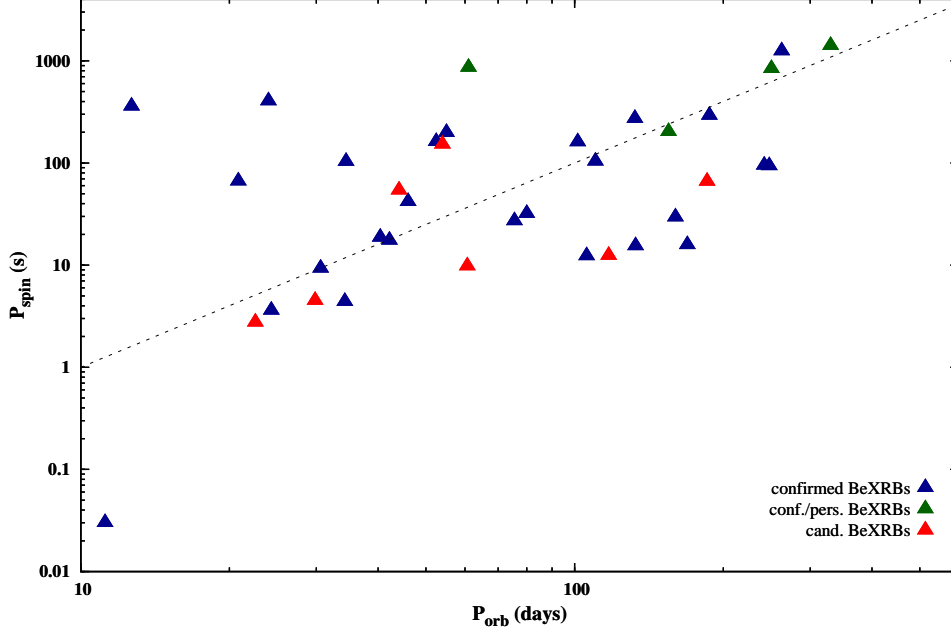


Figure 2.4: Corbet diagram for BeXRBs and candidates. The dashed line indicates the relation $P_{spin} \propto P_{orb}^2$ given by Corbet (1986).

the probability, it results in a coefficient of 0.44 and p-value of 0.05 which is not significant again to state a relationship. The second test for the linear-log relation of the parameters gives a coefficient of 0.351 and p-value of 0.182. The meaningful results are acquired only when all the data are used, including Be/ γ -ray binaries, with $\rho=0.45$ and $p=0.047$ referring to a statistically significant but a weak relation. In Fig. 2.5, we plot e vs $\log P_{orb}$ for Be/X-ray and Be/ γ -ray binaries. Since the correlation gets stronger when systems with γ -ray companions are added, we could then focus on the idea that the relation would mainly holds for these type of sources. Indeed, for 4 Be/ γ -ray binaries we found a positive strong correlation between their eccentricities and their log of orbital periods with $\rho=1$. The purple-solid line in Fig. 2.5 shows the linear regression fit to these parameters. The relation is defined as,

$$e = 0.23 + (\log P_{orb}) * 0.219. \quad (2.1)$$

It must be noted that a similar relation for Be/ γ -ray binaries was previously showed by Casares et al. (2012). They suggested that to trigger VHE radiations the systems with large eccentricities would have long-orbital periods. For short-orbital period binaries, on the other hand, unstable conditions in disk due to the small separation

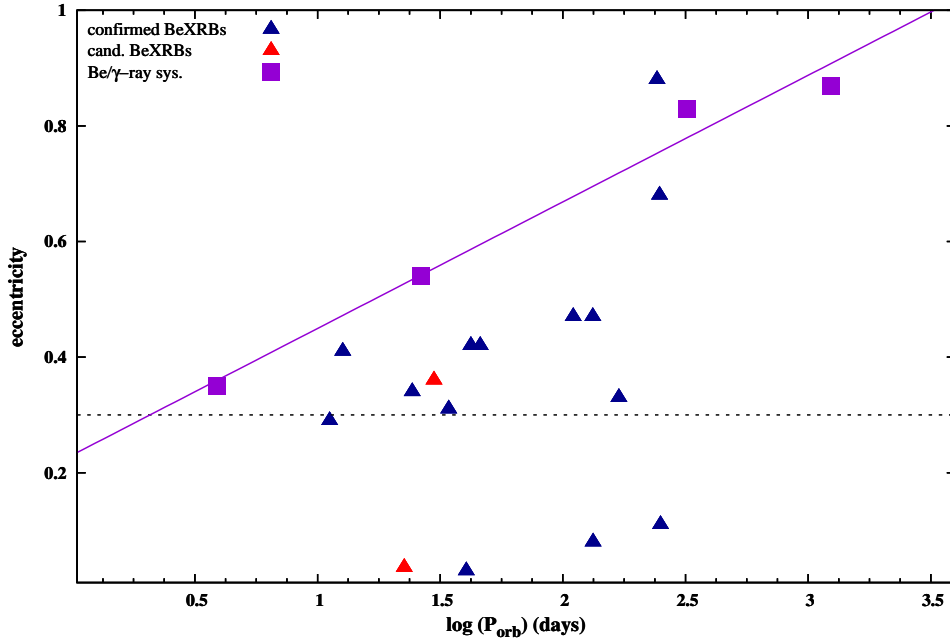


Figure 2.5: Orbital period against eccentricity for the BeXRBs in Table 2.2 and γ -ray binaries with Be companions in Table 2.3. The dashed horizontal line corresponds to the value of $e=0.3$ at/above where most of the systems are located. A linear regression fit to Be/ γ binaries is overplotted with a purple-solid line.

from the companion would lead to emit the high-energy radiation. We should point out that they have used 5 Be/ γ -ray sources, one of which was recently identified as a first Be/Black-Hole system (Munar-Adrover et al. 2014).

Yet, a convincing relation is not obtained between e and P_{orb} parameters for BeXRBs, intuitively we can state that most of the systems are located at/above $e \geq 0.3$ (black-dashed line in Fig.2.5).

2.7 $H\alpha$ and $H\beta$ Strength vs P_{orb}

It has been strictly accepted that the NS in Be/X-ray systems prevents the extension of the decretion disk by exerting the tidal/resonant torques on it (see Chap. 1.1.2). The main observational evidence supporting this physical mechanism is assumed to be the correlation between the maximum EW value of $H\alpha$ emission and the orbital period suggested by Reig et al. (1997a). To show this correlation, we reconstruct

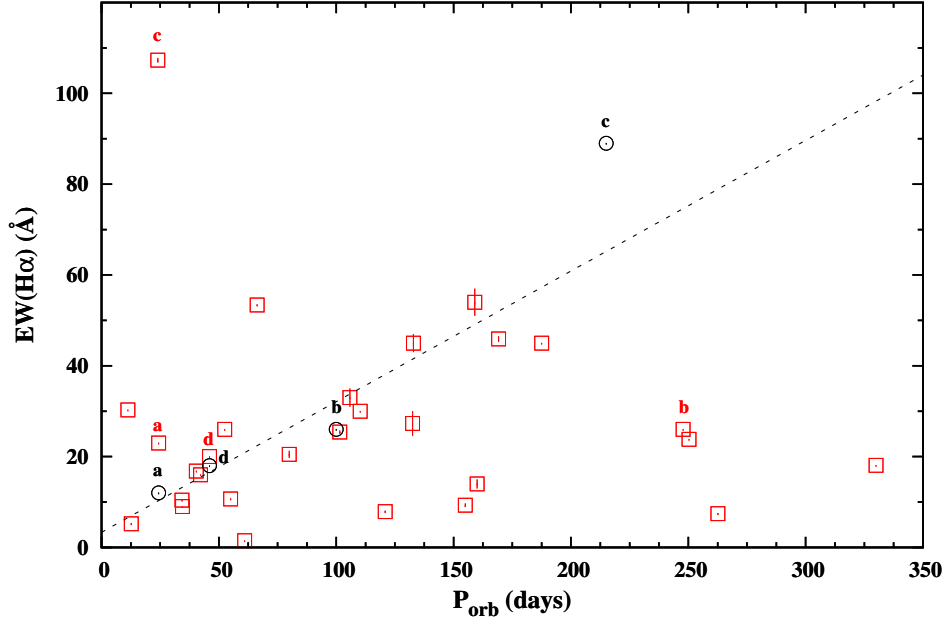


Figure 2.6: Variation of maximum $H\alpha$ EW with respect to the orbital period. Red squares are updated values of the systems given Table 2.2. The linear regression fit to the values given in Reig et al. (1997a) is shown with a dashed-line which is not compatible with our measurements since most of the values have changed. Four of these systems, corresponding to a) 4U 0115+634, b) GRO J1008–57 c) 1A118–616 and d) EXO 2030+275, with the values out of date from Reig et al. (1997a), are also indicated with the black-circles.

the plot given in Reig et al. (1997a) with updated values of the systems in Table 2.2 (see Fig. 2.6). However we could not find a relation between these two parameters as previously stated. Furthermore, both Spearman and Pearson tests returned with the insignificant p -values (0.53 and 0.39) indicating that EW of $H\alpha$ and P_{orb} were disassociated.

It should be noted there were only 11 BeXRBs in the original P_{orb} –EW($H\alpha$) diagram including 1 LMC source (A 0535–668) and 2 sources whose orbital periods determined from the Corbet Diagram (GRO J1008–57 and 1A 1118–615). Removing the LMC source from the list 4 sources have been displaced in our plot. They are 4U 0115+634, GRO J1008–57, 1A 1118–615 and EXO 2030+275 of which old and updated values are also shown in the Figure 2.6. We can definitely suggest that

the previously suggested correlation does not exist at least for the Galactic BeXRBs at present. In fact, Reig (2007) improved their original diagram by adding 12 SMC sources and updating some of the previously used $H\alpha$ and P_{orb} values (except GRO J1008–57) given in Reig et al. (1997a) (see Fig. 1.4). It is clear that even if the data points have been revised, the 2007 diagram has still been out of date.

The relation between the maximum EW of $H\beta$ emission ever observed and P_{orb} was also checked but no clear dependence or correlation was found with these parameters. The data points are largely scattered as seen in Figure 2.7. However, in Figure 2.8 we find a clear relation in the log-log plot of maximum EW of $H\beta$ and $H\alpha$ emissions. We obtain a Pearson correlation coefficient (R) of 0.7015 and probability of $p=2.1 \times 10^{-4}$. The linear regression fit to the data produces the following relation;

$$\log(H\beta) = 0.847 * \log(H\alpha) - 0.742. \quad (2.2)$$

The above relation found from 22 sample suggests that $H\beta$ emission increases with the increasing $H\alpha$ emission. Indeed, such a relation can be expected since both $H\alpha$ and $H\beta$ lines are produced in the decretion disk of the Be star. However, these two lines are emitted from the different parts of the disk: $H\alpha$ line is formed mainly in the outer parts, e.g. 5–20 R_* (Hummel & Vrancken 1995), whereas the inner parts, 2–5 R_* (Mennickent 1991), close to the central star emit $H\beta$ radiation. Assuming that $H\alpha$ strengths give an estimate of the emitted regions, it is then possible to see a similar behavior for $H\beta$. The other possibility, on the other hand, is that the regions responsible for the Balmer emissions are not strictly divided for the individual lines, instead they might be overlapped. However, due to the changing temperature gradients through the disk, this suggestion is naturally eliminated.

2.8 Summary

In this chapter we present a new and comprehensive catalog of Be/X-ray binaries and candidates in the Galaxy. With this new list, the number of confirmed Be/X-ray binaries in the Galaxy have increased to 37 additionally with 26 candidates discovered mainly through the *INTEGRAL* detections.

The spectral distribution of BeXRB population in the Galaxy can be characterized

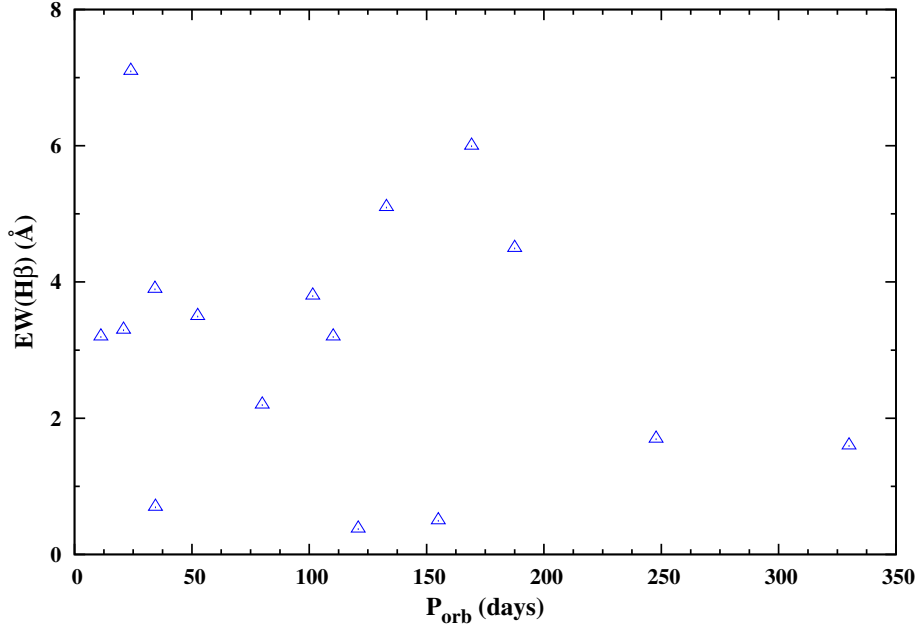


Figure 2.7: Variation of maximum H β EW with respect to the orbital period. There is not a clear relation between these two parameters.

by a narrow spectral range of B0–B2. There are a few systems between O8–B0 and B2–B3. This suggests that the Be phenomenon is generally seen at earlier spectral types. From the distribution of the X-ray activities among the BeXRBs, one can infer that normal outbursts are the most common types. The outbursts of giants are always associated with flares or Type I outbursts. The number of Be/X-ray binaries showing persistent X-ray emission is much higher than the systems exhibiting both Type I and Type II outbursts.

In addition to this, updated properties of each system have been investigated in a general frame which allow us to revise the known characteristics of Be/X-ray systems. Through this, we have updated the Corbet Diagram with 61 sources and confirmed that the Be/X-ray binaries have a distinct location in the plot supporting the relation of $P_{spin} \propto P_{orb}^2$. Yet, we could not find a correlation between the eccentricity of the orbit and its period. But for sure, majority of BeXRBs have eccentric orbits ($e \gtrsim 0.3$). Contrary, Be/ γ -ray binaries show a relation of $e \propto \log(P_{orb})$. Note that, this is also the updated formulation of Casares et al. (2012) found for Be/ γ -ray systems.

Another result obtained from this work is the uncorrelation between the maximum

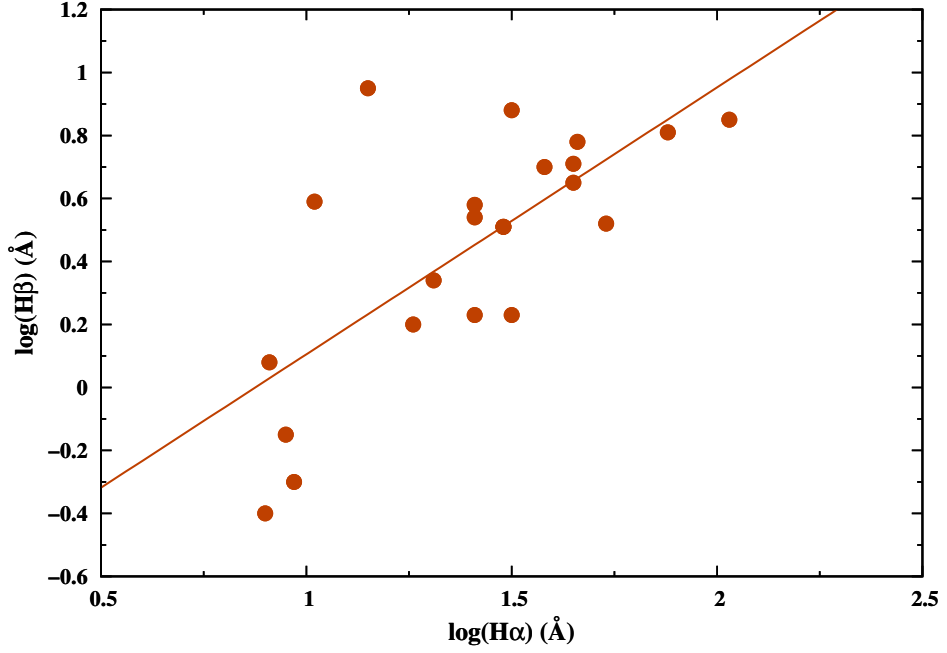


Figure 2.8: Maximum $H\beta$ emission as a function the maximum $H\alpha$ emission.

EW of $H\alpha$ emission and the orbital period despite its theoretical background have been clearly proved previously. The original diagram of $H\alpha-P_{orb}$ contains 11 sources whereas our updated version has 29. Indeed the correlation tests have resulted in insignificant correlation coefficients indicating that these two parameters are not related significantly. Although it is assumed that the systems with large orbits (long orbital periods) are the consequences of the low/none tidal torques exerted by NS on the decretion disk, we suggest that the maximum $H\alpha$ EW alone does not indicate the existence of this relation. In fact, the results from the interferometric observations for the isolated Be stars show that the flux of net $H\alpha$ emission is correlated with the emitting disk radius. Therefore, systematic long-baseline interferometric observations as well as spectroscopic observations should be done to check whether this relation is also hold for the Be/X-ray systems.

We also examine the possible correlation between the maximum $H\beta$ EW and P_{orb} , but we could not find a meaningful result. Instead, we show that maximum EW measurement of $H\alpha$ proportional to that of $H\beta$ indicating that they have the same origin.

CHAPTER 3

LONG-TERM MONITORING OF BE/X-RAY BINARIES

Majority of the Be/X-ray binaries show long-term variations in their photometric and spectroscopic data related to the changes in the size and/or in the density of the decretion disk with a time scale from weeks to years (see Chapter 1.1.1). Therefore, the optical/IR telescopes dedicated to monitoring of these systems are quite important for presenting a window through which we can study the dominant and/or possible physical mechanisms/conditions for the Be star and its environment. Since the decretion disk is the mass reservoir for both optical and X-ray outbursts, the relation between those wavelengths in the long-term base also has a particular importance.

During our long-term monitoring programme dedicated to the above mentioned purposes, we have observed 15 Be/X-ray binary systems, with well-determined orbital parameters, from the catalog given in Chapter 2 for the period 2004–2014. However, due to the weather conditions and technical issues, we could not observe each source for each season. Therefore we have selected three of them that exhibit similar type X-ray outbursts to present in this Chapter. Our main purpose for choosing these systems is to examine whether they have similar optical/IR observational features that can be explained by the common physical mechanisms. The sample includes EXO 0331+530, XTE J1946+274 and SAX J2103.5+4545. We also used quick-look X-ray results provided by the *RXTE* All Sky Monitor team,¹ and *Swift*/BAT transient monitor results² provided by the *Swift*/BAT team (Krimm et al. 2013) to investigate the relation between the X-ray and optical/infrared bands.

¹ http://xte.mit.edu/ASM_lc.html

² <http://swift.gsfc.nasa.gov/results/transients/>

3.1 Observations and Data Reduction

3.1.1 Optical/IR Photometric Observations

As a part of our monitoring campaign the optical counterparts to the systems has been continually observed in the optical and in IR bands with three different telescopes at two different observatories: from the Teide Observatory (Observatorio del Teide) on Tenerife (Spain), observations made with the 80-cm IAC80 and with the 1.5-m TCS telescopes and from the TÜBİTAK National Observatory (Antalya, Turkey) with the ROTSEIIId telescope. The Be/X-ray binary system EXO 0331+530 was only observed with the ROTSEIIId telescope whereas for XTE J1946+274 and SAX J2103.5+4545 two other telescopes were also used.

For the IAC80 and TCS telescopes we obtained CCD images in the B and V bands with integration times of 30 s. In infrared, J, H and K-short (K_s) simultaneous observations were performed using the CAIN camera with integration times of 150 s. All images were reduced in the standard way using the pipelines available for both telescopes. We applied straightforward aperture photometry using apertures of 1.5 times the full width at half maximum (FWHM). Several comparison stars within the field of view were checked for variability during each night and throughout the entire data set. Calibration of the optical data was performed using the zero point magnitude offsets and extinction coefficients listed for the Observatorio del Teide. Infrared data were calibrated using the 2MASS survey as a photometric reference.

The main part of the long-term optical CCD observations of the sources include the 0.45-m reflecting ROTSEIIId³ telescope data achieved during the period of April 2004–2007 for EXO 0331+530, from September 2011 to July 2012 for XTE J1946+274 and lastly for SAX J2103.5+4545 from September 2011 to May 2014. ROTSEIIId telescope, operates without filters is equipped with a 2048×2048 pixel CCD. For a total field of view (FOV) $1.85^\circ \times 1.85^\circ$, the pixel scale is defined as $3''.3 \text{ pixel}^{-1}$ (Akerlof et al. 2003). During the observations, a total of 594, 2014 and 1720 CCD frames were collected for EXO 0331+530, XTE J1946+274 and SAX J2103.5+4545

³ The Robotic Optical Transient Search Experiment, ROTSE, is a collaboration of Lawrence Livermore National Lab, Los Alamos National Lab, and the University of Michigan (<http://www.rotse.net>)

Table 3.1: Selected photometric reference stars in the neighborhood of the optical counterpart of EXO 0331+530 (BQ Cam) and SAX J2103.5+4545 (GSC 03588-00834) with the ROTSEIIIId telescope.

Star	RA (J2000)	Dec (J2000)	USNO-A2 R mag
BQ Cam	03:34:59.90	+53:10:24.0	14.2
Star 1	03:34:52.90	+53:11:53.6	13.8
Star 2	03:35:11.46	+53:08:56.3	13.3
Star 3	03:35:03.77	+53:12:09.1	13.2
GSC 03588-00834	21:03:35.7	+45:45:04.0	14.4
Star 1	21:03:20.58	+45:43:09.1	12.9
Star 2	21:03:21.99	+45:44:55.5	13.8
Star 3	21:03:40.32	+45:46:22.6	13.0

respectively. Dark and flat-field corrections of all images were done automatically by a pipeline immediately after the pointing. Instrumental magnitudes of all the corrected images were obtained using an aperture of 3 pixels (10 arcsec) in diameter by SExtractor Package (Bertin & Arnouts 1996a). By comparing all the stars in each frames with USNO-A2.0 catalog R -band magnitudes, calibrated ROTSEIIIId magnitudes were acquired. For the differential magnitudes of EXO 0331+530 and SAX J2103+4545, we selected 3 reference stars located in the neighboring of the optical companions and subtracted their magnitudes from the Be stars' (see Table 3.1). For the timing analysis of XTE J1946+274 the time series were corrected to the barycenter by using JPL DE200 ephemerides (Kızıloğlu et al. 2005, for the details of ROTSEIIIId data reduction).

3.1.2 Optical Spectroscopic Observations

Optical spectroscopic observations of the companions of the systems were obtained from three different telescopes: the Russian-Turkish 1.5-m telescope (RTT150) at the TÜBİTAK National Observatory in Antalya (Turkey), the 2.56-m Nordic Optical Telescope (NOT) located at the Observatorio del Roque de los Muchachos (La Palma, Spain), and the the 1.5-m Telescope at the Observatorio de Sierra Nevada (OSN-CSIC) in Granada (Spain).

The spectroscopic data from RTT150 were obtained with the TÜBİTAK Faint Object Spectrometer and Camera (TFOSC). It is equipped with a 2048×2048 , $15 \mu\text{m}$ pixel Fairchild 447BI CCD whose FOV is $13'.3 \times 13'.3$. We used slit $67 \mu\text{m}$ ($1''.24$) with Grism 8 having an average dispersion of 1.1 \AA pixel and providing a $5800\text{--}8300 \text{ \AA}$ wavelength coverage. The reduction of RTT150 spectra was done using the Long-Slit package of MIDAS.⁴ Bias correction, flat-fielding and removal of cosmic-ray hits were carried out with standard MIDAS routines.

The low-resolution OSN spectra ($R \approx 1400$) were acquired using Albireo spectrograph centred on $H\alpha$ wavelength (6562.8 \AA) whereas NOT spectrum was obtained with the Andalucía Faint Object Spectrograph and Camera (ALFOSC),⁵ using Grism 7, with a dispersion of $1.5 \text{ \AA}/\text{pixel}$, and $0''.5\text{--}1''$ slits. The reduction of this data set was performed using standard procedures within IRAF,⁶ including bias subtraction, removal of pixel-to-pixel sensitivity variations, optimal spectral extraction, and wavelength calibration based on arc-lamp spectra.

All spectroscopic data were normalized with a spline fit to continuum and corrected to the barycenter after the wavelength calibration. The full width at half maximum (FWHM) and equivalent width (EW) measurements of $H\alpha$ lines were acquired by fitting Gaussian functions to the emission profiles using the ALICE subroutine of MIDAS.

3.2 EXO 0331+530

The recurrent hard X-ray transient EXO 0331+530 (V032+53) was first detected with the *Vela* 5B observatory in 1973 during its giant outburst, reaching a peak intensity of ~ 1.6 Crab in 3–12 keV energy band (Terrell & Priedhorsky 1984). The system had passed a ten-year X-ray quiescent phase when 4.4 s pulsations were detected with *Tenma* and *EXOSAT* satellites (Stella et al. 1985). These X-ray activities, a series of Type I outbursts, lasted about three months separated by the orbital period, 34.25 d, of

⁴ <http://www.eso.org/projects/esomidas>

⁵ The data presented here were obtained [in part] with ALFOSC, which is provided by the Instituto de Astrofísica de Andalucía (IAA) under a joint agreement with the University of Copenhagen and NOTSA.

⁶ IRAF is distributed by the National Optical Astronomy Observatory, optical images which is operated by the Association of Universities for Research in Astronomy (AURA) under cooperative agreement with the National Science Foundation.

the system. During these outbursts, rapid random fluctuations in the X-ray emission in addition to the pulse-profile variations were also reported (Unger et al. 1992). The system underwent another outburst, classified as Type II, in 1989 which led to the discovery of a CRSF at 28.5 keV and QPO centered at 0.051 Hz (Makishima et al. 1990; Takeshima et al. 1994).

The optical companion of the system, BQ Cam, is an O8–9 type main sequence star at a distance of ~ 7 kpc (Negueruela et al. 1999). It has been widely observed both in optical and IR wavelengths since its identification. The optical spectrum is characterised by the highly variable emissions of $H\alpha$, $H\beta$ and $H\gamma$ in addition to the HeI lines whereas photometric data with IR excess (Bernacca et al. 1984; Coe et al. 1987; Honeycutt & Schlegel 1985; Unger et al. 1992). The brightenings in optical/IR light-curves are usually accompanied with the X-ray outburst phases as in the case of giant 2004 outburst of the system. Goranskij & Barsukova (2004) predicted this outburst based on the optical brightening of the source in optical/IR band. During the outburst, three additional CRSFs at 27, 51 and 74 keV were detected in *RXTE* observations (Coburn et al. 2005) and confirmed by the subsequent *INTEGRAL* data (Pottschmidt et al. 2005). Tsygankov et al. (2006) showed that energy of these features are linearly related to the luminosity of the source indicating the different X-ray states. The following X-ray activities of the system was in 2008, 2009 and 2010 with relatively weaker peak fluxes (Krimm et al. 2009c, 2008a; Nakajima et al. 2010). Since then, system has still been in X-ray quiescent state.

In this work, we present the results of the long-term photometric and spectroscopic observations of the optical counterpart to EXO 0331+530, known as BQ Cam, comparing with the simultaneous X-ray observations. It should be noted although the X-ray properties of the NS have been examined by the various authors since the discovery of the system, the studies regarding the relation between the optical companion and the NS for the optical wavenlengths in the literature are quite out-of-date. Therefore, our results have particular importance since they include the recent spectroscopic/photometric observations.

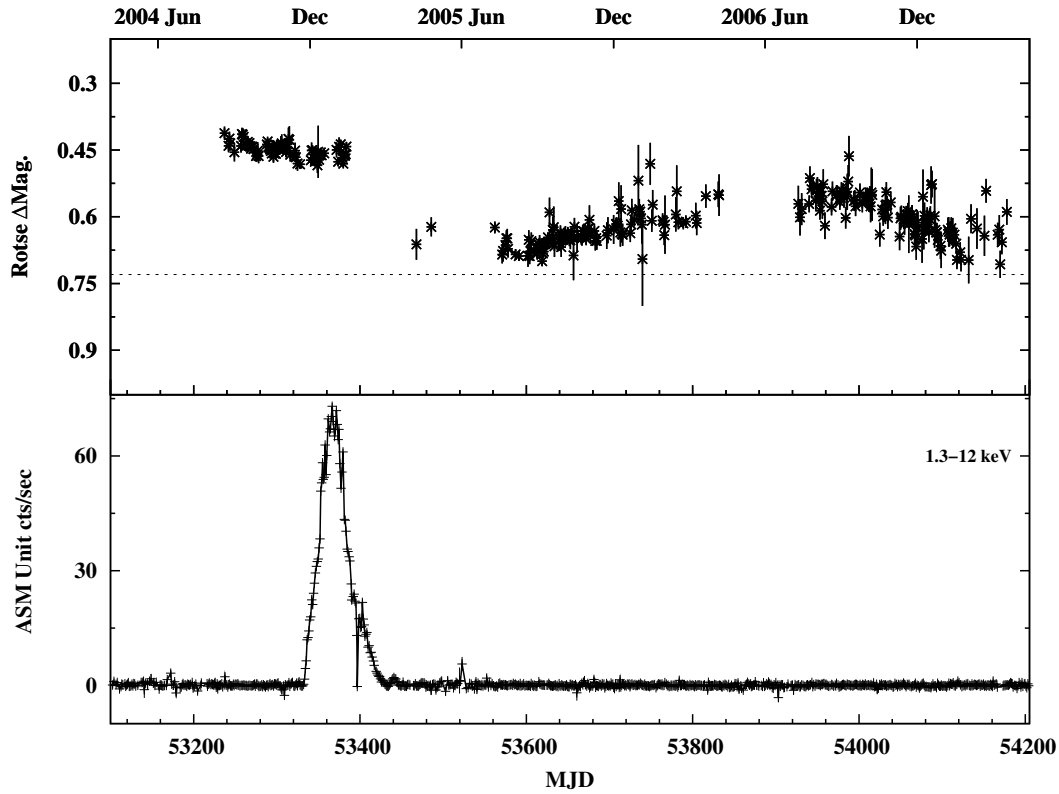


Figure 3.1: ROTSEIIIId daily averaged differential light curve (upper panel) and the *RXTE*/ASM light curve (1.3–12 keV) of EXO 0331+350 for the time interval MJD 53100–54205. The horizontal black-dashed line in the Rotse panel denotes quiescent differential magnitude (~ 0.73) of the source.

3.2.1 Results

3.2.1.1 Optical Photometric Observations

In Figure 3.1, the results of ROTSEIIIId observations of BQ Cam together with the *RXTE*/ASM data for the time interval April 2004–2007 (MJD 53100–54205) are given. A slow decrease in the brightness of the source, ~ 0.25 mag, from 22 August 2004 to 12 July 2005 coinciding with the X-ray outburst is clearly seen. Nearly six months before the X-ray activity, Goranskij & Barsukova (2004) reported a ~ 0.5 mag. brightening (2002–2004) of the source in the *V* band. According to this, we probably see the falling part of this optical outburst. A month after the decrease in

the Rotse magnitude, the X-ray outburst (Type II) was triggered in Nov 2004 (MJD ~ 53331). It means that the optical outburst lasts ~ 3.5 years. Although our data do not cover the onset of the optical outburst, a positive relation between the X-ray flux and the Rotse magnitude is obvious. Reaching a peak flux of ~ 73 mCrab in 1.3–12 keV energy band, the X-ray activity entered a fading state around the end of 2004 (MJD 53367) which lasted about 9 months. The decrease in the optical brightness, on the other hand, continues until July 2005. At that point, a new brightening phase of the source in the optical band started. During that period (MJD ~ 53576 – 54180), unlike the previous outburst, the X-ray flux remains nearly constant even after this slow (~ 2 years), and weak (~ 0.2 mag) optical variation.

After a ~ 3.5 year quiescence in X-rays and ~ 5 months in optical wavelengths, the system underwent a new active period. Similar to the X-ray outburst in between 2004–2005, optical companion entered that brightening state nearly a 1.5 y before the NS. The Rotse and *Swift*/BAT light-curves (15–50 keV) of the source from 24 June 2008 to 8 January 2013 are shown in Figure 3.2. When the enhancement in the optical brightness reached a value of ~ 0.25 mag. a new X-ray outburst was triggered around 17 October 2008 (MJD 54756) roughly six days before the periastron passage of the NS (vertical red-dashed lines in Fig.3.2). This large flare lasted about 40 days and reached a flux of ~ 214 mCrab within 3 weeks. It should be pointed out that the optical magnitude of the source shows a sudden decrease when the X-ray outburst declines. Fading of the optical companion continues till the end of January 2009 (MJD ~ 54850) and soon after it turned back to its brightening state. The X-ray flux goes back to its quiescent state again until the optical magnitudes approach to a peak value of 0.25 corresponding to a 0.5 mag. enhancement comparing to the quiescent brightness of BQ Cam. A new X-ray phase of the system started in November 2009 again a few days after the periastron passage (MJD ~ 55140) of the NS. That activity includes five small but periodic outbursts separated by the orbital period (34.25 d) of the system classified as Type I. The second outburst of these series is the most powerful one with a peak flux of ~ 110 mCrab. The optical magnitude, on the other hand, started to decrease with declining of the second outburst (MJD ~ 55201). The X-ray activities finished by the end of the May 2010 (MJD ~ 55312) while the optical magnitude was still fading. It ceased around August 2011 (MJD ~ 55780) and lasted

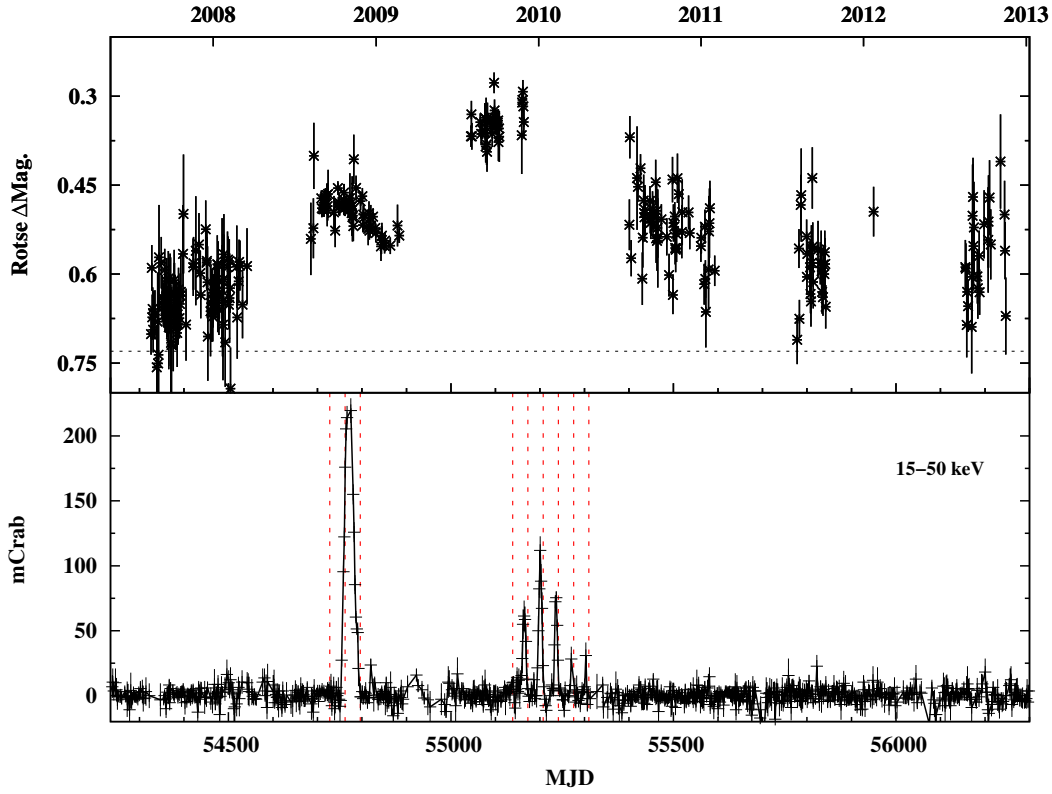


Figure 3.2: Comparison of *Swift*/BAT light-curve (15–50 keV) with a bin size equal to 2 days with the ROTSEIIIId magnitudes of EXO 0331+350, for the time interval MJD 54275–56300. The horizontal black-dashed line in the Rotse panel denotes quiescent differential magnitude (~ 0.73) of BQ Cam whereas the vertical red-dashed line in the X-ray panel represents the time of the periastron passages of the NS.

~ 4 years.

Therefore, the time scale for the optical outbursts of EXO 0331+330 can be given as ~ 2 –4 years depending onto its three activities. In addition they generally start nearly 1.5–2.5 years before the X-ray activity. On the other hand, we see much shorter time scales for the X-ray outbursts; 35–40 d (orbital period) for the giant outburst and 15–18 d (half of the period) for the normal outbursts. To sum up, it is obvious from the observations that the Be star in the system spends most of its time in the long and consecutive optical brightening phases.

3.2.1.2 H α Observations

The long-term H α line monitoring of BQ Cam for September 2006–January 2014 is shown in Figure 3.3. In contrast to the previous works stating the H α profile variations (Negueruela et al. 1998, 1999), we do not see such variability patterns during the observation period. Instead, all the line profiles are nearly-symmetric in a single-peaked form despite the lack of the observations for the period 2010–2011.

Having the same single-peaked emission profile on a long-term basis, H α line strength does not show a constant trend during the spectroscopic observations (see Table 3.2). In Figure 3.4, the evolution of EW and FWHM measurements of the emission line is shown. The first two measurements of the line coincide with the declining phase of the optical outburst seen in the time interval MJD 53576–54180. The EW values decrease as the star fades away which can be attributed to the weakening of the accretion disk. Besides, this decreasing pattern continues even after the second optical outburst triggered (MJD \sim 54324). It means that we see a reverse relation between the optical magnitude and the width of the emission line until 4 March 2009 (MJD 54894) when the lowest value of H α is reached. After about seven months, the EW reaches a value of 5.21 Å. Although this sudden increase in the line width well fits with the rising of optical magnitude, we cannot make any further explanation regarding the behavior of the emission line due to the inadequate data for 2010–2011. In 2012–2014, we see that the strength of the H α line keeps its varying pattern. However, again, since we do not have any photometric observations of the source it is not possible to examine its relation with the optical magnitudes. But we can surely state that these variations are not related to the X-rays as no recent X-ray activity of the source has been reported for this period.

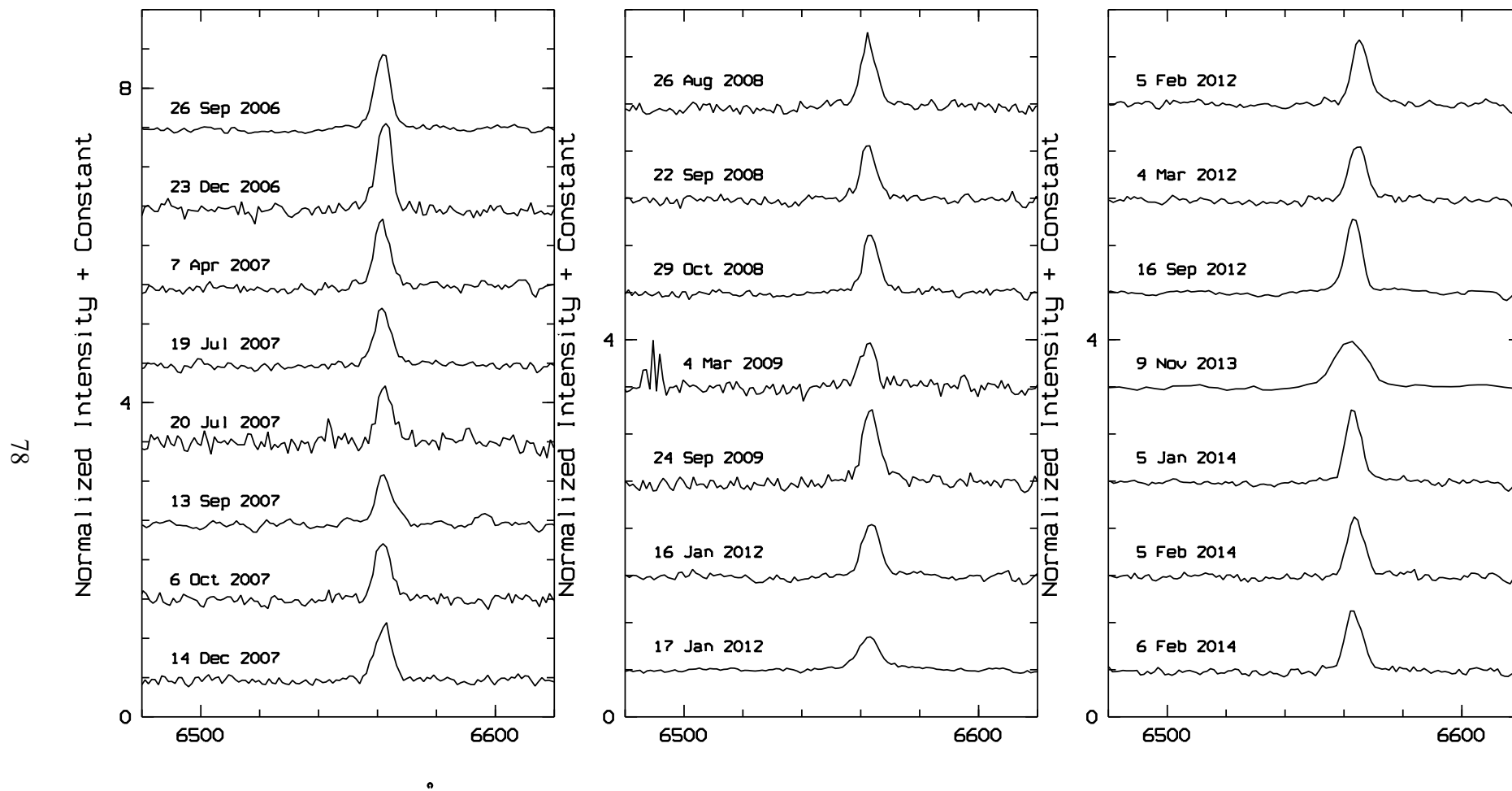


Figure 3.3: H α line profiles of EXO 0331+530 observed between 2006–2014. The single-peaked emission of the line does not change on a long-term basis.

Table 3.2: H α line EW and FWHM measurements for EXO 0331+530. Negative values of EW indicate that the line is in emission.

DATE	MJD	EW(H α) (\AA)	FWHM(H α) (\AA)
2006-Sep-26	54004.9238	-6.21 \pm 0.71	6.18 \pm 0.38
2006-Dec-23	54092.9543	-7.05 \pm 0.56	5.83 \pm 0.55
2007-Apr-07	54197.7388	-5.85 \pm 0.33	6.48 \pm 0.83
2007-Jul-19	54300.0279	-5.11 \pm 0.10	6.83 \pm 0.22
2007-Jul-20	54301.0591	-4.80 \pm 0.49	6.40 \pm 0.68
2007-Sep-13	54356.9962	-3.82 \pm 0.18	6.20 \pm 0.67
2007-Oct-06	54379.0510	-5.26 \pm 0.18	6.62 \pm 0.40
2007-Dec-14	54448.8768	-4.62 \pm 0.17	6.42 \pm 0.29
2008-Aug-26	54704.9757	-4.70 \pm 0.09	6.31 \pm 0.48
2008-Sep-22	54731.0652	-3.97 \pm 0.09	6.49 \pm 0.62
2008-Oct-29	54768.8500	-4.45 \pm 0.10	6.69 \pm 0.26
2009-Mar-04	54894.7260	-3.13 \pm 0.23	6.36 \pm 0.34
2009-Sep-24	55098.9814	-5.21 \pm 0.12	6.56 \pm 0.44
2012-Jan-16	55942.8952	-4.38 \pm 0.07	7.22 \pm 0.28
2012-Jan-17	55943.7739	-4.86 \pm 0.07	9.38 \pm 0.62
2012-Feb-05	55962.8764	-5.45 \pm 0.10	7.42 \pm 0.20
2012-Mar-04	55990.8104	-4.22 \pm 0.09	6.82 \pm 0.17
2012-Sep-16	56186.0446	-5.83 \pm 0.10	6.84 \pm 0.28
2013-Nov-09	56605.0347	-7.44 \pm 0.08	13.73 \pm 0.66
2014-Jan-05	56662.8496	-5.25 \pm 0.14	6.48 \pm 0.67
2014-Feb-05	56693.7630	-4.34 \pm 0.20	6.62 \pm 0.37
2014-Feb-06	56694.8018	-4.93 \pm 0.33	7.28 \pm 0.40

In contrast to the variations in EW values, the FWHM values stay approximately constant until the end of 2012. At that point, the FWHM values start to follow nearly the same pattern of EW. Indeed, showing a similar behavior is not unusual for EW and FWHM. Because the width of the emission profile is directly related to the rotational velocity of the Be star. Hanuschik (1989) gives the relation between the H α widths

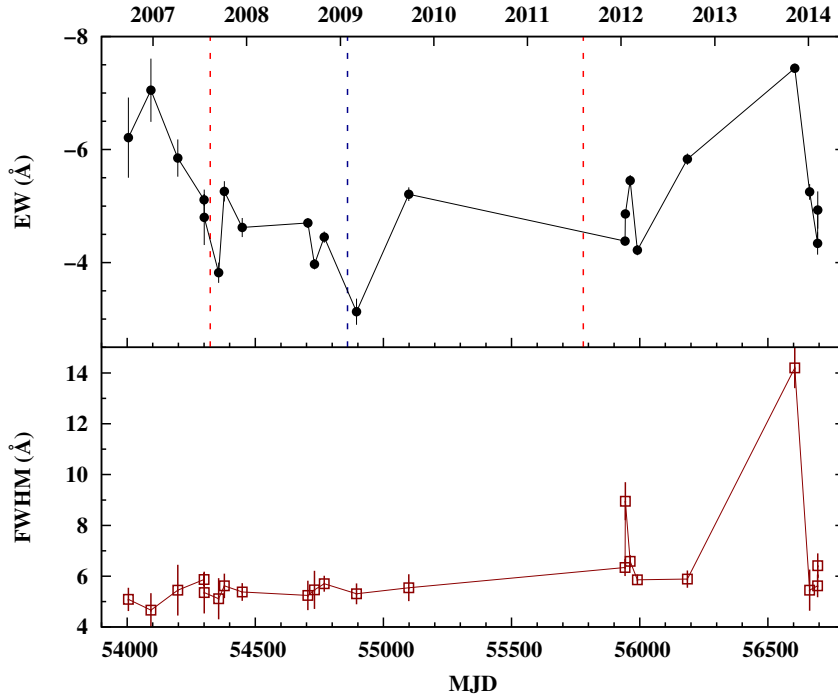


Figure 3.4: Evolution of the EW and FWHM measurements of the $H\alpha$ emission line. The red-dashed vertical line denotes the beginning and ending of the optical outburst seen in ROTSEIIIId light curve (see also Fig.3.2) whereas black-dashed line shows the time of the turning point from decreasing to increasing trend just after (~ 10 d) the strong X-ray outburst around MJD ~ 54850 .

and the projected rotational velocity, $vsini$, as follows,

$$\log \left(\frac{FWHM(H\alpha)}{1.23 \times vsini + 70} \right) = -0.08 \times \log EW(H\alpha) + 0.14, \quad (3.1)$$

where EW is in \AA , FWHM and $vsini$ are in units of km s^{-1} . The projected rotational velocity of the source is found to be $vsini \sim 159 \text{ km s}^{-1}$, using the the average values of 5.04 \AA and 322.39 km s^{-1} for the EW and FWHM respectively. For the true rotational velocity of EXO 0331+530, we have assumed the inclination angle of the system as $i \lesssim 18.9^\circ$ suggested by Zhang et al. (2005). Therefore, the lower limit to the true rotational velocity would be 491 km s^{-1} . Using the typical mass and radius values for a late O-type star ($M \gtrsim 20 M_\odot$ and $R \gtrsim 15 R_\odot$), the break-up velocity is determined as 600 km s^{-1} that is well above the rotational velocity.

3.2.2 Discussion

We can surely infer from the long-term ROTSEIIIId observations of EXO 0331+530 that the source spends most of its time in the optical brightening phases which last $\sim 2\text{--}4$ years. Excluding the second optical outburst between MJD 54324–55780 detected by Rotse, all of the brightening phases accompanied with the X-ray activities starting with a main outburst (Type II) and following series of relatively small outbursts (Type I). Indeed, the similar time scales for the brightenings were previously reported by Goranskii (2001) based on their 18-year (1983–2000) optical photometric observations. It is also important to note that the X-ray outbursts usually occur $\sim 1.5\text{--}2$ years after the optical outbursts. For the 2004 X-ray outburst, the optical magnitude show linear relation with decreasing X-ray flux. This behavior can be well explained by the weakening of the decretion disk during the mass transfer to the NS.

Having a moderate eccentricity of $e=0.31$ with a short orbital period of $P_{orb}=34.25$ d, EXO 0331+530 is one of the BeXRBs that the effect of the truncation exerted by the NS likely to be observed (see Chap. 1.1.2). Due to the small orbit of the companion, the decretion disk cannot expand so much. Thus, it is truncated at a radius smaller than the critical Roche radius. Since the amount of the material supported by the Be star to the disk would be accumulated in time, the increase in the optical brightness can be understood in this way. However the accumulation of the material particularly at the outer part of the disk makes these regions to become optically thick. According to theory by either the radiation-driving warping or a global density wave the outer part of the disk is strongly elongated (Okazaki & Negueruela 2001b). In general, the existence of the global density waves in the decretion disk observationally supported by the V/R variations seen in the emission line profiles. Although the line profile variations for EXO 0331+530 was previously observed by Negueruela et al. (1998) during the period 1990–1991, we do not have any evidence to support this result. Instead, our results contradict with those of Negueruela et al. (1998), since $H\alpha$ lines are always seen in nearly symmetric single-peaked emissions without any significant variations for the time interval 2006–2014. Therefore, we do not have any evidence to support the idea of the the perturbations occurred in the disk as well as the V/R variations.

Formation of an accretion disk during the outbursts (particularly for Type II outburst) have already been revealed for several systems (4U 0115+630, A0532+262, EXO 2030+375) depending on the spin-up of the NS or the presence of the QPO features (Bildsten et al. 1997; Finger et al. 1999; Wilson et al. 2002, and references therein) as well as EXO 0331+530 (Tsygankov et al. 2006). Therefore, it is possible to see that the matter transferred from the accretion disk of the Be star to the NS is not immediately results in X-ray outbursts. Instead, an amount of material should be accumulated in the disk of the NS before the accretion leads to an X-ray outburst. So that the observed delay between the optical and X-ray outburst can be explained.

Recently Okazaki et al. (2013) suggested a new scenario for the formation of Type I and Type II outbursts. According to that, Type I outbursts occurred due to the radiatively inefficient accretion flow (RIAF) from the tidally truncated disks whereas Type II outbursts are produced by the Bondi-Hoyle-Lyttleton (BHL) accretion of the material transferred from the outermost part of a Be disk that is misaligned with orbital plane. These scenarios explain the X-ray outbursts of 4U 0115+634 and A 0535+262 and observed optical spectroscopic/photometric features of them. However, EXO 0331+530 does not fit well in this picture since the spectroscopic/photometric results do not match with these sources in the sample. Besides, the presence of the misalignment of the Be disk with the orbital plane which was suggested by Negueruela et al. (1999) has still been dubious depending on the recovered system parameters measured by Zhang et al. (2005). It is obvious that the observed optical and X-ray features of EXO 0331+530 cannot be completely explained by the suggested mechanisms.

3.3 XTE J1946+274

The hard X-ray transient XTE J1946+274 is one of the poorly-understood sources among Be/X-ray binaries although its X-ray behavior have been studied in detail since its discovery with ASM on board the *RXTE* in 1998 (Smith & Takeshima 1998). The system showed two main transient X-ray active phases detected with different X-ray satellites between 1998 and 2011. The first and the longest X-ray activity lasted about ~ 3 years (between September 1998–August 2001) including 13 consecutive

outbursts (Wilson et al. 2003a). During the initial outburst of these series, having the peak X-ray flux of ~ 110 mCrab in 2-60 keV, it was revealed that the system had an X-ray pulsar with a spin period of 15.83 ± 0.02 s (Smith & Takeshima 1998; Wilson et al. 1998b) orbiting around its Be companion with a period of 169.2 days in an 0.33 eccentric orbit (Campana et al. 1999; Wilson et al. 2003a). In addition the existence of a cyclotron resonance scattering feature (CRSF) at ~ 35 keV was reported by Heindl et al. (2001) using the 1998 outburst observations of High Energy X-Ray Timing Experiment (HEXTE) and Proportional Counter Array (PCA) on *RXTE*.

After a ~ 9 year quiescence in X-rays, the system underwent a new outburst phase starting on 2010 June 4, reaching a value of 140 mCrab in the 15–50 keV energy band within ~ 22 days on *Swift*/Burst Alert Telescope (BAT) hard X-ray transient monitor (Krimm et al. 2010d; Müller et al. 2012). Similar to the previous active phase of the source, the second outburst period was again in a series including an initial giant outburst followed by four fainter ones (Caballero et al. 2010; Camero-Arranz et al. 2010; Müller et al. 2010). The presence of another CRSF feature at ~ 25 keV was discovered indicating the variation of cyclotron lines between the different outbursts (Müller et al. 2012).

In general, X-ray active phases of XTE J1946+274 include two outbursts per orbital period that are possible to be produced if the Be disk and the orbital plane are offset (Priedhorsky & Holt 1987). However for XTE J1946+274 the outbursts do not coincide with the time of periastron and apastron passages of the neutron star that would be expected to happen for similar misaligned Be/X-ray systems (Müller et al. 2012; Wilson et al. 2003a, and references therein). Therefore the additional mechanisms would be responsible for this unique behavior.

The optical/IR counterpart to XTE J1946+274 was discovered by Verrecchia et al. (2002) nearly ~ 3 years after the first X-ray activity of the system. It is a relatively faint $V = 16.9$, reddened B0–1 IV–Ve type star having strong $H\alpha$ and $H\beta$ emission lines in its spectra suggesting the presence of the decretion disk. Subsequent optical spectroscopic observations revealed the profile variations of $H\alpha$ emission lines implying the existence of global density perturbations in the disk (Wilson et al. 2003a).

In this work we present the results of the the first long-term optical/IR observations of XTE J1946+274. Since the hard X-ray transient XTE J1946+274 spends most of its life in X-ray quiescent phase, our spectroscopic and photometric data mainly cover this inactive periods between the X-ray brightening phases (see Fig. 3.5). The observations of XTE J1946+274 separated to 3 parts: quiescent state I, covering the period between the 2 outburst phases starting from MJD 53465 (April 2005) to 55350 (June 2010), active state, for the interval MJD 55350–55800 and quiescent state II which includes the recent observations. We used optical/IR data from our monitoring programme on Be/X-ray binaries involving several ground-based astronomical observatories (Camero et al. 2014, the first paper of this monitoring campaign), in addition to the survey data of the different space-borne telescopes to investigate the relation between the X-ray and optical/infrared bands.

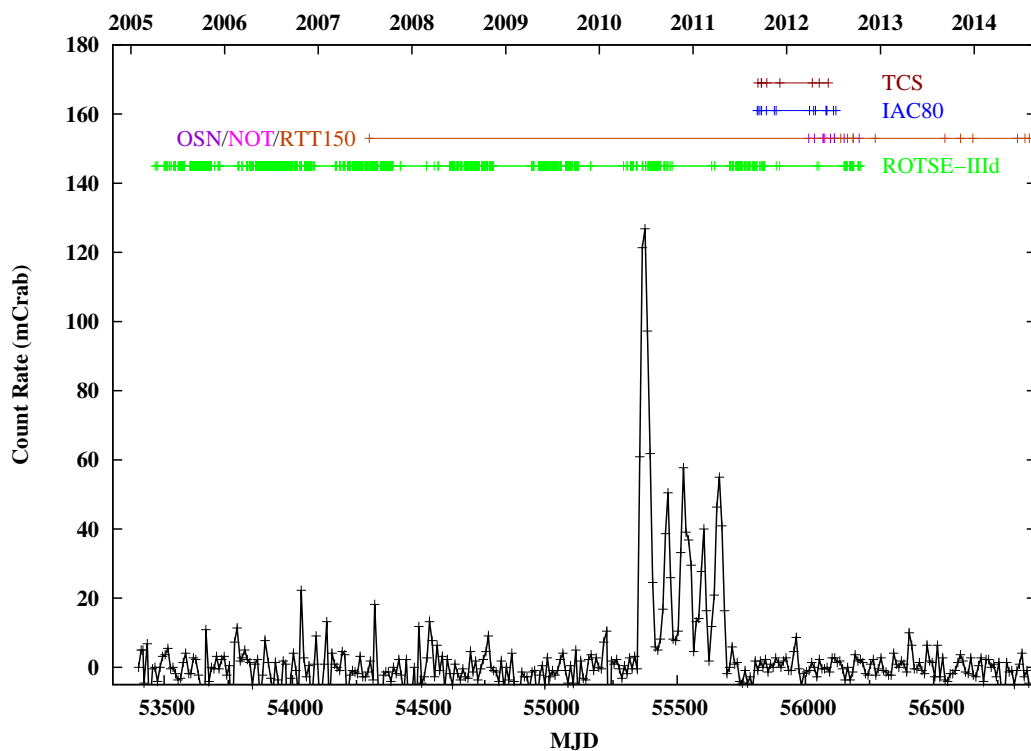


Figure 3.5: *Swift*/BAT light-curve (15–50 keV) with a bin size equal to 10 d. Tick marks on the segments located above the light-curve denote the times of the optical/IR photometric data from the ground-based telescopes ROTSEIIIId (green), IAC80 (blue) and TCS (red) and the optical spectroscopic observations come from OSN (purple), NOT (magenta) and RTT150 (orange) (see also Table 3.3).

3.3.1 Results

3.3.1.1 Quiescent State I (MJD 52130–55350)

The optical counterpart to XTE J1946+274 was monitored with ROTSEIIIId telescope through this period starting at MJD 53465 corresponding to ~ 12 orbits of the neutron star. Due to large gaps between the observations, the data separated into 6 sets in order to seek the possible variations clearly (see Fig. 3.6). However during this quiescent phase of XTE J1946+274, the photometric data do not show a significant variation which could be attributed to a large scaled activity in the decretion disk of the optical companion. On the other hand we see a relatively slow brightening (~ 0.08 mag) of the source between the individual segments. The measured average Rotse magnitudes for 6 panels are 14.96 ± 0.06 , 14.95 ± 0.08 , 14.91 ± 0.09 , 14.93 ± 0.09 , 14.88 ± 0.08 and 14.89 ± 0.09 represented by the black-dashed lines respectively in Figure 3.6.

We also searched for a periodic variability in the light curve of quiescent period I using Lomb-Scargle (Lomb 1976; Scargle 1982, 1989) and Clean (Roberts et al. 1987) algorithms. The power spectra obtained from these analysis can be seen in Figure 3.7 in a log-log plot. Frequency analysis was applied to all photometric data, including 1747 points, over a range from 0 to 17.49 d^{-1} (Nyquist frequency). However except the power at frequency 1 d^{-1} , the effect of the daily observations, the time series of the quiescent I phase do not show any periodic variations (see Fig. 3.7).

The only optical spectroscopic measurement in the literature coincides with this period belongs to Wilson et al. (2003a) who suggest the existence of perturbations in the circumstellar disk with the X-ray turn-off regarding to the $H\alpha$ profile variations between 2001 June 29 (MJD 52032) and 2001 July 17 (MJD 52107). In general $H\alpha$ is always seen in single-peaked emission with an average EW value of $\sim 42 \text{ \AA}$ in their work. Furthermore due to the narrowness of the line profile ($\text{FWHM} = 8.6 \text{ \AA}$) they suggested that the Be star might be viewed nearly pole-on as a result of the relatively low inclination angle. Similarly, $H\alpha$ profile of 2007 July 18 is a narrow (see Table 3.3) single-peaked emission with EW of 37.35 \AA as seen in Figure 3.8. Nevertheless we cannot make a firm interpretation about the physical conditions in the decretion disk since we do not have any other spectroscopic observations of the source through this

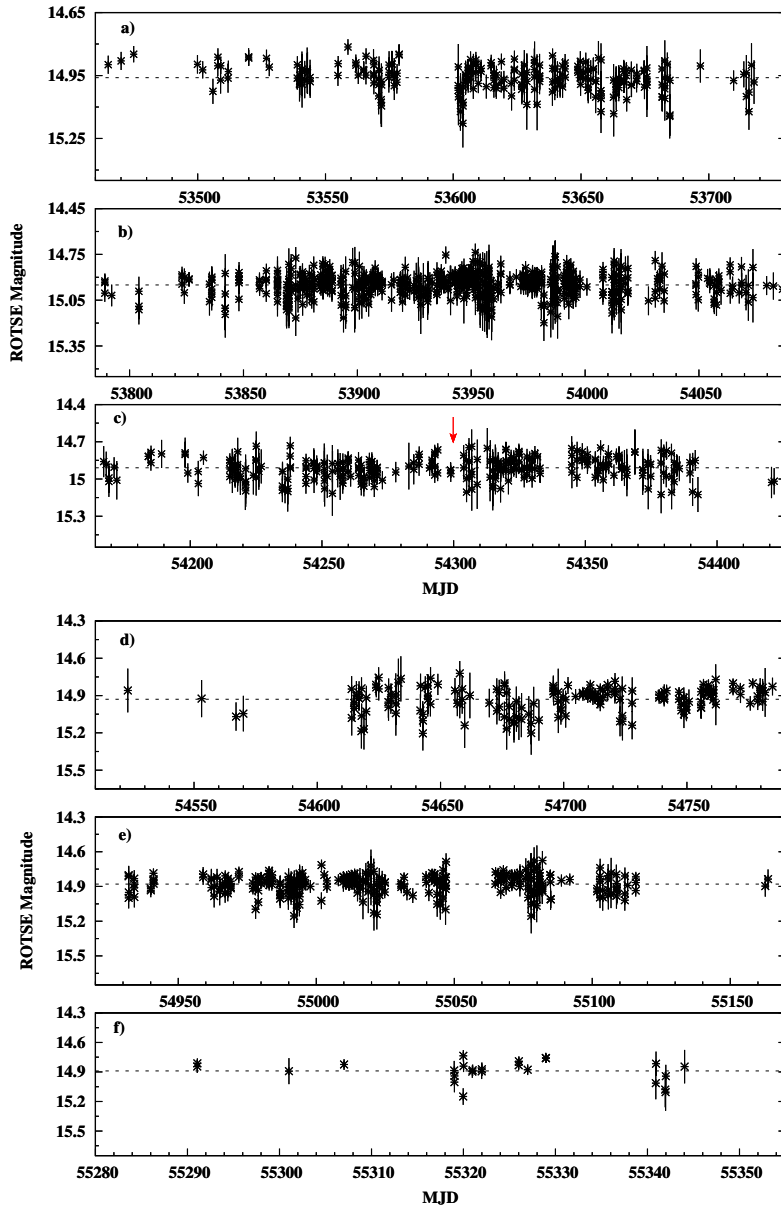


Figure 3.6: ROTSE IIIId light curves of the optical counterpart to XTE J1946+274 for the quiescent phase I. The LCs are separated to six parts (a–f) on a \sim yearly basis. The red arrow in the panel (c) indicates the time of the spectroscopic observation performed with RTT150. The average magnitude of each panel is represented by the black-dashed lines denoting 14.96 ± 0.06 , 14.95 ± 0.08 , 14.91 ± 0.09 , 14.93 ± 0.09 , 14.88 ± 0.08 and 14.89 ± 0.09 respectively.

period.

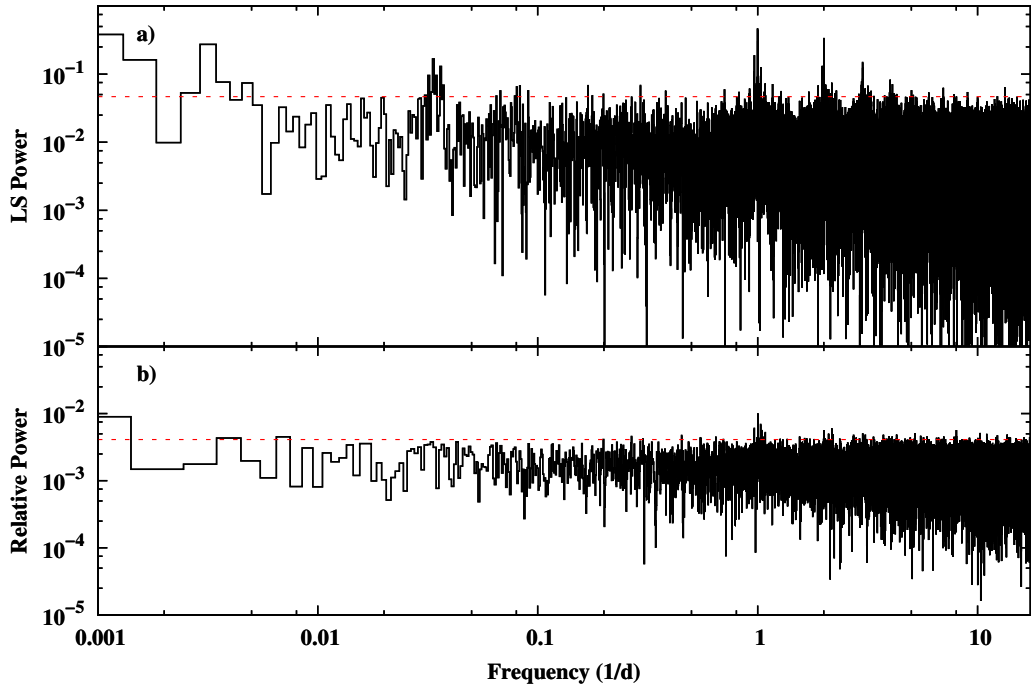


Figure 3.7: Power spectra of ROTSEIII data of XTE J1946+274 obtained with Lomb-Scargle (upper) and Clean algorithms (below). The red-dashed lines in each panel represent the $P=99\%$ confidence levels above which only observational windows are seen.

3.3.1.2 Active State (MJD 55350–55800)

This period covers the last X-ray activity of the source between June 2010–June 2011. The main (giant) outburst lasted ~ 60 days reached a flux of ~ 140 mCrab in 15–50 keV (see Fig. 3.9). The following four outbursts are seen in a series, typical to Type I outbursts, with a separation of 60–90 days. In contrast to the other Be/X-ray systems showing recurrent series of normal outbursts, they do not coincide with the time of periastron passage of the NS. Scattering around the average magnitude of ~ 14.9 , the Rotse magnitude of the optical companion does not seem to be affected before/after the X-ray active phase despite the lack of the data during the normal outbursts. Although, the giant outbursts indicate the large-scaled disruptions of the accretion disk due to the accretion of the large amount of material to the NS, it is obvious that this picture is not valid for XTE J1946+274.

Table 3.3: H α equivalent width (EW) measurements of optical counterpart to XTE J1946+274.

DATE	MJD	EW (\AA)	FWHM (\AA)	Telescope
2007-Jul-18	54299.816	-37.35 ± 1.39	9.88 ± 0.27	RTT150
2012-Mar-27	56013.148	-17.73 ± 0.76	11.09 ± 0.46	OSN
2012-Apr-18	56035.132	-28.49 ± 1.20	11.57 ± 0.30	OSN
2012-May-22	56069.014	-41.65 ± 1.31	10.19 ± 0.46	OSN
2012-May-22	56069.039	-40.70 ± 1.39	9.87 ± 0.15	OSN
2012-May-28	56075.024	-45.16 ± 1.36	10.40 ± 0.78	NOT
2012-Jun-19	56097.997	-39.87 ± 1.52	10.30 ± 0.11	OSN
2012-Jul-4	56112.963	-45.07 ± 1.01	9.69 ± 0.74	OSN
2012-Jul-5	56113.030	-47.62 ± 0.95	10.21 ± 0.94	OSN
2012-Jul-29	56137.922	-39.12 ± 0.86	10.12 ± 0.32	RTT150
2012-Aug-11	56150.981	-44.46 ± 1.18	10.62 ± 0.44	OSN
2012-Aug-24	56163.847	-41.64 ± 1.74	10.14 ± 0.31	RTT150
2012-Sep-15	56185.758	-40.00 ± 0.86	9.78 ± 0.31	RTT150
2012-Sep-16	56186.734	-39.65 ± 1.15	9.76 ± 0.31	RTT150
2012-Oct-09	56209.917	-42.18 ± 1.11	11.66 ± 0.26	OSN
2012-Dec-11	56272.669	-42.58 ± 2.04	10.35 ± 0.31	RTT150
2013-Sep-08	56543.815	-40.11 ± 1.35	9.88 ± 0.31	RTT150
2013-Nov-08	56604.714	-36.11 ± 0.58	13.33 ± 0.13	RTT150
2013-Dec-26	56652.890	-38.68 ± 1.79	14.09 ± 0.88	RTT150
2014-Jun-19	56827.041	-39.60 ± 0.97	9.07 ± 0.49	RTT150
2014-Jul-17	56855.813	-42.79 ± 1.10	9.95 ± 0.60	RTT150
2014-Aug-03	56872.859	-41.06 ± 0.80	9.85 ± 0.43	RTT150

3.3.1.3 Quiescent State II (MJD 55800–up to now)

After the 2010–2011 X-ray outburst series, the Be/X-ray binary XTE J1946+274 did not show any transient activity. The source has still been in quiescent phase that has been ongoing for ~ 3 years. In Figure 3.10 the optical light curves taken with B/V/J/H/K_s filters in addition to the Rotse data correspond to the time interval 2011 July–2012 December. The optical/IR magnitudes of the source follow a nearly

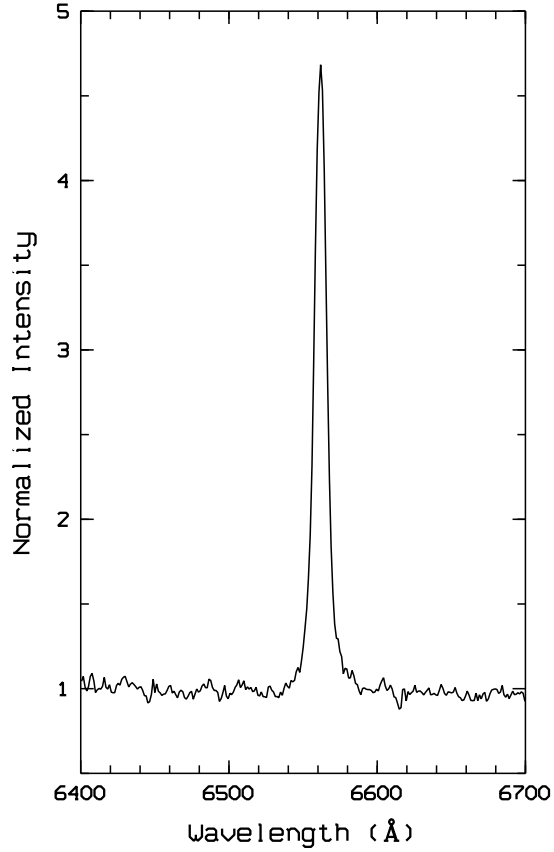


Figure 3.8: $H\alpha$ line emission observed in the spectrum of 2007 Jul 18. The EW and FWHM measurements of the line is compatible with the values detected by Wilson et al. (2003a).

constant trend over the period (see Table 3.4). In fact, this appearance is not different from the one observed during the quiescent state I and the X-ray outburst phase.

On the other hand, we can find the distance to the source using the observed B and V magnitudes. For this estimation, the amount of the extinction has to be determined via the total color excess (reddening), $E(B - V)$, in optical wavelengths. It is defined as,

$$E(B - V) = (B - V)_o - (B - V)_i, \quad (3.2)$$

where $(B - V)_o$ is the observed color excess and $(B - V)_i$ is the intrinsic color excess depending on the spectral and luminosity classification of the star. Owing to the uncertainty in the spectral/luminosity class of XTE J1946+274, the intrinsic color for the source was chosen to be -0.24 for a B0–1 type main sequence star, from the study of Wegner (1994). The total color excess in the optical band is found

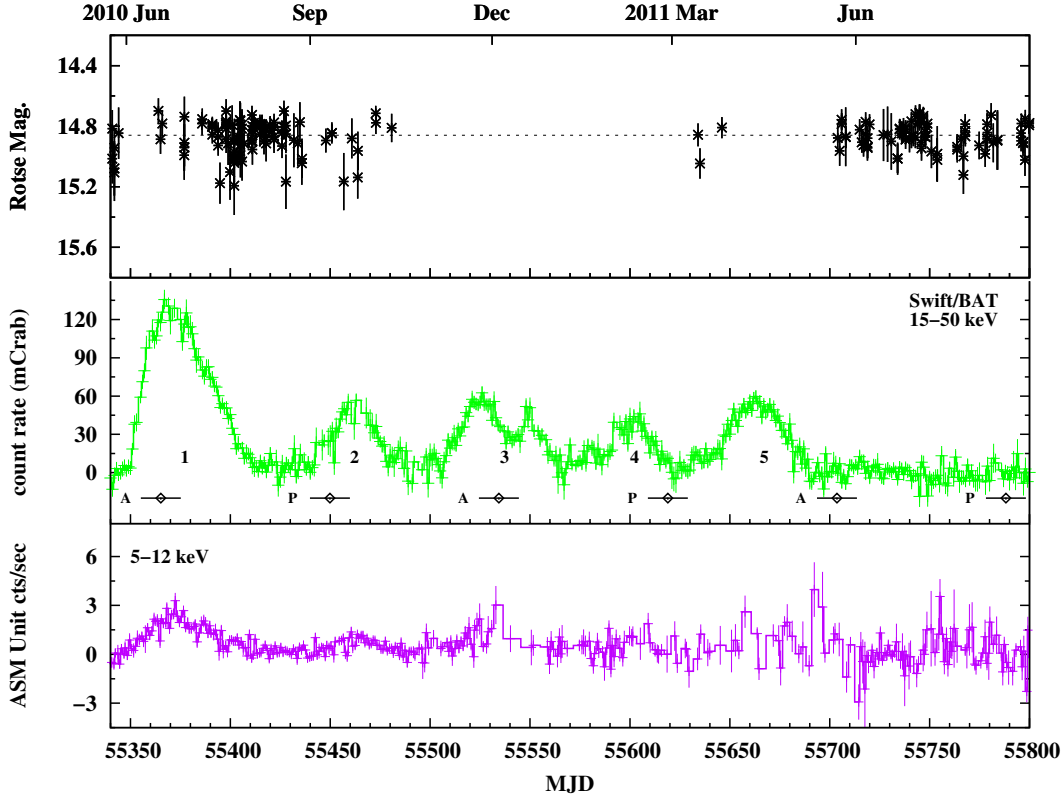


Figure 3.9: Comparison of ROTSEIIIId magnitudes (upper) with the *Swift*/BAT (middle) and *RXTE*/ASM (lower) light curves of XTE J1946+274 during the X-ray activity. The black-dashed line in ROTSEIIIId panel shows the average of 53 data points. The time of the periastron and apastron passages of the NS is marked with diamonds and corresponding letters (A and P) in the middle panel.

as 1.62, using the average observed excess of 1.38 ± 0.04 . The extinction in the visual band is given by,

$$A_V = R \times E(B - V), \quad (3.3)$$

here R is the extinction parameter with a value of 3.1. Thus, we derive the visual extinction of XTE J1946+274 as $A_V = 5.02$. Using the standard distance modulus,

$$d = 10^{\left(\frac{V - M_V + 5 - A_V}{5}\right)} (\text{kpc}), \quad (3.4)$$

where $M_V = 2.95$ is the absolute magnitude of a B1 V type star (Wegner 2006) and V is the observed visual magnitude, the distance to the source is found as ~ 18 kpc. In general, the total excess in optical band is the sum of two components; the circumstellar excess caused by the photons in the decretion disk of the Be star and the excess of

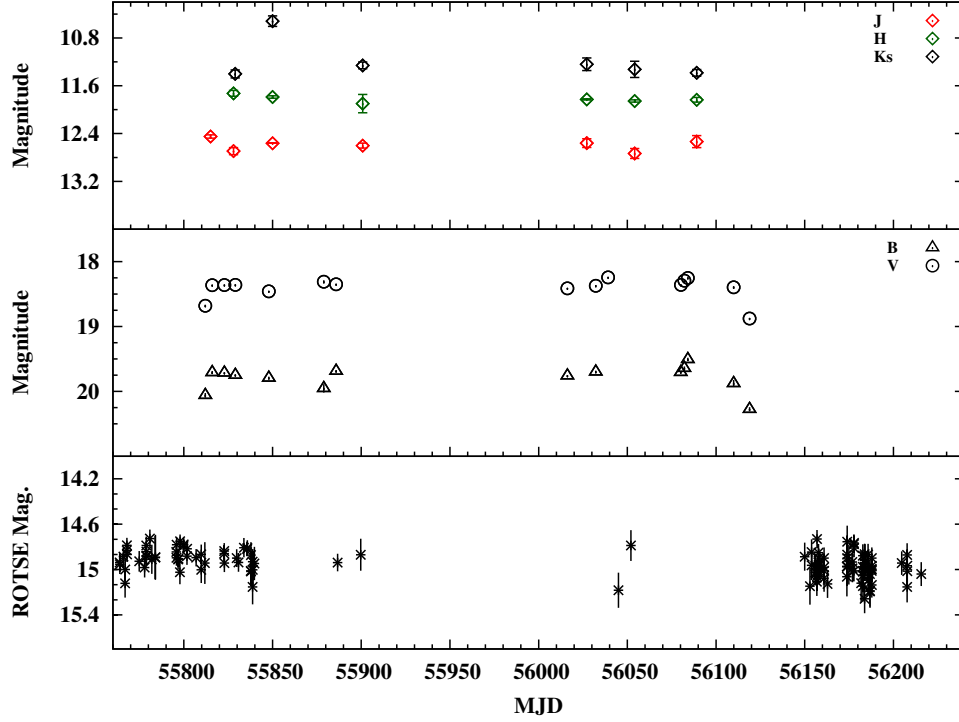


Figure 3.10: Optical/IR light curves of XTE J1946+274 for the quiescent state2.

dust produced in the interstellar medium between the observer and the source. Therefore, to find the real reddening measurement of a Be star, it is important to use the magnitudes observed during the disk-loss phase to eliminate the contribution of the disk. However for the case of XTE J1946+274, the disk is always present since the $H\alpha$ line is never seen in absorption (see Table 3.3). Since the effect of the circumstellar material on the color is very difficult to disentangle, ~ 18 kpc is thought to be a rough estimate of the upper distance limit.

In Figure 3.11, we present the spectroscopic tracing of the $H\alpha$ line profiles observed between 2012–2014. The $H\alpha$ line is always seen in a single-peaked emission even its EW and FWHM measurements show significant variations in Figure 3.12. The first spectroscopic observation of this period has the lowest value of $H\alpha$ emission line, $\sim 18 \text{ \AA}$, ever observed for XTE J1946+274. The weakness of this emission comparing to the typical values of XTE J1946+274 might be interpreted as the variations in the decretion disk of the Be star. However, the optical/IR light curves of the source do not indicate such a variation for this period. Assuming that the EW measurement of $H\alpha$ line emission is also related to the amount of the material in the emitting re-

Table 3.4: Optical and IR magnitudes of XTE J1946+274 observed with IAC80 and TCS telescopes respectively.

DATE	MJD	B	V	J	H	K _s
2011-Sep-08	55812.053	20.061±0.036	18.681±0.016	—	—	—
2011-Sep-11	55815.974	19.708±0.023	18.364±0.008	12.450±0.028	—	—
2011-Sep-18	55822.863	19.716±0.011	18.360±0.006	—	—	—
2011-Sep-24	55828.975	19.749±0.013	18.358±0.007	12.694±0.059	11.727±0.049	11.402±0.066
2011-Oct-13	55847.866	19.794±0.020	18.459±0.008	—	—	—
2011-Oct-15	55849.970	—	—	12.562±0.001	11.789±0.020	10.520±0.088
2011-Nov-13	55878.858	19.954±0.064	18.311±0.024	—	—	—
2011-Nov-20	55885.801	19.687±0.016	18.349±0.007	—	—	—
2011-Dec-05	55900.815	—	—	12.602±0.042	11.899±0.153	11.260±0.056
2012-Mar-30	56016.195	19.760±0.011	18.413±0.006	—	—	—
2012-Apr-10	56027.140	—	—	12.56±0.074	11.828±0.010	11.241±0.106
2012-Apr-15	56032.193	19.698±0.018	18.372±0.008	—	—	—
2012-Apr-22	56039.194	—	18.244±0.007	—	—	—
2012-May-07	56054.179	—	—	12.734±0.083	11.856±0.019	11.326±0.136
2012-Jun-02	56080.182	19.707±0.010	18.358±0.005	—	—	—
2012-Jun-04	56082.206	19.643±0.028	18.295±0.010	—	—	—
2012-Jun-06	56084.152	19.507±0.026	18.252±0.001	—	—	—
2012-Jun-11	56089.101	—	—	12.535±0.100	11.835±0.039	11.383±0.055
2012-Jul-01	56109.912	19.878±0.054	18.395±0.017	—	—	—
2012-Jul-10	56118.885	20.276±0.032	18.878±0.011	—	—	—

gion of the disk, the weakness of the EW would be the result of the mass loss either through the accretion of the NS or the truncation of its size despite the lack of an X-ray activity. It is also possible that the weakest value we caught does not represent the lowest one, instead it can be a part of the refilling process of the disk after a disk-loss episode. In fact, a sharp increasing trend of the EW right after this value confirms the suggested idea. The increase in EW lasted about three months reaching its peak value of $\sim 48 \text{ \AA}$. It is also important to note that this is the highest EW value of XTE J1946+274 ever observed. Although the line measurements are scattered between MJD 56069–56209, they are not significantly different than the average EW value.

During the observations of October and December 2013, the widest emissions were detected while EW values were around the average. In general the H α line is seen as a narrow single-peaked emission with an average FWHM value of $\sim 10.5 \text{ \AA}$. It is also

important to note that the EW and FWHM values of the source show an inverse relation despite the expected positive relation (Hanuschik 1989). Yet, using the relation given in 3.1 we have calculated the projected rotational velocity of XTE J1946+274 as $v \sin i \sim 323 \text{ km s}^{-1}$ via the average values of EW and FWHM parameters. From the orbital solution of the system, Wilson et al. (2003a) suggested the inclination of XTE J1946+274 to be $\gtrsim 46^\circ$. From this angle, the true rotational velocity, v_{rot} , of the Be star is estimated as $323\text{--}449 \text{ km s}^{-1}$. Taking the mass of the star as $16 M_\odot$ (Wilson et al. 2003a) and $8 R_\odot$ as the limit radius for a B type star, the critical break-up velocity, v_{crit} , is found to be $\sim 618 \text{ km s}^{-1}$. Thus, we find the critical fraction, defined as the ratio of the equatorial rotational velocity to the break-up velocity, of XTE J1946+274 as $w \sim 0.5\text{--}0.72$.

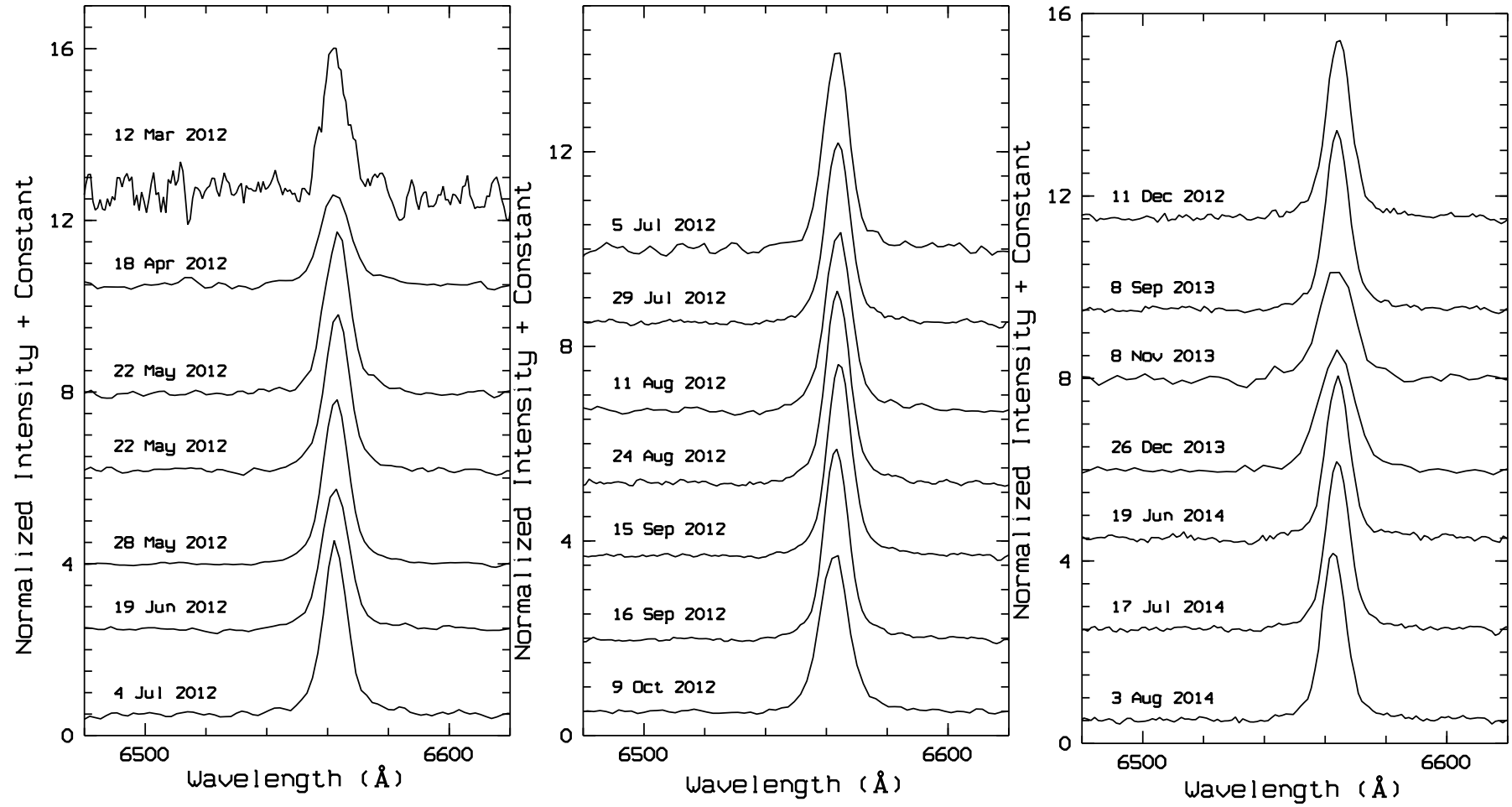


Figure 3.11: $H\alpha$ line profiles of XTE J1946+274 observed between 2012 March–2014 August. The single-peaked emission of the line does not change on a long-term basis.

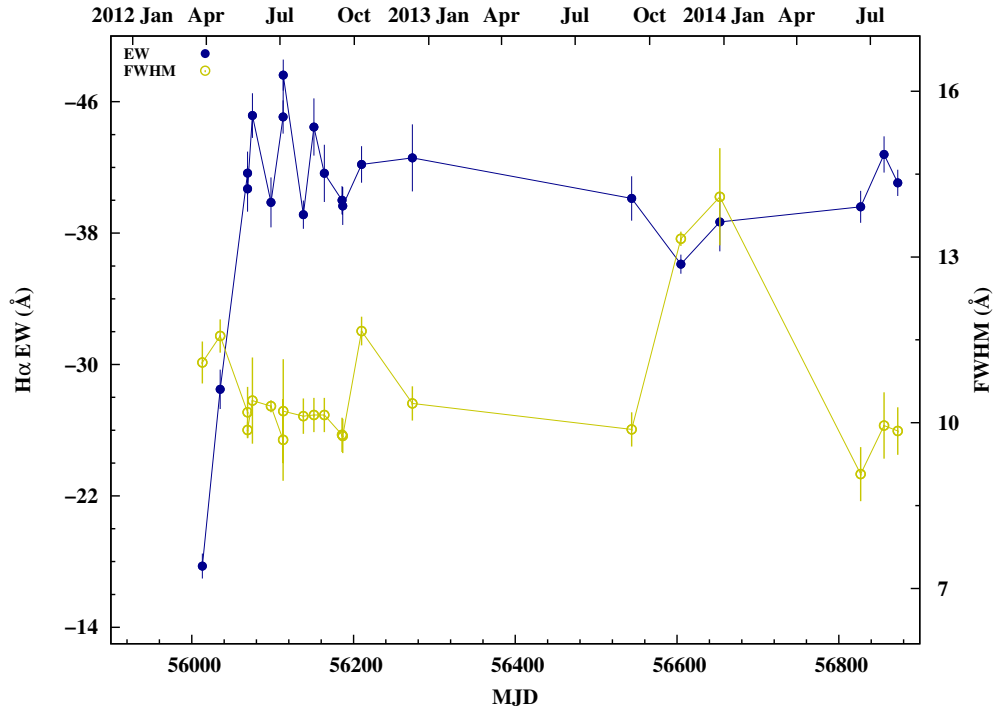


Figure 3.12: The variation of EW and FWHM measurements of $H\alpha$ emission line during the observations. An inverse relation between the two measurements is seen until end of 2013. Note that during the observations both the lowest and the highest values of $H\alpha$ emission for XTE J1946+274 were detected.

3.3.2 Summary and Discussion

In this work, we have presented the first long-term optical/IR observations of XTE J1946+274. Since its discovery, this hard X-ray transient showed two similar X-ray outburst periods with a separation of about a decade. Thus, XTE J1946+274 is one of the BeXRBs that spends most of its time in an X-ray quiescent phase. The uniqueness of the system comes from its X-ray outburst behaviour that is not connected to the orbital passages of the NS as seen in the case of the similar misaligned systems, e.g. EXO 2030+375. The shifts in the outburst phases with respect to the periastron/apastron passages of the NS is thought to be result of the global perturbations triggered by the truncation of the disk radius. However, we have not see any trace of such density wave occurred in the decretion disk that shows itself as the variation of the emission profiles in the spectroscopic data. Wilson et al. (2003a) attributed the variations in the $H\alpha$ emission profile to the existence of the perturbations in the disk

and added the difficulties of detection of the density perturbations in XTE J1946+274 since the relatively small viewing angle restricts the size of the projected area to be observed. According to that, only the large-scaled perturbations can be seen in the disk of XTE J1946+274. In contrast to this idea, Silaj et al. (2010) suggested that emission line profile shapes could not be used to estimate the inclination angle of the system since for a given inclination angle different types of profile shapes might be produced as a result of the density changes in the disk-thermal structure. This means that, conversely the suggested picture of Wilson et al. (2003a) for XTE J1946+274, we should have seen the profile changes if there had occurred any density variations in the decretion disk, despite the small inclination angle of the system.

Our spectroscopic data reveal that the $H\alpha$ line is always seen in narrow, single-peaked emission without any remarkable changes. On the other hand, the evolution of EW measurements indicates a probable disk-loss or disk-fading period before May 2012. Although, either the optical/IR light curves of the source or X-ray data do not support this idea, the enhancement seen in the EW values just after the lowest point might be attributed to an increase in the amount of the disk material. In general, XTE J1946+274 shows strong $H\alpha$ emissions in its spectra. Having a moderate eccentricity of $e=0.33$, and the orbital period of 169.2 days, XTE J1946+ is also unique in the sense of its strong emissions staying nearly constant over the long term observations. It is obvious that the decretion disk of the source remains same even before/after the outburst phases. Comparison of optical/IR light curves with the X-ray also confirms this structure. As a result, the light curves of different energy bands do not show a correlation.

Using the EW and FWHM measurements we also estimated the rotational velocity of the source as 323–449 km s⁻¹. This result indicates that the Be star in XTE J1946+274 is rotating at %50–70 of its break-up velocity typical to the stars for the same type.

3.4 SAX J2103.5+4545⁷

The X-ray transient SAX J2103.5+4545 was discovered with the *BeppoSAX* satellite in 1997 while showing X-ray pulsations of ~ 358 s (Hulleman et al. 1998). The X-ray spectrum of the source in 2–25 keV was well described by an absorbed power-law fit with a photon index of 1.27 ± 0.14 ($N_H = 3.1 \times 10^{22}$ cm $^{-2}$). Having a 12.68 d orbital period (Baykal et al. 2000) and a 358.6 s spin period, SAX J2103.5+4545 is one of the unusual Be/X-ray binaries that falls in wind-fed supergiant region of Corbet diagram (Corbet 1984).

During the second outburst of the system in 1999, detected by the ASM on board the *RXTE*, Baykal et al. (2002) found a correlation between the spin-up rate and the X-ray flux suggesting the existence of an accretion disk during the periastron passage of the NS. In addition, using the *XMM/Newton* observations, İnam et al. (2004) reported the discovery of a transient QPO feature at 22.7 s. The system was in X-ray active phase again in 2001 March, 2002 June, 2007 May, 2010 October and in 2012 June showing a relatively similar X-ray behavior described as a large flare followed by a main outburst (Camero Arranz et al. 2007; Galis et al. 2007; Krimm et al. 2010a; Sguera et al. 2012). In general, SAX J2103.5+454 shows periodic Type I outbursts and X-ray activities similar to the Type II outbursts (Camero Arranz et al. 2007).

The system contains a highly reddened B0 V type emission line star ($V = 14.2$) as the optical counterpart, locating at a distance of 6.8 kpc exhibiting disk-loss and disk-renewal phases correlated with the X-ray outbursts (Baykal et al. 2002; Reig et al. 2004b, 2010a). Blay et al. (2004) showed that change of $H\alpha$ line from emission to absorption coincides with the high and low X-ray luminosity states of the source respectively. Similarly, the enhancement of the brightness in optical/IR wavelengths is usually treated as the precursor of the upcoming X-ray activity (Kiziloglu et al. 2010). Recently, in March 2014, the system entered a new optical and X-ray active phase detected by *INTEGRAL* and optical/IR telescopes respectively (Camero-Arranz et al. 2014b; Ducci et al. 2014).

In this work, we present a long-term study of SAX J2103.5+4545 since 2010. For

⁷ This work is a part of a large collaboration accepted to be published in A&A (Camero et al. 2014)

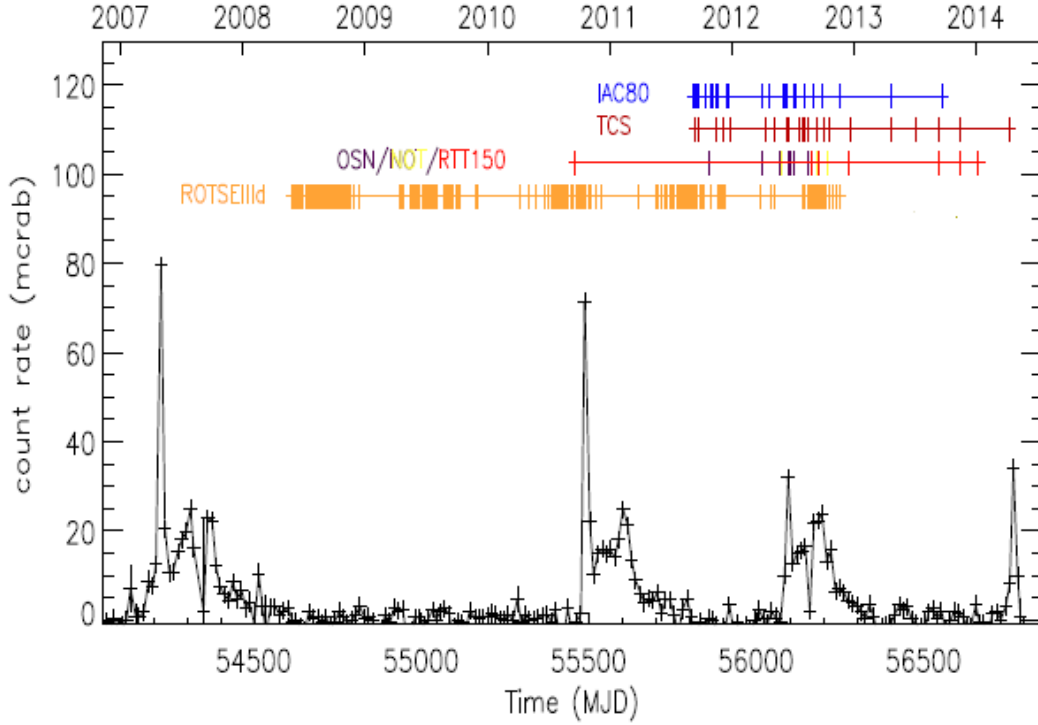


Figure 3.13: *Swift*/BAT light-curve of SAX J2103.5+4545 in 15–50 keV energy band with a bin size equal to the orbital period of 12.68 d. The time span of the optical/IR photometric data from the ground-based telescopes ROTSEIIIId (orange), IAC80 (blue) and TCS (red) are represented by the tickmarks on the segments located above the light-curve. The optical spectroscopic observations performed with OSN (purple), NOT (yellow) and RTT150 (light red) are also denoted in the plot (see also Table 3.7).

this purpose we used optical/IR data from our dedicated campaign involving several ground-based astronomical observatories. In Figure 3.13 the time span of these observations is presented with the *Swift*/BAT light curve.

3.4.1 Results

3.4.1.1 Optical/IR Photometry

In Figure 3.14, the long-term optical/IR observations together with the *Swift*/BAT light curve of SAX J2103.5+4545 are shown (see Tables 3.5 and 3.6). The obser-

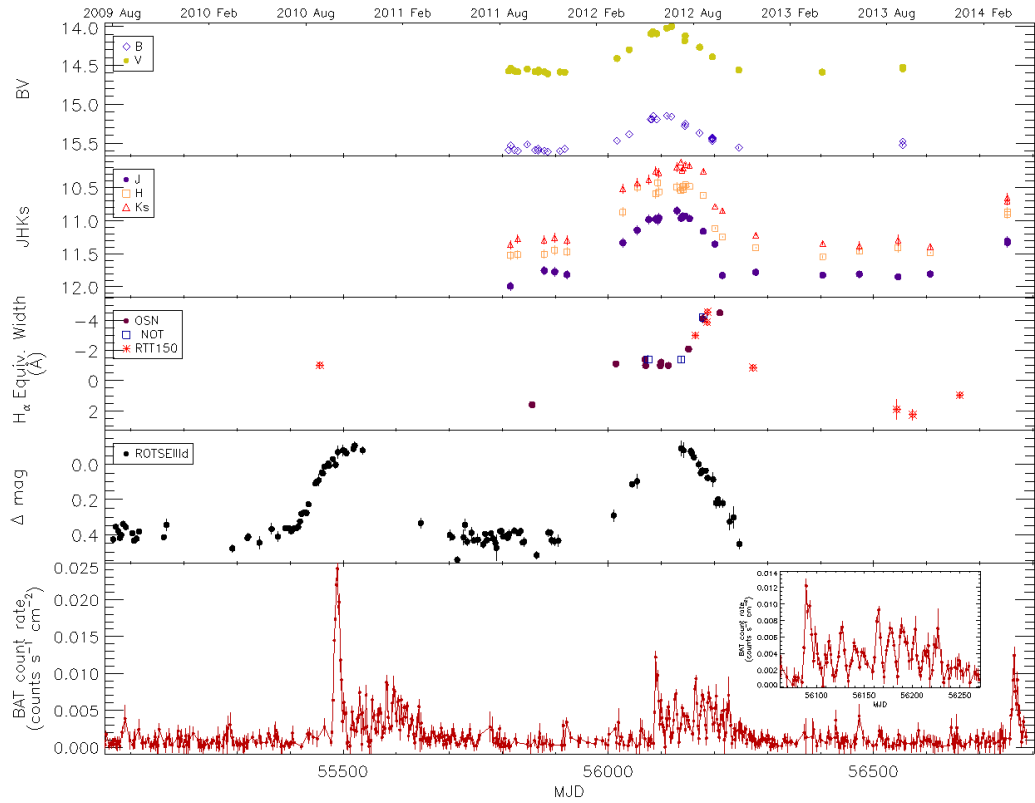


Figure 3.14: Comparison of optical/IR and X-ray light curves of SAX J2103.5+4545. The evolution of the EW measurements of $H\alpha$ line is also added (the third panel) to check the previously suggested relation between the X-ray flux and the line strengths by Blay et al. (2004). The small panel in *Swift*/BAT light curve (with 2-day binning) represents the correlation between the X-ray outbursts and the orbital period of the system for the 2012 X-ray activity (adapted from Camero et al. (2014)).

vations cover the last two outbursts of the system detected in X-ray wavelengths in addition to the recent activity started in March 2014. It is obvious from the figure that the optical/IR magnitudes of the Be star are correlated with the X-ray flux of the NS.

The Rotse differential magnitude (the fourth panel) of the source between May 2010–August 2010 (MJD \sim 55320–55410) shows a smooth rise indicating the beginning of the optical outburst that lasts \sim 1 year. Approximately three months before the peak of this outburst (MJD \sim 55420), the system becomes active in X-rays with an intense flare followed by the weaker periodic outbursts detected in each orbit.

Table 3.5: Optical photometric observations of the optical counterpart to SAX J2103.5+4545 performed with the IAC80 telescope.

Date	MJD	B	V	Date	MJD	B	V
2011/09/08	55812.071	15.587±0.007	14.571±0.004	2012/06/13	56091.144	15.196±0.006	14.092±0.003
2011/09/12	55816.049	15.528±0.008	14.535±0.003	2012/06/30	56108.939	15.148±0.008	14.022±0.003
2011/09/18	55822.883	15.589±0.005	14.574±0.003	2012/07/10	56118.926	15.159±0.006	13.999±0.003
2011/09/24	55828.994	15.600±0.006	14.581±0.003	2012/08/04	56143.970	15.28±0.02	14.184±0.015
2011/10/13	55847.055	15.52±0.01	14.547±0.005	2012/08/06	56145.018	15.25±0.01	14.120±0.006
2011/10/27	55861.925	15.591±0.005	14.582±0.005	2012/09/02	56172.113	15.35±0.01	14.266±0.006
2011/10/27	55861.922	-	14.580±0.003	2012/09/02	56172.110	15.37±0.01	-
2011/11/02	55867.990	15.57±0.01	14.585±0.007	2012/09/25	56195.944	15.47±0.01	-
2011/11/02	55867.992	15.60±0.01	14.563±0.003	2012/09/25	56195.945	15.43±0.02	-
2011/11/13	55878.875	15.599±0.009	14.583±0.004	2012/09/25	56195.947	15.45±0.02	-
2011/11/20	55885.819	15.609±0.005	14.608±0.003	2012/09/25	56195.948	15.44±0.01	-
2011/12/13	55908.871	15.603±0.006	14.585±0.003	2012/09/25	56195.952	15.45±0.01	-
2011/12/22	55917.841	15.574±0.005	14.588±0.003	2012/09/25	56195.953	15.44±0.02	14.389±0.006
2012/03/30	56016.221	15.471±0.006	14.412±0.003	2012/11/14	56245.918	15.56±0.01	14.559±0.007
2012/04/22	56039.218	15.384±0.004	14.300±0.002	2013/04/21	56403.281	-	14.587±0.006
2012/06/02	56080.187	15.195±0.004	14.093±0.002	2013/09/19	56554.946	15.48±0.01	14.526±0.005
2012/06/04	56082.195	15.195±0.006	14.092±0.003	2013/09/19	56554.947	15.53±0.01	14.542±0.005
2012/06/06	56084.166	15.150±0.004	14.067±0.002				

After the activity in X-rays, both ROTSEIIIId and optical/IR magnitudes (the first and the second panel) show nearly a constant trend until March 2012 (MJD \sim 56000). The following X-ray activity starts around \sim 2012 June (MJD \sim 56070), nearly 3 months after the optical brightening, as seen in the previous case lasting \sim 7 months. The system was in a quiescent phase both in optical/IR and in X-ray wavelengths until 2014 March. From the IR magnitudes of the source (the second panel), it can be inferred that the recent X-ray activity started again \sim 3 months after the optical/IR brightening.

In general, the optical/IR outbursts of SAX J2103.5+4545 last for 8–9 months during which the peaks of the activities are always reached before the X-ray maxima. Although the time of the onset of the optical/IR brightenings does not coincide with the X-ray activities, the system goes to the quiescent state in different wavelengths simultaneously.

Table 3.6: IR observations of the optical counterpart to SAX J2103.5+4545 taken with the TCS telescope.

Date	MJD	J	H	Ks
2011/09/11	55815.125	11.99±0.07	11.52±0.07	11.36±0.07
2011/09/24	55828.999	-	11.51±0.07	11.27±0.07
2011/11/13	55878.906	11.75±0.07	11.50±0.07	11.29±0.07
2011/12/03	55898.849	11.77±0.07	11.44±0.07	11.26±0.07
2011/12/26	55921.838	11.81±0.07	11.47±0.07	11.30±0.07
2012/04/10	56027.180	11.33±0.07	10.87±0.07	10.52±0.07
2012/05/07	56054.201	11.14±0.07	10.49±0.07	10.43±0.07
2012/05/29	56076.185	10.98±0.07	-	10.38±0.07
2012/06/11	56089.201	10.97±0.07	10.59±0.07	10.25±0.07
2012/06/15	56093.084	10.99±0.07	10.42±0.07	-
2012/06/17	56095.119	10.96±0.07	10.56±0.07	10.27±0.07
2012/07/21	56129.194	10.85±0.07	10.49±0.07	10.19±0.07
2012/07/29	56137.112	10.96±0.03	10.54±0.03	10.112±0.008
2012/07/31	56139.023	10.953±0.005	10.50±0.01	10.23±0.03
2012/08/02	56141.053	10.927±0.009	10.472±0.003	-
2012/08/02	56141.067	-	10.53±0.02	10.21±0.03
2012/08/06	56145.120	10.934±0.011	10.453±0.015	10.15±0.02
2012/08/13	56152.969	10.964±0.004	10.481±0.002	10.16±0.04
2012/09/08	56178.980	11.160±0.008	10.612±0.002	10.25±0.03
2012/10/01	56201.010	11.354±0.008	11.11±0.02	10.782±0.008
2012/10/14	56214.890	11.83±0.03	11.24±0.01	10.84±0.04
2012/12/16	56277.849	11.780±0.003	11.41±0.01	11.22±0.02
2013/04/22	56404.166	11.824±0.002	11.54±0.02	11.35±0.02
2013/06/30	56473.117	11.81±0.06	11.46±0.03	11.38±0.07
2013/09/11	56546.076	11.85±0.03	11.41±0.07	11.29±0.08
2013/11/10	56606.907	11.81±0.03	-	-
2013/11/10	56606.913	-	11.48±0.01	11.39±0.04
2014/11/10	56606.913	-	11.48±0.01	11.39±0.04
2014/04/05	56752.182	11.31 ±0.07	10.87±0.07	10.70±0.07
2014/04/05	56752.187	11.33 ±0.07	10.90±0.07	10.65±0.07

Using ROTSEIIIId data, we also searched for the possible periodic short-term variations, but we could not detect any significant frequencies could be attributed to the NRP of the Be companion. We found the recurrence time of the optical outbursts of SAX J2103.5+4545 as less than ~ 2 years which was quite shorter than the previ-

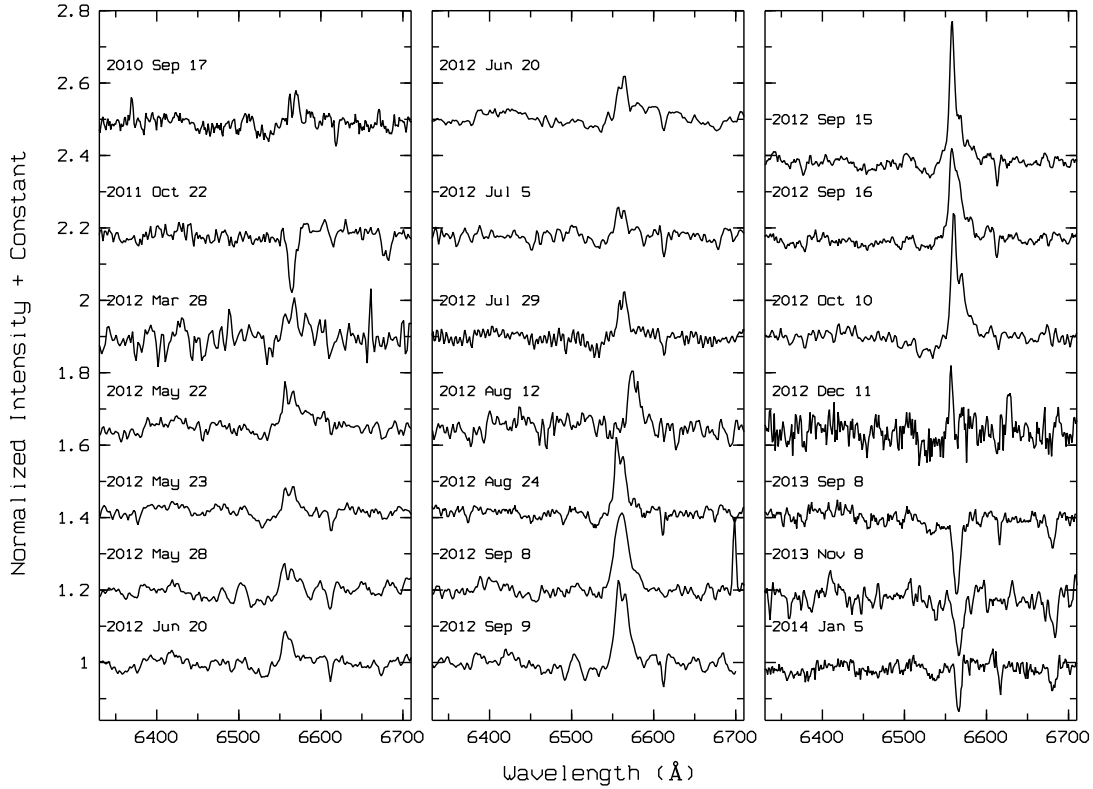


Figure 3.15: Evolution of the H α line profile for SAX J2103.5+4545.

ously suggested one (Reig et al. 2010a).

3.4.1.2 H α Line Variations and Decretion Disk of Be Star

During the spectroscopic observations between Sep 2010–Jan 2014, the H α line shows significant variations indicating the disk-loss and disk-filling phases of the Be companion (see Fig. 3.14 and Fig. 3.15). Although the exact time of the transition from emission to absorption profiles is not clear from our data, we can definitely state that during the 2010 outburst, at least at the time of the X-ray rising state, the decretion disk of the Be star was present. The following spectrum, taken on 22 October 2011, however, is typical to the spectrum of those of the stars with the same spectral type without any emission lines. It is clear that the disk material has been lost during/after the X-ray activity by making the Be star diskless. Similar to the pattern seen for the optical/IR outbursts, the H α line was detected in emission ~ 2 months before the 2012 X-ray activity. The EW measurements of H α line stayed nearly constant until the maximum magnitude was reached in optical/IR wavelengths. It is important to

note that the strength of the line started to increase when the source entered a fading state both in optical/IR and in X-rays. In addition, it just took $\sim 3\text{--}4$ months to lost the materials in the decretion disk, after the maximum value of the EW was reached on 15 September 2012. The $H\alpha$ line has been detected in absorption since September 2013.

In general, the system enters the brightening phase in the optical/IR wavelengths when the decretion disk is absent that can be seen from the evolution of the $H\alpha$ line profiles between 2010–2014, presented in Figure 3.15. Then, the Be star loses its circumstellar material after the active states.

For a double-peaked emission profile, the variation between the two peaks is defined as the V/R ratio (see Chap. 1.1.1) caused by the global density waves in the decretion disk. Figure 3.16 reveals that the V/R ratios of the $H\alpha$ line for SAX J2103.5+4545 represent rapid changes on short times scales (see also Table 3.7). The separation between the V and R emissions, ΔV , was also indicated in the figure by fitting Gaussian functions to each peak. We see an inverse relation between the EW of the $H\alpha$ line (the third panel in Fig. 3.13) and the ΔV values of the peaks till 9 September 2012 (MJD 56179). At that point, a rapid increase both in ΔV and V/R ratios was recorded implying the truncation of the Be disk. Applying the formalism of Hanuschik (1989) given in Equation 3.1, to the average EW and FWHM measurements, we have calculated the projected rotational velocity of SAX J2103.5+4545 as $v \sin i \sim 292 \text{ km s}^{-1}$, which is of the same order as the value of 240 km s^{-1} reported by Reig et al. (2004b).

The relatively small peak value of the $H\alpha$ line EW in emission indicates a small Be disk truncated by the neutron star through its short orbit. The distance between the V and R peaks of the $H\alpha$ line can be regarded with the measure of the $H\alpha$ emitting region of the disk for a Be star (Huang 1972),

$$\left(\frac{\Delta V}{2v \sin i} \right) = \left(\frac{R_{disk}}{R_*} \right)^{-j}, \quad (3.5)$$

where $j=0.5$ for Keplerian rotation ($j=1$ from the angular momentum conservation), R_{disk} is the radius of $H\alpha$ emitting region and R_* denotes the radius of the central star. Taking the average value of ΔV (381.12 km s^{-1}) and the previously found rotational velocity for this source, the size of the $H\alpha$ emitting region of SAX J2103.5+4545 is

Table 3.7: H α line width measurements of the optical counterpart to SAX J2103.5+4545. Positive values indicate that the line is in absorption.

DATE	MJD	Telescope ^a	EW (\AA)	FWHM (\AA)	Profile ^b	ΔV^c (± 50)
2010-Sep-17	55456.707	RTT150	-1.02 ± 0.08	9.47 ± 0.10	V \approx R	365.63
2011-Oct-22	55856.007	OSN	$+1.44 \pm 0.12$	8.45 ± 0.26	ABS	–
2012-Mar-28	56014.133	OSN	-1.34 ± 0.24	10.36 ± 0.32	V<R	494.74
2012-May-22	56069.168	OSN	-1.73 ± 0.21	15.94 ± 0.31	V>R	498.86
2012-May-23	56070.170	OSN	-1.07 ± 0.26	15.26 ± 0.08	V \approx R	445.33
2012-May-28	56075.101	NOT	-1.19 ± 0.28	17.07 ± 0.14	V>R	429.81
2012-Jun-20	56098.058	OSN	-1.57 ± 0.30	14.04 ± 0.15	V>R	363.29
2012-Jun-20	56098.996	OSN	-1.88 ± 0.35	14.13 ± 0.36	V<R	394.94
2012-Jul-05	56113.058	OSN	-0.94 ± 0.18	11.84 ± 0.36	V>R	371.55
2012-Jul-29	56137.180	NOT	-1.41 ± 0.19	11.47 ± 0.30	V<R	334.22
2012-Aug-12	56151.096	OSN	-2.19 ± 0.18	11.98 ± 0.38	V>R	301.07
2012-Aug-24	56163.952	RTT150	-3.00 ± 0.06	10.28 ± 0.24	V>R	283.86
2012-Sep-08	56178.071	OSN	-4.44 ± 0.26	18.52 ± 0.52	SPE	–
2012-Sep-09	56179.134	NOT	-3.85 ± 0.24	17.71 ± 0.35	V>R	442.71
2012-Sep-15	56185.919	RTT150	-3.87 ± 0.16	10.00 ± 0.08	V>R	383.86
2012-Sep-16	56186.898	RTT150	-4.56 ± 0.09	14.09 ± 0.37	V>R	387.64
2012-Oct-10	56210.017	OSN	-4.37 ± 0.24	12.03 ± 0.32	V>R	390.89
2012-Dec-11	56272.703	RTT150	-0.70 ± 0.12	4.73 ± 0.46	V<R	209.51
2013-Sep-08	56543.791	RTT150	$+1.91 \pm 0.68$	10.66 ± 0.69	ABS	–
2013-Nov-08	56604.870	RTT150	$+2.26 \pm 0.40$	11.81 ± 0.26	ABS	–
2014-Jan-05	56662.733	RTT150	$+0.96 \pm 0.14$	5.75 ± 0.41	ABS	–

^(a) Resolution of the spectra for each instrument. RTT150: R \approx 2200; OSN: R \approx 1400; NOT: R \approx 1300–2600.

^(b) ABS, absorption; SPE, single-peaked emission.

^(c) ΔV , separation between the violet and red peaks of the double-peaked emission profiles. Units in km s $^{-1}$

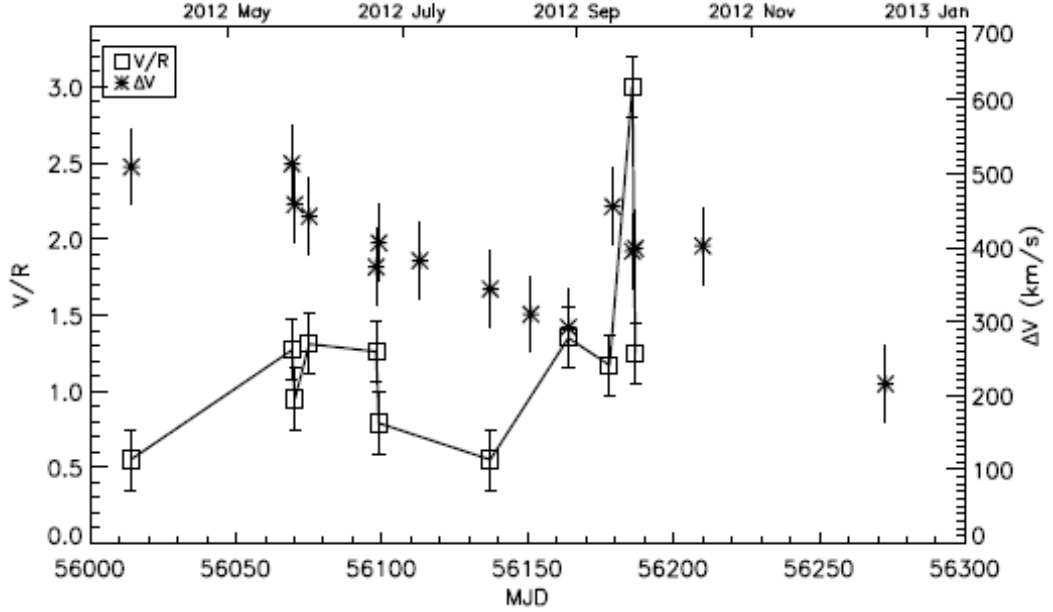


Figure 3.16: Variations V/R ratios (open squares) of the $H\alpha$ emission line during the observations. The peak separation ΔV between the peaks is also indicated with stars.

found to be $R_{disc} \sim 2.35 R_*$, compatible with Reig et al. (2010a). Furthermore, the radius of the Be disk of SAX J2103.5+4545 was found to be similar to the size of the Roche lobe and similar to the periastron distance (Reig et al. 2010a), which probably propitiated the formation of sudden and strong X-ray flares when the neutron star made direct contact with the Be disk during the periastron passages.

The present study restricts the time scale upper limit of the production and disintegration of the Be disk to ~ 10 months, the shortest known for BeXRBs, probably due to its narrow orbit. From Table 3.7 we see that in 2012 EW of the $H\alpha$ line emission reached its maximum in ~ 6.5 months (from MJD 56013.89–56210.02). Since the X-ray activity was triggered around MJD 56050 (~ 36 days after the $H\alpha$ was found in emission), this means that it most probably took no more than those ~ 6.5 months for the disk to grow. Two months later, in 2012 December (MJD 56272.2) the disk was still present but shortened. Although we found this line in absorption in the next available data in 2013 September (MJD 56543.79), from the X-ray observations we can infer that the transient disk was already not present ~ 1.6 months later (around MJD 56320). Analysis of data from 2007 led Reig et al. (2010a) to reach similar conclusions and find a time scale of ~ 1.3 – 1.5 yr.

This source is also particular because of the variability observed in the strength and shape of the $H\alpha$ line. Asymmetric line profiles may arise owing to one-armed density waves in the circumstellar disk, as suggested by the global disk oscillation model (Okazaki 1997; Papaloizou & Savonije 2006). Furthermore, cyclic changes in the V/R ratio observed in many stars were also found to be consistent with the presence of a one-armed density wave in the disk precessing around the central star (Porter & Rivinius 2003). In this study, we observed rapid V/R ratio variations in SAX J2103.5+4545; however, our sample did not allow us confidently to predict a cyclic pattern. Furthermore, rapid changes in line profile shapes are explained as the result of dynamical effects due to the misalignment of the disk orbital plane and the stellar equator (Porter & Rivinius 2003). Recent studies propose that density changes in the disk thermal structure may be also the origin (Silaj et al. 2010, and references therein).

3.4.2 Summary

In this work we have presented the results of our multiwavelength campaign for the Be/X-ray binary system SAX J2103.5+4545. We have performed the spectral and photometric temporal analysis in order to investigate the transient behaviour exhibited by this source since 2007. These new observations were put into the context of historical data and discussed in terms of the neutron star Be-disk interaction.

The optical outbursts in 2010 and 2012 lasted for about 8–9 months (as did probably the one in 2007 and will probably do the one in 2014), and were most probably due to mass ejection events from the Be star. From our long-term optical/IR monitoring of this source, a correlation between the IR variability and the X-ray intensity was found. The IR enhancement episode of 2012 extended for the same period of time as in the optical band. The optical/IR outbursts started about 3 months before the triggering of the X-ray activity. However, the optical/IR brightness and the $H\alpha$ EW were anti-correlated; that is, the maximum of the EW of this line was reached during the decline of the brightness of the BVJHKs magnitudes. We confined the disk formation/disintegration process to within about 10 months. We only observed $H\alpha$ line profiles in absorption at the beginning and end of the optical/IR activity, an indication

that no disk was present around the Be star. We observed fast H α line variability, and asymmetric double-peaked and single-peaked profiles during the evolution of the Be disk. This behaviour might be explained in terms of one-armed density waves in the circumstellar disk.

CHAPTER 4

SEARCHING OF PERIODIC SHORT-TERM VARIATIONS IN BE/X-RAY BINARIES

The mechanism(s) underlying the so called "Be phenomenon" has always been the main issue for understanding the full picture of the Be stars. Although it has been previously assumed that the rapid rotation of the star is the key feature for making a Be star from a B star, recent studies add the non-radial pulsations (NRP) to the context as a new candidate to explain this phenomenon. The reason behind this need arises from the fact that the rapid-rotation is not so efficient for the mass ejection from the Be star to the circumstellar environment despite its high values ($V_{rot} \approx 0.7-0.9V_{crit}$, see also Chapter 3 for the individual sources). Therefore, it has been now widely accepted that NRPs provide an additional amount of moment to the material to be ejected from a Be star. The NRP reveals itself as the short-term variations within the optical light-curves of the Be stars. The time-scale of this short-term variations usually in the range of 0.3–2 days.

Therefore, it is natural to expect that the optical companions in Be/X-ray binaries must show NRPs since the central stars share the same physical properties with the isolated ones. Recently, through the missions dedicated to investigation of NRPs, , e.g. CoRoT, the number of Be stars showing short-term variations have enormously increased. On the other hand, the family of Be/X-ray binaries showing NRPs has still been uncrowded whilst majority of the known HMXBs are the Be/X-ray systems. In fact, there have been only four systems in the Galaxy showing NRPs (see Table 1.1). Thus, investigating the short-term periodic variations in Be/X-ray binaries is important to understand the link between the stellar pulsation and the decretion disk.

Table 4.1: Log of the T100 observations.

Star	Date	Start Time	Stop Time	Exp.(s)	N
IGR J01363+6610	6 Aug 2013	56510.8832	56511.0906	5	663
	18 Feb 2012	55975.7232	55975.8710	30	149
IGR J01583+6713	7 Aug 2013	56511.9034	56512.0098	15	143
	2 Sep 2013	56537.7828	56537.9287	15	400
	3 Sep 2013	56538.8287	56538.9149	15	212
RX J0440.9+4431	2 Sep 2013	56537.9358	56538.0938	2	598
SWIFT J2000.6+3210	24 May 2012	56071.9169	56072.0803	60	154
	14 Jun 2013	56457.8216	56458.0745	15	301
	15 Jun 2013	56458.9229	56459.0710	15	362
	7 Jul 2013	56480.7700	56481.0658	20	715
GS 2138+56	5 Jul 2013	56478.7658	56479.0747	15	859

In this Chapter, we present the results of the optical photometric observations of Be/X-ray binaries between 2012–2013, performed with the T100 Telescope located at the TÜBİTAK National Observatory (Antalya, Turkey), with the aim of searching for NRPs of Galactic BeXRBs. Since this is an ongoing project, the results are preliminary, and will be pursued in the future.

4.1 T100 Observations and Data Reduction

T100 telescope is a 1-m Ritchey-Chrétien type telescope equipped with a 4096×4037 , $15 \mu\text{m}$ pixel Fairchild 486BI CCD whose FOV is $21'.5 \times 21'.5$. To search the periodic short-term variations of selected Be/X-ray binaries we used Bessel R filter with different exposure times for each source. Since the photometric quality of an observation night has crucial effects on the resulting magnitudes, the frames with seeing worse than $1.5''$ were discarded. To achieve a higher S/N rate and short exposure times, the image frames were binned with a factor of 2. In total, we get 5664 high quality frames for 5 sources after the elimination of 1200 frames (see Table 4.1).

For the reduction of the images, a different strategy was followed to get the instrumental magnitudes of the sources. Since T100 does not have a pipeline for the data

reduction, a new code (written by S. Kaan Yerli, 2013, private comm.), was used to deal with our large data set. Briefly, the reduction includes three steps. As the first step, we used IRAF for the standard procedures including bias and dark correction in addition to the flat fielding. After that, we used our two scripts written in the Perl programming-language. For a given coordinate (α and δ) within the observed frame and a radius, the first script, called *astrophot*, adds World Coordinate System (WCS) to the *fits* images using Astrometry.net¹. In addition, it produces the instrumental magnitudes of the frame objects via SExtractor software (Bertin & Arnouts 1996b). As the last step, measured instrumental magnitudes for the interested sources (coordinates) are picked and sorted according to their dates with the script *astrolight*.

To removed instrumental and atmospheric effects on the magnitude we chose reference stars in the neighbouring of the target sources, assuming that they did not vary in time. We measured the differences between the instrumental magnitudes and their known cataloged brightness. The reference stars used for each target sources with the magnitudes are given in Table 4.2. Despite the wide FOV of the CCD, we only used the one quadrant of these images due to the varying backgrounds in the individuals quadrants. Therefore, for IGR J01583+6712 and SWIFT J2000.6+3210 we could just find 2 reference stars since we had small regions around the target sources. The average of the measured differential magnitudes of the reference stars then used to determine the R-magnitude of the target sources. It should be noted that the removed effects on the instrumental magnitudes do not exactly correspond to a real photometric calibration. In addition, the times of the each photometric observation were corrected to the Barycenter using JPL DE200 ephemerides.

For the search of periodic variations, we used Lomb-Scargle (Lomb 1976; Scargle 1982, 1989) and Clean (Roberts et al. 1987) periodograms which find the discrete Fourier transform of the reduced time-series.

¹ <http://nova.astrometry.net/>

Table 4.2: Photometric reference stars used to find the differential magnitudes of the observed sources with T100. The reference star names and magnitudes denotes the USNO-B1.0 catalog ID and R_1 magnitudes respectively.

Star	RA (J2000)	Dec (2000)	R mag
IGR J01363+6610	01:35:49.86	+66:12:43.30	12.37
1561-0031110	01:36:20.55	+66:10:12.20	13.88
1562-0030520	01:36:31.32	+66:12:58.00	14.21
1562-0030553	01:36:37.42	+66:13:55.20	12.55
IGR J01583+6712	01:58:18.40	+67:13:23.50	13.18
1571-0044837	01:58:24.05	+66:11:29.68	12.56
1572-0050060	01:58:30.99	+67:13:20.13	13.75
RX J0440.9+4431	04:40:59.33	+44:31:49.34	10.22
1344-01124540	04:41:10.06	+44:27:31.45	12.59
1344-00112680	04:41:33.77	+44:25:17.95	10.46
1345-00112757	04:41:38.53	+44:31:37.69	11.43
SWIFT J2000.6+3210	20:00:21.85	+32:11:23.38	14.98
1221-0532931	20:00:22.97	+44:27:31.45	14.59
1221-0533231	20:00:34.16	+44:27:31.45	14.12
GS 2138+56	21:39:30.7	+56:59:10.53	13.81
1470-0418886	21:38:34.12	+57:00:47.58	12.79
1469-0410062	21:39:22.16	+56:56:48.78	12.02
1469-0410277	21:39:34.96	+56:57:17.11	12.40

4.2 Results and Discussion

In Figure 4.1, the reduced R-filter light-curves of IGR J01363+6610, RX J0440.9+4431 and GS 2138+56 are represented. For the Be/X-ray binary IGR J01363+6610, we observed a brightening of 40 mmag within ~ 4.3 h. Similarly, RX J0440.9+4431 were detected to show a variation of 60 mmag during the ~ 3.4 h observations. Having the longest observation time (~ 7.4 h) among these three sources, GS 2138+56 also showed a very different pattern of a variability. However the time-scales of these variations for the three sources are not typical for the Be/X-ray systems since they are quite faster than expected. Despite the large numbers of the data (see Table 4.1), they were observed only one night in a very limited time. Therefore we could not find any

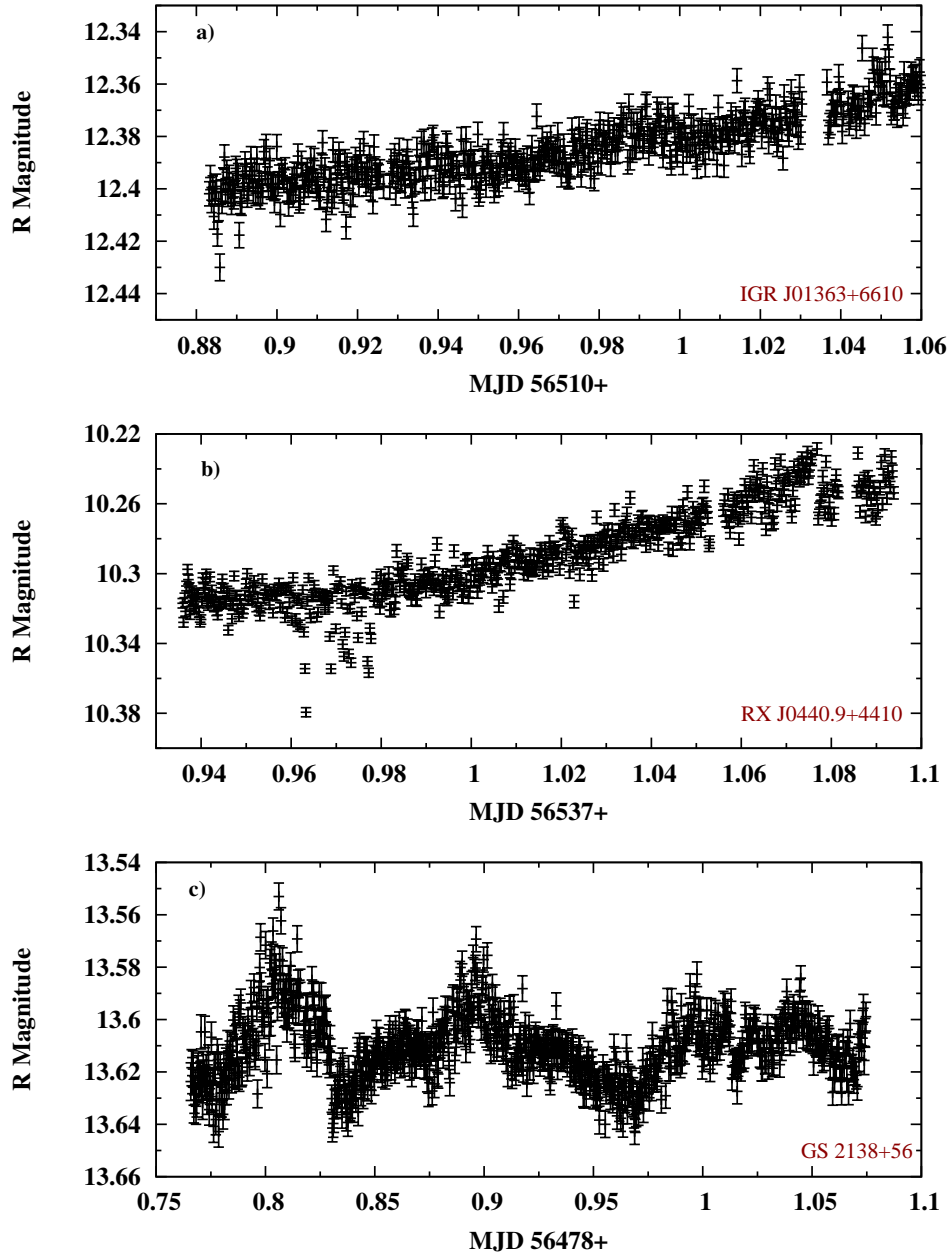


Figure 4.1: Light-curves of a) IGR J01363+6610, b) RX J0440.9+4431 and c) GS 2138+56 for the observation runs 6 August , 2 September and 5 July 2013 respectively.

frequencies in their periodograms that can be shown as a preliminary result.

For IGR J01583+6713, we collected 904 data points achieved from four runs. The lightcurves of each observation are shown in Figure 4.2. We measured a ~ 45 mmag brightening of the source within 2 seasons. The search of periodicity in overall light-

curves however were not resulted in significant frequencies. The power spectra of the source obtained from Clean and Lomb-Scargle algorithms are shown in upper panel of Figure 4.4. Although the two highest frequencies seen in Lomb-Scargle (LS) periodogram, 0.482 and 1.801 d^{-1} are in the range of typical non-radial pulsation periods, both absence of their harmonics and appearing even below the 2σ confidence levels make these detections dubious. Besides, the power spectrum of Clean algorithm is nothing but the spectral window.

Lastly, we observed SWIFT J2000.6+3210 in four observation nights and get 1532 data points. The lightcurves of each night are shown in Figure 4.3. The source does not show a clear brightening or a fading trend during the observations unlike the other sources. But as in the previous source, the timing analysis were not resulted in reliable frequencies (see bottom panel of Fig. 4.4). From the LS spectrum of the source the two highest frequencies, 1.06 and 2.74 d^{-1} are again quite below the significance level of 2σ .

As a result, we could not detect any significant periodic variations in the light-curves of the five Be/X-ray systems. But, we should point out that both J01583+6713 and SWIFT J2000.6+3210 deserve to be pursued in the future to check the presence of the detected frequencies.

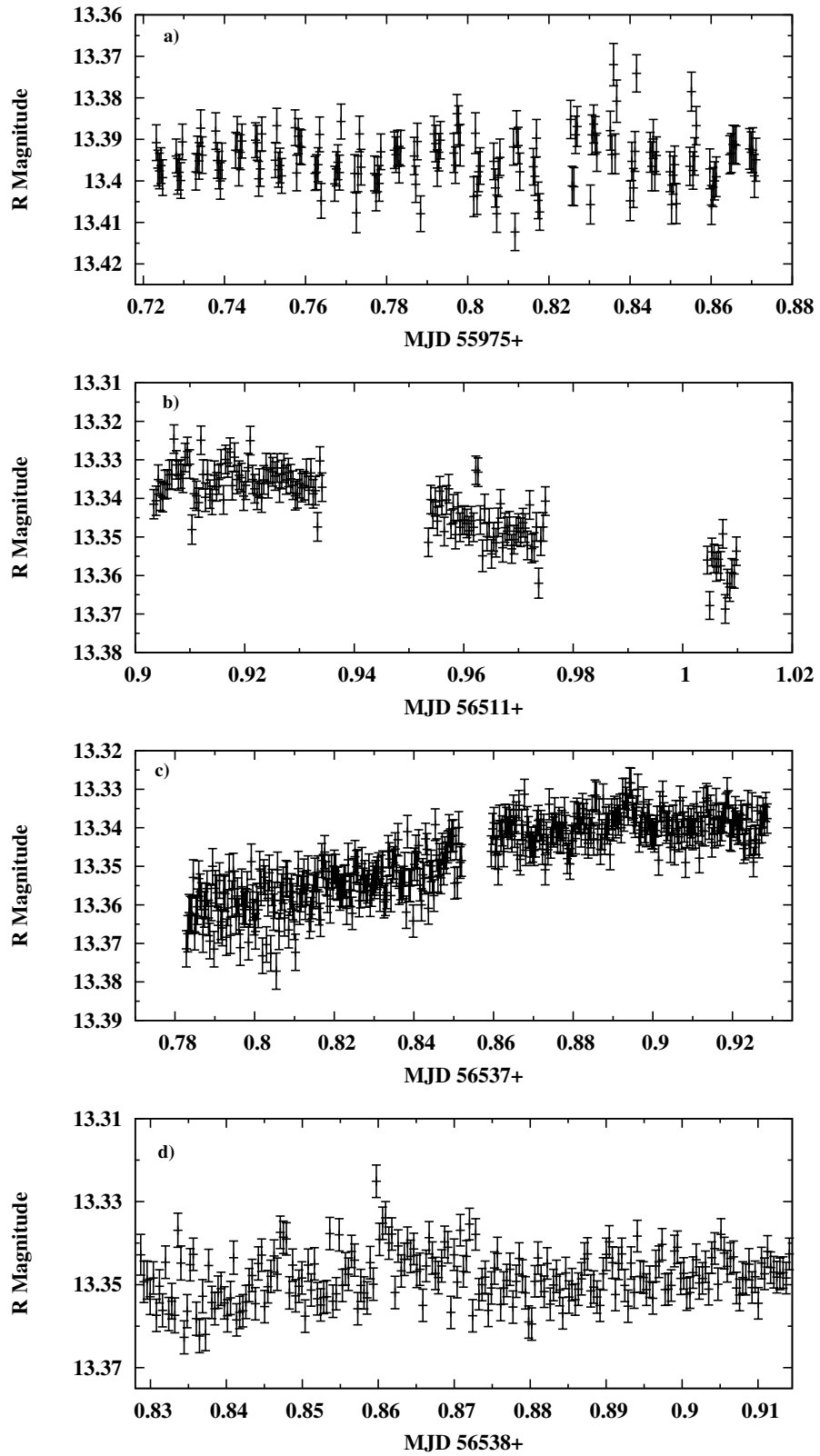


Figure 4.2: R magnitudes of IGR J01583+6713 for the different observing runs (see Table 4.1).

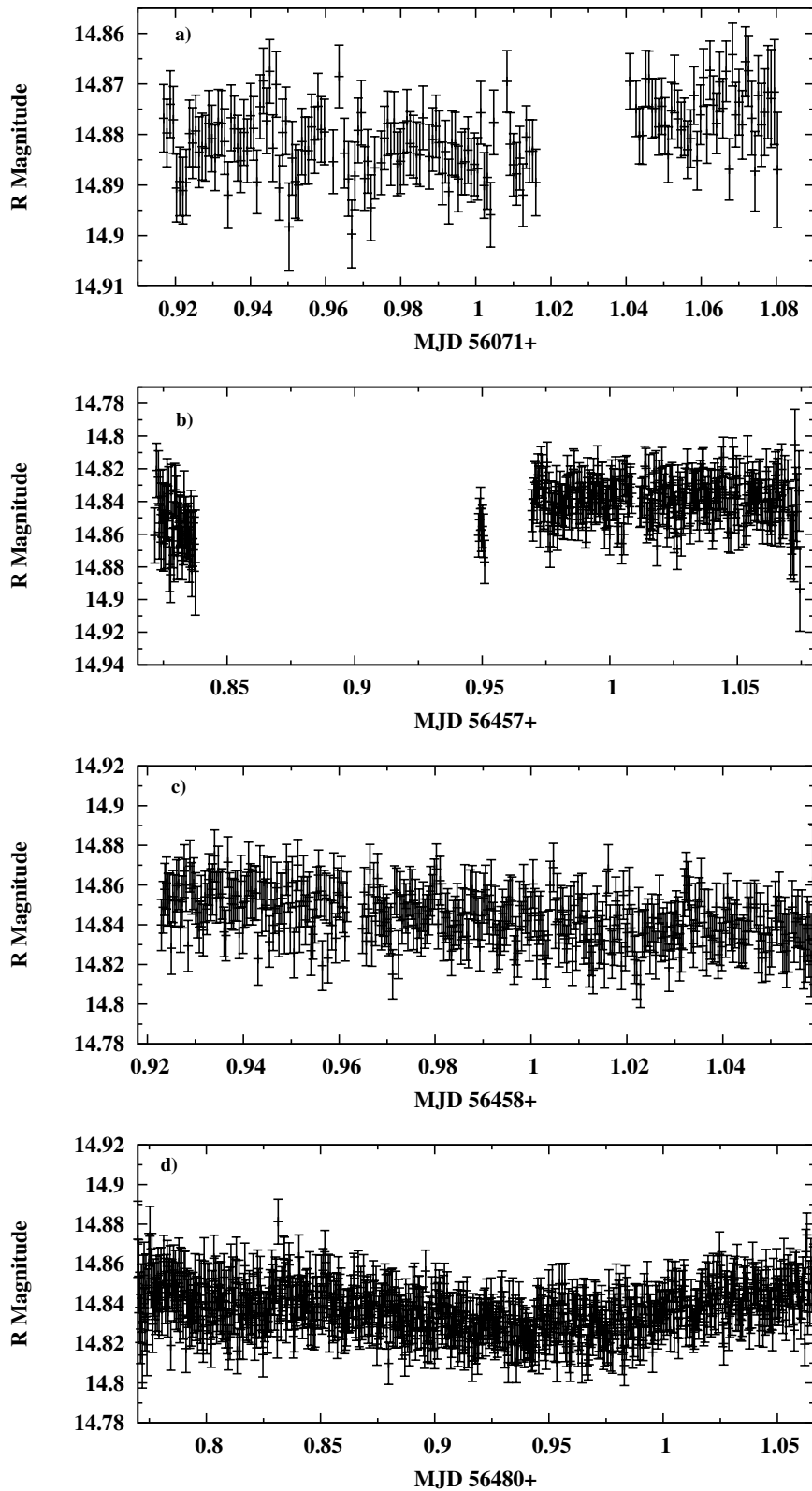


Figure 4.3: Light-curves of SWIFT J2000.6+3210 for the four different observation nights (see Table 4.1).

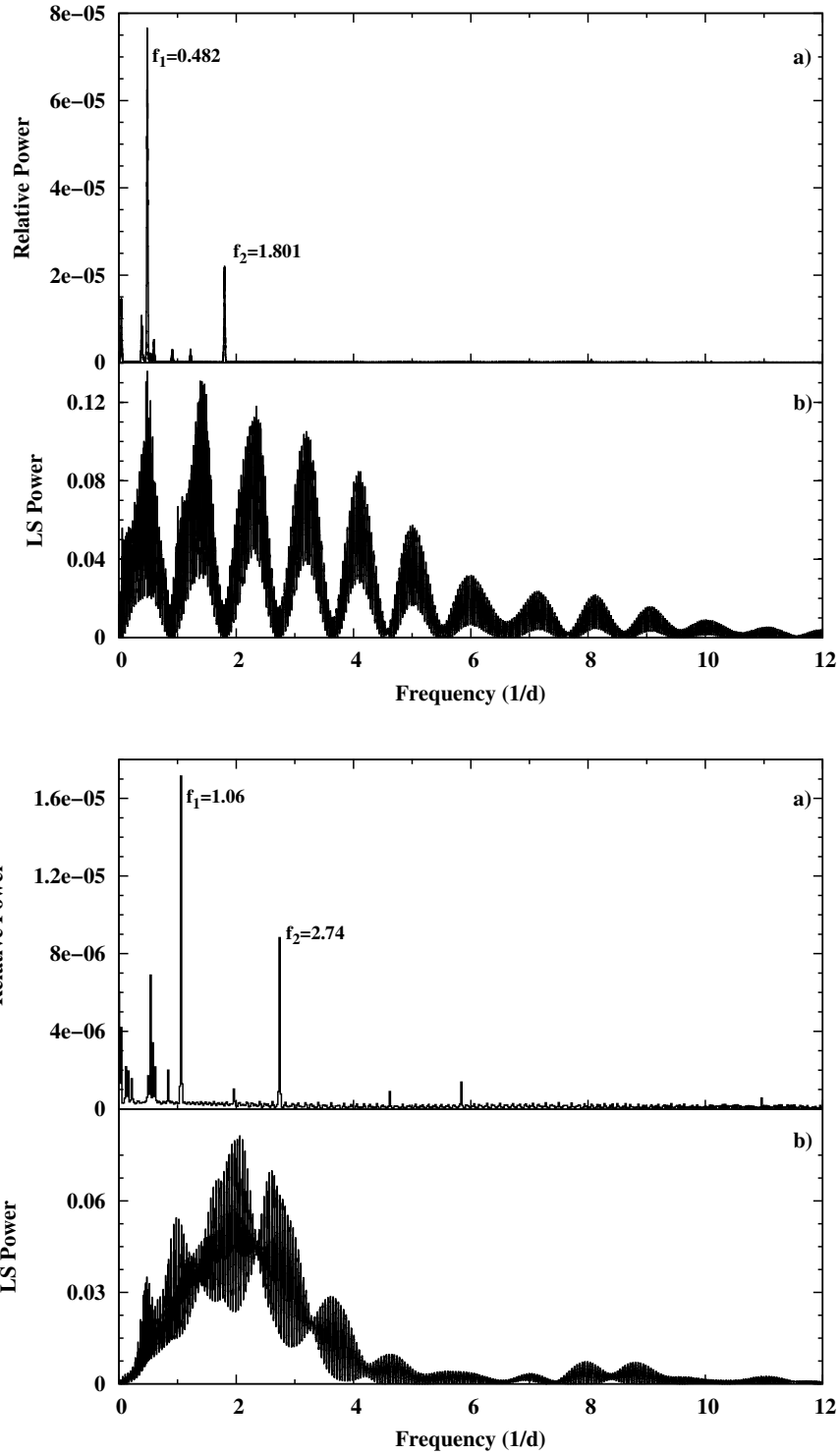


Figure 4.4: (Upper Panel) Power spectra of IGR J01583+6713 obtained from Clean (a) and Lomb-Scargle (b) algorithms. The two highest frequencies of 0.482 and 1.801 d^{-1} are also shown in LS periodogram. (Bottom Panel) Power spectra of SWIFT J2000.6+3210 obtained from Clean (a) and Lomb-Scargle (b) algorithms. The two highest frequencies of 1.06 and 2.74 d^{-1} are also shown in LS periodogram.

CHAPTER 5

CONCLUSIONS

In this work, we have mainly focused on the observational features of Be/X-ray binaries and their responsible physical mechanisms. For this purpose, we first made a thorough review of the literature for each Be/X-ray binary identified so far and create a comprehensive catalog of the systems and the probable potential candidates in the Galaxy. With this new list number of Be/X-ray binaries increased to 63 including the candidates. In contrast to the first catalog of Be/X-ray binaries published in 2005 (Raguzova & Popov 2005), we have examined Be/ γ -ray systems in a different class, since their general properties are quite different from those seen in Be/X-ray binaries. Furthermore, we removed the γ -Cas and γ -Cas analogs from the list due to the unknown nature of their compact companions.

By investigating the spectral distribution of BeXRBs in the Galaxy, we confirmed that the optical companions of these systems mainly took place between BO and B2 spectral types. The confinement in the earlier spectral types indicates that Be phenomenon is not common for the late type stars probably due to the mass transfer processes during the binary evolution. From the distribution of the X-ray outbursts, on the other hand, we revealed that majority of the BeXRBs shows Type I outbursts. Outbursts of giants are always associated with flares or Type I outbursts. The number of Be/X-ray binaries showing persistent X-ray emission is much higher than the systems exhibiting both Type I and Type II outbursts. We also updated the Corbet diagram for the BeXRBs whose orbital parameters have been recently discovered or revised. As expected, BeXRBs are located at a distinct region on the diagram as a result of the correlation between the spin periods and the orbital periods of the sys-

tems. Although most of the BeXRBs have eccentric orbits, it seems that they are not correlated with their eccentricities. Yet, it is possible to find a moderate relation for these parameters in the case of Be/ γ -ray binaries. Interestingly, from a sample of 29 BeXRBs in the Galaxy, we could not find a correlation between their maximum $H\alpha$ EW and the orbital periods contradicting with the previous results. It is possible that for some of the recently discovered (but confirmed) BeXRBs in the sample we have not observed the maximum EW measurements yet. But even we removed these sources the uncorrelation stays the same. We should note that, a relation between these two parameters has a particular importance since it has been assumed to be the observational evidence of the tidal effects of the NS on the decretion disk. As a result, we did not confirm this mechanism with our new $H\alpha$ EW- P_{orb} diagram. But increasing the number of sources with the other confirmed BeXRBs and with the new EW values, it is likely to observe a different pattern in the diagram. We also examine the possible correlation between the maximum $H\beta$ EW and P_{orb} , but we could not find a significant result. Instead, we show that maximum EW measurement of $H\alpha$ is proportional to that of $H\beta$ indicating that they have the same origin.

From the long-term ROTSEIII observations of EXO 0331+530, we showed that the source spent most of its time in the optical brightening phases lasted $\sim 2-4$ years. Excluding the second optical outburst between MJD 54324–55780 detected by ROTSE, all of the brightening phases are accompanied with the X-ray activities starting with a main outburst (Type II) and followed by series of relatively small outbursts (Type I). The X-ray outbursts usually occur after $\sim 1.5-2$ years after the optical outburst are triggered. For the 2004 X-ray outburst, the optical magnitudes show a linear relation with decreasing X-ray flux. This behavior can be explained by the weakening of the decretion disk during the mass transfer to the NS. Although the line profile variations for EXO 0331+530 was previously observed to be showing V/R variations, we do not have any evidence to support this result. Instead, our results contradict with those of Negueruela et al. (1998), since $H\alpha$ lines are always seen in nearly symmetric single-peaked emissions without any significant variations for the time interval 2006–2014. Therefore, we do not have any evidence to support the idea of the perturbations occurred in the disk as well as the V/R variations. From the EW measurements of the $H\alpha$ emissions we found the rotational velocity of the source to be 491 km s^{-1}

corresponding to the $\sim 80\%$ of the break-up velocity.

The optical/IR and X-ray observations of one of the poorly studied BeXRBs, XTE J1946+274, have also been presented in this work. The comparison of optical/IR and X-ray observations reveals that the outbursts phases are not related to the optical brightness of the Be star. In addition, the X-ray outburst behavior of XTE J1946+274 is not connected to the orbital passages of the NS as seen in the case of the similar misaligned systems, e.g. EXO 2030+375. The shifts in the outburst phases with respect to the periastron/apastron passages of the NS is thought to be the result of the global perturbations triggered by the truncation of the disk radius. However, we did not see any trace of such density waves occurred in the decretion disk appearing as the variation of the emission profiles in the spectroscopic data. Similar to the results of EXO 0331+530, the spectra of XTE J1946+274 are dominated by the strong $H\alpha$ emissions that are always seen in narrow, single peaks without any remarkable changes. On the other hand, the evolution of EW measurements indicates a probable disk-loss or disk-fading episode before May 2012. Although, this result is not supported by either the optical/IR magnitude variations or any X-ray activities, the enhancement seen in the EW values just after the lowest point might be attributed to an increase in the amount of the disk material. Using the EW and FWHM measurements we also estimated the rotational velocity of the source as 323–449 km s⁻¹. This result indicates that the Be star in XTE J1946+274 is rotating at 50–70% of its break-up velocity typical to the stars for the same type.

For SAX J2103.5+4545, we have performed the spectral and photometric temporal analysis in order to investigate the transient behavior exhibited by this source since 2007. These new observations were put into the context of historical data and discussed in terms of the neutron star Be-disk interaction. The optical outbursts in 2010 and 2012 lasted for about 8–9 months (as did probably the one in 2007 and will probably do the one in 2014), and were most probably due to mass ejection events from the Be star. From our long-term optical/IR monitoring of this source, a correlation between the IR variability and the X-ray intensity was found. The IR enhancement episode of 2012 extended for the same period of time as in the optical band. The optical/IR outbursts started about 3 months before the triggering of the X-ray activity. However, the optical/IR brightness and the $H\alpha$ EW were anti-correlated; that is, the

maximum of the EW of this line was reached during the decline of the brightness of the BVJHKs magnitudes. This source is also particular because of the variability observed in the strength and shape of the $H\alpha$ line. Asymmetric line profiles may arise owing to one-armed density waves in the circumstellar disc, as suggested by the global disk oscillation model. In this study, we observed rapid V/R ratio variations in SAX J2103.5+4545; however, our sample did not allow us confidently to predict a cyclic pattern. Furthermore, rapid changes in line profile types are explained as the result of dynamical effects due to the misalignment of the disk orbital plane and the stellar equator. We confined the disk formation/disintegration process to within about 10 months. We only observed $H\alpha$ line profiles in absorption at the beginning and end of the optical/IR activity, an indication that no disk was present around the Be star. We observed fast $H\alpha$ line variability, and asymmetric double-peaked and single-peaked profiles during the evolution of the Be disk. This behavior might be explained in terms of one-armed density waves in the circumstellar disk.

The search of non-radial pulsations in the photometric data of IGR J01363+6610, IGR J01583+6713, RX J0440.9+4431, SWIFT J2000.6+3210 and GS 2138+56 have not been resulted in significant periods. The large gaps between the data due to the bad weather conditions and the lack of the continuous monitoring made the periodograms of the sources dominated by the insignificant frequencies. Yet, the results are still preliminary since this is an ongoing project. Although we found that the brightness of three sources in the sample shows small variations within 3–5 hours, this results could only be explained with the further observations. We have also worked on the implementation of a code to manipulate Astrometry.net, SExtractor and produce light curves of large data sets in an automatic way. The code has been written by S.K.Yerli (2013, private comm.) and the new version might be implemented for TUG T100 in future.

REFERENCES

- Aab, O. E. 1985, SvA, 29, 195
- Abdo, A. A., Ackermann, M., Ajello, M., et al. 2010, ApJS, 188, 405
- Abdo, A. A., Ackermann, M., Ajello, M., et al. 2009a, ApJ, 701, L123
- Abdo, A. A., Ackermann, M., Ajello, M., et al. 2009b, ApJ, 706, L56
- Acciari, V. A., Aliu, E., Arlen, T., et al. 2009, ApJ, 698, L94
- Acuner, Z., Inam, S. C., Sahiner, S., et al. 2014, arXiv:1405.3803A
- Aharonian, F., Akhperjanian, A. G., Anton, G., et al. 2009, A&A, 507, 389
- Aharonian, F., Akhperjanian, A. G., Aye, K.-M., et al. 2005, Science, 309, 746
- Aharonian, F., Akhperjanian, A. G., Bazer-Bachi, A. R., et al. 2006, A&A, 460, 743
- Aharonian, F. A., Akhperjanian, A. G., Bazer-Bachi, A. R., et al. 2007, A&A, 469, L1
- Akerlof, C. W., Kehoe, R. L., McKay, T. A., et al. 2003, PASP, 115, 132
- An, H., Dufour, F., Kaspi, V. M., & Harrison, F. A. 2013, ApJ, 775, 135
- Angelini, L., Church, M. J., Parmar, A. N., Balucinska-Church, M., & Mineo, T. 1998, A&A, 339, L41
- Antoniou, V., Hatzidimitriou, D., Zezas, A., & Reig, P. 2009, ApJ, 707, 1080
- Apparao, K. M. V. 2001, A&A, 371, 672
- Apparao, K. M. V., Bradt, H. V., Dower, R. G., et al. 1978, Nat, 271, 225
- Apparao, K. M. V., Naranan, S., Kelley, R. L., & Bradt, H. V. 1980, A&A, 89, 249
- Aragona, C., McSwain, M. V., & De Becker, M. 2010, ApJ, 724, 306

- Aragona, C., McSwain, M. V., Grundstrom, E. D., et al. 2009, *ApJ*, 698, 514
- Balona, L. A. 1995, *MNRAS*, 277, 1547
- Baykal, A., Göğüş, E., Çağdaş İnam, S., & Belloni, T. 2010, *ApJ*, 711, 1306
- Baykal, A., İnam, S. Ç., & Beklen, E. 2006, *MNRAS*, 369, 1760
- Baykal, A., İnam, S. C., Gogus, E., & Belloni, T. M. 2009, *The Astronomer's Telegram*, 2250, 1
- Baykal, A., İnam, S. Ç., Stark, M. J., et al. 2007, *MNRAS*, 374, 1108
- Baykal, A., Kızıloğlu, Ü., Kızıloğlu, N., Beklen, E., & Özbey, M. 2008, *A&A*, 479, 301
- Baykal, A., Stark, M. J., & Swank, J. 2000, *ApJ*, 544, L129
- Baykal, A., Stark, M. J., & Swank, J. H. 2002, *ApJ*, 569, 903
- Becker, R. H., Swank, J. H., Boldt, E. A., et al. 1977, *ApJ*, 216, L11
- Beklen, E., Finger, M. H., & GBM Pulsar Project Team. 2009, *The Astronomer's Telegram*, 2275, 1
- Bellm, E. C., Fuerst, F., Pottschmidt, K., et al. 2014, *arXiv:1403.5249B*
- Belloni, T., Hasinger, G., Pietsch, W., et al. 1993, *A&A*, 271, 487
- Belloni, T., Homan, J., Campana, S., Markwardt, C. B., & Gehrels, N. 2006, *The Astronomer's Telegram*, 687, 1
- Berghoefer, T. W., Schmitt, J. H. M. M., Danner, R., & Cassinelli, J. P. 1997, *A&A*, 322, 167
- Bernacca, P. L., Iijima, T., & Stagni, R. 1984, *A&A*, 132, L8
- Bertin, E. & Arnouts, S. 1996a, *A&AS*, 117, 393
- Bertin, E. & Arnouts, S. 1996b, *A&AS*, 117, 393
- Bignami, G. F., Caraveo, P. A., Lamb, R. C., Markert, T. H., & Paul, J. A. 1981, *ApJ*, 247, L85

- Bikmaev, I. F., Burenin, R. A., Revnivtsev, M. G., et al. 2008, *Astronomy Letters*, 34, 653
- Bildsten, L., Chakrabarty, D., Chiu, J., et al. 1997, *ApJS*, 113, 367
- Bird, A. J., Bazzano, A., Bassani, L., et al. 2010, *ApJS*, 186, 1
- Bird, A. J., Malizia, A., Bazzano, A., et al. 2007, *ApJS*, 170, 175
- Blay, P., Negueruela, I., Reig, P., et al. 2006, *A&A*, 446, 1095
- Blay, P., Reig, P., Martínez Núñez, S., et al. 2004, *A&A*, 427, 293
- Bodaghee, A., Courvoisier, T. J.-L., Rodriguez, J., et al. 2007, *A&A*, 467, 585
- Bodaghee, A., Walter, R., Zurita Heras, J. A., et al. 2006, *A&A*, 447, 1027
- Boldin, P. A., Tsygankov, S. S., & Lutovinov, A. A. 2013, *Astronomy Letters*, 39, 375
- Bongiorno, S. D., Falcone, A. D., Stroh, M., et al. 2011, *ApJ*, 737, L11
- Bonnet-Bidaud, J. M. & Mouchet, M. 1998, *A&A*, 332, L9
- Borozdin, K., Gilfanov, M., Sunyaev, R., et al. 1990, *Soviet Astronomy Letters*, 16, 345
- Bosch-Ramon, V. & Paredes, J. M. 2004, *A&A*, 425, 1069
- Bozzo, E., Ferrigno, C., Falanga, M., & Walter, R. 2011, *A&A*, 531, A65
- Bradt, H. V., Clark, G. W., Dower, R., et al. 1977, *Nat*, 269, 21
- Braes, L. L. E. & Miley, G. K. 1972, *Nat*, 235, 273
- Brandt, S., Shaw, S., Hill, A., et al. 2008, *The Astronomer's Telegram*, 1400, 1
- Caballero, I., Ferrigno, C., Klochkov, D., et al. 2011, *The Astronomer's Telegram*, 3204, 1
- Caballero, I., Kretschmar, P., Santangelo, A., et al. 2007, *A&A*, 465, L21
- Caballero, I., Pottschmidt, K., Bozzo, E., et al. 2010, *The Astronomer's Telegram*, 2692, 1

- Camero, A., Zurita, C., Gutierrez Soto, J., et al. 2014, arXiv:1405.4216
- Camero-Arranz, A., Finger, M., Jenke, P., & Connaughton, V. 2011a, *The Astronomer's Telegram*, 3805, 1
- Camero-Arranz, A., Finger, M. H., Jenke, P., & Connaughton, V. 2011b, *The Astronomer's Telegram*, 3408, 1
- Camero-Arranz, A., Finger, M. H., Wilson-Hodge, C., & Jenke, P. 2010, *The Astronomer's Telegram*, 2677, 1
- Camero-Arranz, A., Finger, M. H., Wilson-Hodge, C. A., et al. 2012a, *ApJ*, 754, 20
- Camero-Arranz, A., Nespoli, E., Gutierrez-Soto, J., & Zurita, C. 2012b, *The Astronomer's Telegram*, 4187, 1
- Camero-Arranz, A., Ozbey-Arabaci, M., Fabregat, J., et al. 2014a, *The Astronomer's Telegram*, 6043, 1
- Camero Arranz, A., Wilson, C. A., Finger, M. H., & Reglero, V. 2007, *A&A*, 473, 551
- Camero-Arranz, A., Zurita, C., Fabregat, J., Finger, M. H., & Peris, V. 2014b, *The Astronomer's Telegram*, 6262, 1
- Campana, S., Israel, G., & Stella, L. 1999, *A&A*, 352, L91
- Carciofi, A. C., Okazaki, A. T., Le Bouquin, J.-B., et al. 2009, *A&A*, 504, 915
- Casares, J., Negueruela, I., Ribó, M., et al. 2014, *Nat*, 505, 378
- Casares, J., Ribó, M., Ribas, I., et al. 2005, *MNRAS*, 364, 899
- Casares, J., Ribó, M., Ribas, I., et al. 2012, *MNRAS*, 421, 1103
- Cassinelli, J. P., Brown, J. C., Maheswaran, M., Miller, N. A., & Telfer, D. C. 2002, *ApJ*, 578, 951
- Chakrabarty, D., Grunsfeld, J. M., Prince, T. A., et al. 1993, *ApJ*, 403, L33
- Chakrabarty, D., Koh, T., Bildsten, L., et al. 1995, *ApJ*, 446, 826
- Chakrabarty, D., Wang, Z., Juett, A. M., Lee, J. C., & Roche, P. 2002, *ApJ*, 573, 789

- Chenevez, J., Budtz-Jorgensen, C., Lund, N., et al. 2004, *The Astronomer's Telegram*, 223, 1
- Cherepashchuk, A. M., Molkov, S., Foschini, L., et al. 2003, *The Astronomer's Telegram*, 159, 1
- Chernyakova, M., Lutovinov, A., Rodríguez, J., & Revnivtsev, M. 2005, *MNRAS*, 364, 455
- Chernyakova, M., Neronov, A., Aharonian, F., Uchiyama, Y., & Takahashi, T. 2009, *MNRAS*, 397, 2123
- Chernyakova, M., Shtykovsky, P., Lutovinov, A., et al. 2004, *The Astronomer's Telegram*, 251, 1
- Chevalier, C. & Ilovaisky, S. A. 1975, *IAU Circ.*, 2778, 1
- Chevalier, C. & Ilovaisky, S. A. 1998, *A&A*, 330, 201
- Clark, D. J., Sguera, V., Bird, A. J., et al. 2010, *MNRAS*, 406, L75
- Clark, G. & Cominsky, L. 1978, *IAU Circ.*, 3161, 1H
- Clark, G. W. 2000, *ApJ*, 542, L131
- Clark, G. W., Schmidt, G. D., & Angel, J. R. P. 1975, *IAU Circ.*, 2843, 1
- Clark, J. S., Tarasov, A. E., Okazaki, A. T., Roche, P., & Lyuty, V. M. 2001, *A&A*, 380, 615
- Clark, J. S., Tarasov, A. E., Steele, I. A., et al. 1998, *MNRAS*, 294, 165
- Coburn, W., Heindl, W. A., Gruber, D. E., et al. 2001, *ApJ*, 552, 738
- Coburn, W., Kretschmar, P., Kreykenbohm, I., et al. 2005, *The Astronomer's Telegram*, 381, 1
- Coe, M. J., Bird, A. J., Hill, A. B., et al. 2007, *MNRAS*, 378, 1427
- Coe, M. J., Buckley, D. A. H., Fabregat, J., et al. 1997, *A&AS*, 126, 237
- Coe, M. J. & Payne, B. J. 1985, *Ap&SS*, 109, 175

- Coe, M. J., Payne, B. J., Hanson, C. G., & Longmore, A. J. 1987, *MNRAS*, 226, 455
- Coe, M. J., Reig, P., McBride, V. A., Galache, J. L., & Fabregat, J. 2006, *MNRAS*, 368, 447
- Coe, M. J., Roche, P., Everall, C., et al. 1994a, *MNRAS*, 270, L57
- Coe, M. J., Roche, P., Everall, C., et al. 1994b, *A&A*, 289, 784
- Coleiro, A., Chaty, S., Zurita Heras, J. A., Rahoui, F., & Tomsick, J. A. 2013, *A&A*, 560, A108
- Collmar, W. & Zhang, S. 2014, *A&A*, 565, A38
- Cook, M. C. & Warwick, R. S. 1987, *MNRAS*, 227, 661
- Corbet, R., Barbier, L., Barthelmy, S., et al. 2006, *The Astronomer's Telegram*, 779, 1
- Corbet, R., Barbier, L., Barthelmy, S., et al. 2005, *The Astronomer's Telegram*, 649, 1
- Corbet, R. & Peele, A. 1997a, *IAU Circ.*, 6647, 2
- Corbet, R., Peele, A., & Remillard, R. 1997, *IAU Circ.*, 6556, 3
- Corbet, R. H. D. 1984, *A&A*, 141, 91
- Corbet, R. H. D. 1986, *MNRAS*, 220, 1047
- Corbet, R. H. D., Barthelmy, S. D., Baumgartner, W. H., et al. 2010a, *The Astronomer's Telegram*, 2598, 1
- Corbet, R. H. D., Cheung, C. C., Kerr, M., et al. 2011, *The Astronomer's Telegram*, 3221, 1
- Corbet, R. H. D., in't Zand, J. J. M., Levine, A. M., & Marshall, F. E. 2009, *ApJ*, 695, 30
- Corbet, R. H. D. & Krimm, H. A. 2009, *The Astronomer's Telegram*, 2008, 1
- Corbet, R. H. D. & Krimm, H. A. 2010, *The Astronomer's Telegram*, 3079, 1

- Corbet, R. H. D., Krimm, H. A., Barthelmy, S. D., et al. 2010b, *The Astronomer's Telegram*, 2570, 1
- Corbet, R. H. D., Krimm, H. A., & Skinner, G. K. 2010c, *The Astronomer's Telegram*, 2559, 1
- Corbet, R. H. D. & Levine, A. M. 2006, *The Astronomer's Telegram*, 843, 1
- Corbet, R. H. D., Markwardt, C. B., & Tueller, J. 2007, *ApJ*, 655, 458
- Corbet, R. H. D., Marshall, F. E., Peele, A. G., & Takeshima, T. 1999, *ApJ*, 517, 956
- Corbet, R. H. D. & Mason, K. O. 1984, *A&A*, 131, 385
- Corbet, R. H. D. & Mukai, K. 2002, *ApJ*, 577, 923
- Corbet, R. H. D. & Mukai, K. 2008, *The Astronomer's Telegram*, 1861, 1
- Corbet, R. H. D., Pearlman, A. B., & Pottschmidt, K. 2010d, *The Astronomer's Telegram*, 2766, 1
- Corbet, R. H. D. & Peele, A. G. 1997b, *ApJ*, 489, L83
- Corbet, R. H. D. & Peele, A. G. 2000, *ApJ*, 530, L33
- Corbet, R. H. D. & Remillard, R. 2005, *The Astronomer's Telegram*, 377, 1
- Corbet, R. H. D., Smale, A. P., Menzies, J. W., et al. 1986, *MNRAS*, 221, 961
- Cusumano, G., La Parola, V., Romano, P., et al. 2010, *MNRAS*, 406, L16
- Cusumano, G., Maccarone, M. C., Nicastro, L., Sacco, B., & Kaaret, P. 2000, *ApJ*, 528, L25
- Cusumano, G., Segreto, A., La Parola, V., et al. 2013, *MNRAS*, 436, L74
- Cutri, R. M., Skrutskie, M. F., van Dyk, S., et al. 2003, *VizieR Online Data Catalog*, 2246, 0
- Dachs, J., Hummel, W., & Hanuschik, R. W. 1992, *A&AS*, 95, 437
- D'Ai, A., La Parola, V., Cusumano, G., et al. 2011, *A&A*, 529, A30
- Davidson, K. & Ostriker, J. P. 1973, *ApJ*, 179, 585

DeCesar, M. E., Boyd, P. T., Pottschmidt, K., et al. 2013, *ApJ*, 762, 61

Delgado-Martí, H., Levine, A. M., Pfahl, E., & Rappaport, S. A. 2001, *ApJ*, 546, 455

Denis, M., Roques, J. P., Barret, D., et al. 1993, *A&AS*, 97, 333

Densham, R. H. & Charles, P. A. 1982, *MNRAS*, 201, 171

Devasia, J., James, M., Paul, B., & Indulekha, K. 2011a, *MNRAS*, 414, 1023

Devasia, J., James, M., Paul, B., & Indulekha, K. 2011b, *MNRAS*, 417, 348

Di Salvo, T., Burderi, L., Robba, N. R., & Guainazzi, M. 1998, *ApJ*, 509, 897

Doroshenko, V., Suchy, S., Santangelo, A., et al. 2010, *A&A*, 515, L1

Dower, R. G., Bradt, H. V., Doxsey, R. E., et al. 1978, *Nat*, 273, 364

Drave, S. P., Bird, A. J., Flocchi, M., et al. 2011, *The Astronomer's Telegram*, 3434, 1

Drave, S. P., Bird, A. J., Sidoli, L., et al. 2014, *MNRAS*, 439, 2175

Drave, S. P., Bird, A. J., Townsend, L. J., et al. 2012a, *A&A*, 539, A21

Drave, S. P., Sguera, V., Bird, A. J., et al. 2012b, *The Astronomer's Telegram*, 4218, 1

Drave, S. P., Sguera, V., Flocchi, M., et al. 2013, *The Astronomer's Telegram*, 5079, 1

Drilling, J. S. 1975, *AJ*, 80, 128

Dubus, G. 2013, *A&ARv*, 21, 64

Dubus, G., Cerutti, B., & Henri, G. 2008, *A&A*, 477, 691

Ducci, L., Jourdain, E., Wilms, J., & Bozzo, E. 2014, *The Astronomer's Telegram*, 6154, 1

Ebisawa, K., Bourban, G., Bodaghee, A., Mowlavi, N., & Courvoisier, T. J.-L. 2003, *A&A*, 411, L59

Elvis, M., Plummer, D., Schachter, J., & Fabbiano, G. 1992, *ApJS*, 80, 257

Epchtein, N., de Batz, B., Copet, E., et al. 1994, *Ap&SS*, 217, 3

Esposito, P., Israel, G. L., Sidoli, L., et al. 2013, *MNRAS*, 433, 2028

Evangelista, Y., Donnarumma, I., Del Monte, E., et al. 2008, *The Astronomer's Telegram*, 1619, 1

Evans, P. A., Beardmore, A. P., Krimm, H. A., & Lien, A. Y. 2014, *The Astronomer's Telegram*, 6243, 1

Eyles, C. J., Skinner, G. K., Willmore, A. P., & Rosenberg, F. D. 1975, *Nat*, 254, 577

Fabregat, J., Reglero, V., Coe, M. J., et al. 1992, *A&A*, 259, 522

Fabrycky, D. 2005, *MNRAS*, 359, 117

Falcone, A. D., Grube, J., Hinton, J., et al. 2010, *ApJ*, 708, L52

Fernie, J. D. 1983, *ApJS*, 52, 7

Ferrigno, C., Falanga, M., Bozzo, E., et al. 2011, *A&A*, 532, A76

Ferrigno, C., Farinelli, R., Bozzo, E., et al. 2013, *A&A*, 553, A103

Finger, M. H., Bildsten, L., Chakrabarty, D., et al. 1999, *ApJ*, 517, 449

Finger, M. H. & Camero-Arranz, A. 2010, *The Astronomer's Telegram*, 2537, 1

Finger, M. H., Cominsky, L. R., Wilson, R. B., Harmon, B. A., & Fishman, G. J. 1994, in *American Institute of Physics Conference Series*, Vol. 308, *The Evolution of X-ray Binaries*, ed. S. Holt & C. S. Day, 459

Finger, M. H., Wilson, R. B., & Chakrabarty, D. 1996a, *A&AS*, 120, C209

Finger, M. H., Wilson, R. B., & Harmon, B. A. 1996b, *ApJ*, 459, 288

Fiocchi, M., Drave, S. P., Chenevez, J., et al. 2012, *The Astronomer's Telegram*, 4135, 1

Fiocchi, M., Sguera, V., Sidoli, L., et al. 2014, *The Astronomer's Telegram*, 5782, 1

Fiocchi, M., Sidoli, L., Bird, A. J., Drave, S. P., & Sguera, V. 2013, *The Astronomer's Telegram*, 5104, 1

Forman, W., Jones, C., Cominsky, L., et al. 1978, *ApJS*, 38, 357

Frail, D. A. & Hjellming, R. M. 1991, *AJ*, 101, 2126

Frank, J., King, A., & Raine, D. J. 2002, *Accretion Power in Astrophysics: Third Edition*

Frémat, Y., Zorec, J., Hubert, A.-M., & Floquet, M. 2005, *A&A*, 440, 305

Galis, R., Beckmann, V., Bianchin, V., et al. 2007, *The Astronomer's Telegram*, 1063, 1

Galloway, D., Remillard, R., Morgan, E., & Swank, J. 2003a, *The Astronomer's Telegram*, 118, 1

Galloway, D. K., Morgan, E. H., & Levine, A. M. 2004, *ApJ*, 613, 1164

Galloway, D. K., Remillard, R., & Morgan, E. 2003b, *The Astronomer's Telegram*, 121, 1

Galloway, D. K., Wang, Z., & Morgan, E. H. 2005, *ApJ*, 635, 1217

Garrison, R. F., Hiltner, W. A., & Schild, R. E. 1977, *ApJS*, 35, 111

Giacconi, R., Gursky, H., Paolini, F. R., & Rossi, B. B. 1962, *Physical Review Letters*, 9, 439

Giacconi, R., Murray, S., Gursky, H., et al. 1974, *ApJS*, 27, 37

Giacconi, R., Murray, S., Gursky, H., et al. 1972, *ApJ*, 178, 281

Gies, D. R., Bagnuolo, Jr., W. G., Baines, E. K., et al. 2007, *ApJ*, 654, 527

Giovannelli, F. & Graziati, L. S. 1992, *SSRv*, 59, 1

Giunta, A., Bozzo, E., Bernardini, F., et al. 2009, *MNRAS*, 399, 744

González-Galán, A., Negueruela, I., Castro, N., et al. 2014, *A&A*, 566, A131

Goranskii, V. P. 2001, *Astronomy Letters*, 27, 516

Goranskij, V. & Barsukova, E. 2004, *The Astronomer's Telegram*, 245, 1

Grebenev, S. & Sunyaev, R. 1991, *IAU Circ.*, 5294, 2

- Grebenev, S. A., De Cesare, G., Chenevez, J., et al. 2005, *The Astronomer's Telegram*, 647, 1
- Grebenev, S. A., Molkov, S. V., & Sunyaev, R. A. 2006, *The Astronomer's Telegram*, 744, 1
- Grebenev, S. A. & Sunyaev, R. A. 2007, *Astronomy Letters*, 33, 149
- Grebenev, S. A., Ubertini, P., Chenevez, J., et al. 2004a, *The Astronomer's Telegram*, 350, 1
- Grebenev, S. A., Ubertini, P., Chenevez, J., Orr, A., & Sunyaev, R. A. 2004b, *The Astronomer's Telegram*, 275, 1
- Gregory, P. C. 2002, *ApJ*, 575, 427
- Gregory, P. C. & Taylor, A. R. 1978, *Nat*, 272, 704
- Grillo, F., Sciortino, S., Micela, G., Vaiana, G. S., & Harnden, Jr., F. R. 1992, *ApJS*, 81, 795
- Grindlay, J. E., Petro, L. D., & McClintock, J. E. 1984, *ApJ*, 276, 621
- Grove, J. E., Kurfess, J. D., Philips, B. F., Strickman, M. S., & Ulmer, M. P. 1995, *International Cosmic Ray Conference*, 2, 1
- Grundstrom, E. D., Blair, J. L., Gies, D. R., et al. 2007a, *ApJ*, 656, 431
- Grundstrom, E. D., Boyajian, T. S., Finch, C., et al. 2007b, *ApJ*, 660, 1398
- Grundstrom, E. D., Caballero-Nieves, S. M., Gies, D. R., et al. 2007c, *ApJ*, 656, 437
- Gutiérrez-Soto, J., Neiner, C., Fabregat, J., et al. 2011a, in *IAU Symposium*, Vol. 272, *IAU Symposium*, ed. C. Neiner, G. Wade, G. Meynet, & G. Peters, 451–456
- Gutiérrez-Soto, J., Reig, P., Fabregat, J., & Fox-Machado, L. 2011b, in *IAU Symposium*, Vol. 272, *IAU Symposium*, ed. C. Neiner, G. Wade, G. Meynet, & G. Peters, 505–506
- Haberl, F. 1994, *A&A*, 283, 175
- Haberl, F., Angelini, L., & Motch, C. 1998a, *A&A*, 335, 587

Haberl, F., Angelini, L., Motch, C., & White, N. E. 1998b, *A&A*, 330, 189

Hadasch, D., Torres, D. F., Tanaka, T., et al. 2012, *ApJ*, 749, 54

Haefner, R. 1988, *Information Bulletin on Variable Stars*, 3260, 1

Halpern, J. P. 2006, *The Astronomer's Telegram*, 847, 1

Halpern, J. P. & Tyagi, S. 2005a, *The Astronomer's Telegram*, 681, 1

Halpern, J. P. & Tyagi, S. 2005b, *The Astronomer's Telegram*, 682, 1

Hanuschik, R. W. 1989, *Ap&SS*, 161, 61

Hardorp, J., Rohlfs, K., Slettebak, A., & Stock, J. 1959, *Hamburger Sternw. Warner & Swasey Obs.*, 0

Harlaftis, E. T., Dhillon, V. S., & Castro-Tirado, A. 2001, *A&A*, 369, 210

Harmanec, P., Habuda, P., Štefl, S., et al. 2000, *A&A*, 364, L85

Harris, J. & Zaritsky, D. 2004, *AJ*, 127, 1531

Heindl, W. A., Coburn, W., Gruber, D. E., et al. 2001, *ApJ*, 563, L35

Hellier, C. 1994, *IAU Circ.*, 5994, 2

Heras, J. A. Z., Chaty, S., & Rodriguez, J. 2007, *The Astronomer's Telegram*, 1035, 1

Hermesen, W., Swanenburg, B. N., Bignami, G. F., et al. 1977, *Nat*, 269, 494

Hill, A. B., Walter, R., Knigge, C., et al. 2005, *A&A*, 439, 255

Hinton, J. A., Skilton, J. L., Funk, S., et al. 2009, *ApJ*, 690, L101

Høg, E., Fabricius, C., Makarov, V. V., et al. 2000, *A&A*, 355, L27

Honeycutt, R. K. & Schlegel, E. M. 1985, *PASP*, 97, 300

Huang, S.-S. 1972, *ApJ*, 171, 549

Hubert, A. M. & Floquet, M. 1998, *A&A*, 335, 565

Hulleman, F., in 't Zand, J. J. M., & Heise, J. 1998, *A&A*, 337, L25

- Hummel, W. & Hanuschik, R. W. 1997, *A&A*, 320, 852
- Hummel, W. & Vrancken, M. 1995, *A&A*, 302, 751
- Hutchings, J. B. & Crampton, D. 1981, *PASP*, 93, 486
- İçdem, B., Inam, S., & Baykal, A. 2011, *MNRAS*, 415, 1523
- Ikhsanov, N. R. 2001, *A&A*, 367, 549
- Ikhsanov, N. R. & Beskrovnaya, N. G. 2011, *Astrophysics*, 54, 463
- Illarionov, A. F. & Sunyaev, R. A. 1975, *A&A*, 39, 185
- İnam, S. Ç., Baykal, A., Swank, J., & Stark, M. J. 2004, *ApJ*, 616, 463
- in't Zand, J. & Heise, J. 2004, *The Astronomer's Telegram*, 362, 1
- in't Zand, J. J. M., Corbet, R. H. D., & Marshall, F. E. 2001a, *ApJ*, 553, L165
- in't Zand, J. J. M., Halpern, J., Eracleous, M., et al. 2000, *A&A*, 361, 85
- in't Zand, J. J. M., Kuiper, L., den Hartog, P. R., Hermsen, W., & Corbet, R. H. D. 2007, *A&A*, 469, 1063
- in't Zand, J. J. M., Swank, J., Corbet, R. H. D., & Markwardt, C. B. 2001b, *A&A*, 380, L26
- Israel, G. L., Covino, S., Campana, S., et al. 2000a, *MNRAS*, 314, 87
- Israel, G. L., Covino, S., Polcaro, V. F., et al. 2000b, in *Astronomical Society of the Pacific Conference Series*, Vol. 214, IAU Colloq. 175: The Be Phenomenon in Early-Type Stars, ed. M. A. Smith, H. F. Henrichs, & J. Fabregat, 739
- Israel, G. L., Negueruela, I., Campana, S., et al. 2001, *A&A*, 371, 1018
- Ives, J. C., Sanford, P. W., & Bell Burnell, S. J. 1975, *Nat*, 254, 578
- James, M., Paul, B., Devasia, J., & Indulekha, K. 2010, *MNRAS*, 407, 285
- James, M., Paul, B., Devasia, J., & Indulekha, K. 2011, *MNRAS*, 410, 1489
- Janot-Pacheco, E., Ilovaisky, S. A., & Chevalier, C. 1981, *A&A*, 99, 274

- Janot-Pacheco, E., Motch, C., & Mouchet, M. 1987, *A&A*, 177, 91
- Janot-Pacheco, E., Motch, C., & Pakull, M. W. 1988, *A&A*, 202, 81
- Jenke, P., Finger, M., Camero-Arranz, A., & Wilson-Hodge, C. A. 2011, *The Astronomer's Telegram*, 3745, 1
- Jenke, P. & Finger, M. H. 2011, *The Astronomer's Telegram*, 3839, 1
- Jenke, P., Finger, M. H., & Connaughton, V. 2012a, *The Astronomer's Telegram*, 4235, 1
- Jenke, P., Finger, M. H., Wilson-Hodge, C. A., & Connaughton, V. 2012b, *The Astronomer's Telegram*, 4547, 1
- Johnston, S., Ball, L., Wang, N., & Manchester, R. N. 2005, *MNRAS*, 358, 1069
- Johnston, S., Lyne, A. G., Manchester, R. N., et al. 1992a, *MNRAS*, 255, 401
- Johnston, S., Manchester, R. N., Lyne, A. G., et al. 1992b, *ApJ*, 387, L37
- Jones, C. E., Tycner, C., & Smith, A. D. 2011, *AJ*, 141, 150
- Kaaret, P., Piraino, S., Halpern, J., & Eracleous, M. 1999, *ApJ*, 523, 197
- Kaluzienski, L. J. 1976, *IAU Circ.*, 2935, 1
- Karasev, D. I., Lutovinov, A. A., & Burenin, R. A. 2010, *MNRAS*, 409, L69
- Karasev, D. I., Lutovinov, A. A., Revnivtsev, M. G., & Krivonos, R. A. 2012, *Astronomy Letters*, 38, 629
- Karasev, D. I., Tsygankov, S. S., & Lutovinov, A. A. 2008, *MNRAS*, 386, L10
- Kargaltsev, O., Pavlov, G. G., Durant, M., Volkov, I., & Hare, J. 2014, *ApJ*, 784, 124
- Kato, S. 1983, *PASJ*, 35, 249
- Kaur, R., Kumar, B., Paul, B., & Sagar, R. 2008a, *The Astronomer's Telegram*, 1807, 1
- Kaur, R., Paul, B., Kumar, B., & Sagar, R. 2008b, *MNRAS*, 386, 2253
- Kaur, R., Wijnands, R., Patruno, A., et al. 2009, *MNRAS*, 394, 1597

- Kaur, R., Wijnands, R., Paul, B., Patruno, A., & Degenaar, N. 2010, *MNRAS*, 402, 2388
- Kawagoe, A., Mihara, T., Negoro, H., et al. 2013a, *The Astronomer's Telegram*, 5438, 1
- Kawagoe, A., Mihara, T., Sugizaki, M., et al. 2013b, *The Astronomer's Telegram*, 5705, 1
- Keek, S., Kuiper, L., & Hermsen, W. 2006, *The Astronomer's Telegram*, 810, 1
- Kelley, R. L., Doxsey, R. E., Jernigan, J. G., et al. 1981, *ApJ*, 243, 251
- Kelley, R. L., Rappaport, S., & Ayasli, S. 1983, *ApJ*, 274, 765
- Kennea, J. A., Evans, P. A., Krimm, H. A., et al. 2013, *The Astronomer's Telegram*, 5441, 1
- Kholopov, P. N., Samus', N. N., Kukarkina, N. P., Medvedeva, G. I., & Perova, N. B. 1981, *Information Bulletin on Variable Stars*, 2042, 1
- Kinugasa, K., Torii, K., Hashimoto, Y., et al. 1998, *ApJ*, 495, 435
- Kiziloglu, U., Kiziloglu, N., Baykal, A., & Inam, S. C. 2010, *The Astronomer's Telegram*, 2925, 1
- Kiziloglu, U., Kiziloglu, N., Baykal, A., Yerli, S. K., & Ozbey, M. 2008, *Information Bulletin on Variable Stars*, 5821, 1
- Kızıloğlu, Ü., Kızıloğlu, N., & Baykal, A. 2005, *AJ*, 130, 2766
- Kızıloğlu, U., Kızıloğlu, N., Baykal, A., Yerli, S. K., & Özbey, M. 2007, *A&A*, 470, 1023
- Kızıloğlu, Ü., Özbilgen, S., Kızıloğlu, N., & Baykal, A. 2009, *A&A*, 508, 895
- Klochkov, D., Doroshenko, V., Santangelo, A., et al. 2012a, *A&A*, 542, L28
- Klochkov, D., Santangelo, A., Staubert, R., et al. 2012b, *The Astronomer's Telegram*, 3902, 1
- Klochkov, D., Santangelo, A., Staubert, R., & Ferrigno, C. 2008, *A&A*, 491, 833

Kodaira, K., Nishimura, S., Kondo, M., et al. 1985, PASJ, 37, 97

Koh, D. T., Bildsten, L., Chakrabarty, D., et al. 1997, ApJ, 479, 933

Kohoutek, L. & Wehmeyer, R. 1999, A&AS, 134, 255

Koyama, K., Kawada, M., Takeuchi, Y., et al. 1990, ApJ, 356, L47

Kreykenbohm, I., Mowlavi, N., Produit, N., et al. 2005, A&A, 433, L45

Kreykenbohm, I., Shaw, S. E., Bianchin, V., et al. 2007, The Astronomer's Telegram, 1281, 1

Kreykenbohm, I., Wilms, J., Kretschmar, P., et al. 2008, A&A, 492, 511

Krimm, H., Barbier, L., Barthelmy, S., et al. 2006, The Astronomer's Telegram, 769, 1

Krimm, H., Barthelmy, S., Capalbi, M., et al. 2005, GRB Coordinates Network, 4361, 1

Krimm, H. A., Barthelmy, S. D., Barbier, L., et al. 2007a, The Astronomer's Telegram, 1298, 1

Krimm, H. A., Barthelmy, S. D., Barbier, L., et al. 2007b, The Astronomer's Telegram, 1345, 1

Krimm, H. A., Barthelmy, S. D., Baumgartner, W., et al. 2009a, The Astronomer's Telegram, 1999, 1

Krimm, H. A., Barthelmy, S. D., Baumgartner, W., et al. 2009b, The Astronomer's Telegram, 2276, 1

Krimm, H. A., Barthelmy, S. D., Baumgartner, W., et al. 2010a, The Astronomer's Telegram, 2928, 1

Krimm, H. A., Barthelmy, S. D., Baumgartner, W., et al. 2010b, The Astronomer's Telegram, 2538, 1

Krimm, H. A., Barthelmy, S. D., Baumgartner, W., et al. 2010c, The Astronomer's Telegram, 2846, 1

- Krimm, H. A., Barthelmy, S. D., Baumgartner, W., et al. 2010d, *The Astronomer's Telegram*, 2663, 1
- Krimm, H. A., Barthelmy, S. D., Baumgartner, W., et al. 2012a, *The Astronomer's Telegram*, 4008, 1
- Krimm, H. A., Barthelmy, S. D., Baumgartner, W., et al. 2009c, *The Astronomer's Telegram*, 2319, 1
- Krimm, H. A., Barthelmy, S. D., Baumgartner, W., et al. 2012b, *The Astronomer's Telegram*, 4350, 1
- Krimm, H. A., Barthelmy, S. D., Baumgartner, W., et al. 2012c, *The Astronomer's Telegram*, 4573, 1
- Krimm, H. A., Barthelmy, S. D., Baumgartner, W., et al. 2009d, *The Astronomer's Telegram*, 1959, 1
- Krimm, H. A., Barthelmy, S. D., Baumgartner, W., et al. 2008a, *The Astronomer's Telegram*, 1792, 1
- Krimm, H. A., Barthelmy, S. D., Cummings, J., et al. 2008b, *The Astronomer's Telegram*, 1376, 1
- Krimm, H. A., Holland, S. T., Corbet, R. H. D., et al. 2013, *ApJS*, 209, 14
- Krimm, H. A., Kennea, J. A., Holland, S. T., et al. 2012d, *The Astronomer's Telegram*, 3936, 1
- Krimm, H. A., Kennea, J. A., Holland, S. T., et al. 2012e, *The Astronomer's Telegram*, 3933, 1
- Krivonos, R., Revnivtsev, M., Lutovinov, A., et al. 2007, *A&A*, 475, 775
- Krivonos, R., Tsygankov, S., Lutovinov, A., et al. 2012, *A&A*, 545, A27
- Krivonos, R., Tsygankov, S., Lutovinov, A., Turler, M., & Bozzo, E. 2010a, *The Astronomer's Telegram*, 2828, 1
- Krivonos, R., Tsygankov, S., Revnivtsev, M., et al. 2010b, *A&A*, 523, A61

- Kuehnel, M., Ferrigno, C., Esposito, V., et al. 2014, *The Astronomer's Telegram*, 6129, 1
- Kuehnel, M., Kreykenbohm, I., Mueller, S., et al. 2011, *The Astronomer's Telegram*, 3254, 1
- Kuehnel, M., Mueller, S., Kreykenbohm, I., et al. 2012, *The Astronomer's Telegram*, 4564, 1
- Kuulkers, E., Beckmann, V., Shaw, S., et al. 2008, *The Astronomer's Telegram*, 1385, 1
- La Palombara, N., Sidoli, L., Esposito, P., Tiengo, A., & Mereghetti, S. 2009, *A&A*, 505, 947
- La Palombara, N., Sidoli, L., Esposito, P., Tiengo, A., & Mereghetti, S. 2012, *A&A*, 539, A82
- La Parola, V., Cusumano, G., Segreto, A., et al. 2013a, *ApJ*, 775, L24
- La Parola, V., D'Ai, A., Cusumano, G., et al. 2013b, arXiv:1305.3916L
- Lamb, F. K., Pethick, C. J., & Pines, D. 1973, *ApJ*, 184, 271
- Lamb, R. C., Markert, T. H., Hartman, R. C., Thompson, D. J., & Bignami, G. F. 1980, *ApJ*, 239, 651
- Landi, R., Bassani, L., Masetti, N., Bazzano, A., & Bird, A. J. 2011, *The Astronomer's Telegram*, 3272, 1
- Landi, R., Bassani, L., Masetti, N., et al. 2012, *The Astronomer's Telegram*, 4166, 1
- Landi, R., Masetti, N., Capitanio, F., Fiocchi, M., & Bird, A. J. 2009, *The Astronomer's Telegram*, 2355, 1
- Landi, R., Masetti, N., Malizia, A., et al. 2008, *The Astronomer's Telegram*, 1539, 1
- Larionov, V., Lyuty, V. M., & Zaitseva, G. V. 2001, *A&A*, 378, 837
- Lee, U., Osaki, Y., & Saio, H. 1991, *MNRAS*, 250, 432
- Levenhagen, R. S. & Leister, N. V. 2006, *MNRAS*, 371, 252

- Levine, A. & Corbet, R. 2000, IAU Circ., 7523, 2
- Levine, A. M., Bradt, H. V., Chakrabarty, D., Corbet, R. H. D., & Harris, R. J. 2011, ApJS, 196, 6
- Levine, A. M., Rappaport, S., Remillard, R., & Savcheva, A. 2004, ApJ, 617, 1284
- Lewin, W. H. G., Clark, G. W., & Smith, W. B. 1968, ApJ, 152, L49
- Leyder, J.-C., Ferrigno, C., Tuerler, M., & Walter, R. 2009a, The Astronomer's Telegram, 1995, 1
- Leyder, J.-C., Walter, R., & Lubiński, P. 2009b, The Astronomer's Telegram, 1949, 1
- Li, J., Torres, D. F., Zhang, S., et al. 2012a, ApJ, 744, L13
- Li, J., Torres, D. F., Zhang, S., et al. 2012b, ApJ, 761, 49
- Li, X.-D. & van den Heuvel, E. P. J. 1996, A&A, 314, L13
- Liller, W. 1975, IAU Circ., 2780, 1
- Liu, Q. Z., van Paradijs, J., & van den Heuvel, E. P. J. 2006, A&A, 455, 1165
- Lomb, N. R. 1976, Ap&SS, 39, 447
- Lopes de Oliveira, R. 2007, PhD thesis, Instituto de Astronomia, Geofísica e Ciências Atmosféricas, Universidade de São Paulo, R. do Matão 1226, 05508-090 São Paulo, Brazil Observatoire Astronomique, UMR 7550 CNRS, Université Louis Pasteur, 11 rue de l'Université, 67000 Strasbourg, France rlopes@astro.iag.usp.br;
- Lopes de Oliveira, R. & Motch, C. 2011, ApJ, 731, L6
- Lopes de Oliveira, R., Motch, C., Haberl, F., Negueruela, I., & Janot-Pacheco, E. 2006, A&A, 454, 265
- Lopes de Oliveira, R., Motch, C., Smith, M. A., Negueruela, I., & Torrejón, J. M. 2007, A&A, 474, 983
- Lopes de Oliveira, R., Smith, M. A., & Motch, C. 2010, A&A, 512, A22
- Lutovinov, A., Tsygankov, S., & Chernyakova, M. 2012, MNRAS, 423, 1978

Lutovinov, A. A., Mironov, A. I., Burenin, R. A., et al. 2013, *Astronomy Letters*, 39, 513

Lyubimkov, L. S., Rostopchin, S. I., Roche, P., & Tarasov, A. E. 1997, *MNRAS*, 286, 549

Maccarone, T. J., Girard, T. M., & Casetti-Dinescu, D. I. 2014, *MNRAS*, 440, 1626

MacConnell, D. J. 1981, *A&AS*, 44, 387

MacConnell, D. J. 1982, *A&AS*, 48, 355

Makino, F. & GINGA Team. 1988a, *IAU Circ.*, 4661, 2

Makino, F. & GINGA Team. 1988b, *IAU Circ.*, 4583, 1

Makino, F. & GINGA Team. 1988c, *IAU Circ.*, 4575, 1

Makino, F. & GINGA Team. 1988d, *IAU Circ.*, 4577, 1

Makino, F. & GINGA Team. 1988e, *IAU Circ.*, 4587, 1

Makino, F. & GINGA Team. 1990, *IAU Circ.*, 5139, 1

Makino, F., Hasinger, G., Pietsch, W., & Belloni, T. 1990, *IAU Circ.*, 5142, 1

Makishima, K., Ohashi, T., Kawai, N., et al. 1990, *PASJ*, 42, 295

Mangano, V. 2009, *The Astronomer's Telegram*, 1896, 1

Manousakis, A., Beckmann, V., Bianchin, V., et al. 2008, *The Astronomer's Telegram*, 1613, 1

Maraschi, L. & Treves, A. 1981, *MNRAS*, 194, 1P

Markwardt, C. B., Baumgartner, W. H., Skinner, G. K., & Corbet, R. H. D. 2010, *The Astronomer's Telegram*, 2564, 1

Markwardt, C. B. & Swank, J. H. 2005, *The Astronomer's Telegram*, 679, 1

Marshall, F. E., in 't Zand, J. J. M., Strohmayer, T., & Markwardt, C. B. 1999, *IAU Circ.*, 7240, 2

Marshall, F. E., Takeshima, T., & in 't Zand, J. 2000, *IAU Circ.*, 7363, 2

- Martin, R. G., Nixon, C., Armitage, P. J., Lubow, S. H., & Price, D. J. 2014, arXiv1407.5676M
- Masetti, N., Bassani, L., Bazzano, A., et al. 2006a, A&A, 455, 11
- Masetti, N., Landi, R., Sguera, V., et al. 2010a, A&A, 511, A48
- Masetti, N., Mason, E., Bassani, L., et al. 2006b, A&A, 448, 547
- Masetti, N., Mason, E., Morelli, L., et al. 2008a, A&A, 482, 113
- Masetti, N., Morelli, L., Palazzi, E., et al. 2006c, A&A, 459, 21
- Masetti, N., Morelli, L., Palazzi, E., et al. 2006d, The Astronomer's Telegram, 783, 1
- Masetti, N., Parisi, P., Palazzi, E., et al. 2010b, A&A, 519, A96
- Masetti, N., Parisi, P., Palazzi, E., et al. 2013, A&A, 556, A120
- Masetti, N., Parisi, P., Palazzi, E., et al. 2009, A&A, 495, 121
- Masetti, N., Parisi, P., Palazzi, E., et al. 2008b, The Astronomer's Telegram, 1620, 1
- Masetti, N., Pretorius, M. L., Palazzi, E., et al. 2006e, A&A, 449, 1139
- Mason, A. B., Clark, J. S., Norton, A. J., Negueruela, I., & Roche, P. 2009, A&A, 505, 281
- Mason, K. O., Murdin, P. G., Parkes, G. E., & Visvanathan, N. 1978, MNRAS, 184, 45P
- Massi, M., Ros, E., & Zimmermann, L. 2012, A&A, 540, A142
- Mathew, B., Banerjee, D. P. K., Naik, S., & Ashok, N. M. 2013, AJ, 145, 158
- McBride, V. A., Coe, M. J., Negueruela, I., Schurch, M. P. E., & McGowan, K. E. 2008, MNRAS, 388, 1198
- McBride, V. A., Wilms, J., Coe, M. J., et al. 2006, A&A, 451, 267
- McBride, V. A., Wilms, J., Kreykenbohm, I., et al. 2007, A&A, 470, 1065
- McClintock, J. E., Nugent, J. J., Li, F. K., & Rappaport, S. A. 1977, ApJ, 216, L15

McClintock, J. E., Ricker, G. R., & Lewin, W. H. G. 1971, *ApJ*, 166, L73

Mendelson, H. & Mazeh, T. 1989, *MNRAS*, 239, 733

Mennickent, R. E. 1991, *A&AS*, 88, 1

Menzies, J. 1981, *MNRAS*, 195, 67P

Mereghetti, S. & La Palombara, N. 2009, *A&A*, 504, 181

Mereghetti, S., Romano, P., & Sidoli, L. 2008, *A&A*, 483, 249

Mihara, M. N. T., Sugizaki, M., Ueno, S., et al. 2012, *The Astronomer's Telegram*, 4420, 1

Mihara, T., Makishima, K., Kamijo, S., et al. 1991, *ApJ*, 379, L61

Miroshnichenko, A. S., Bjorkman, K. S., & Krugov, V. D. 2002, *PASP*, 114, 1226

Miyasaka, H., Bachetti, M., Harrison, F. A., et al. 2013, *ApJ*, 775, 65

Moldón, J., Johnston, S., Ribó, M., Paredes, J. M., & Deller, A. T. 2011a, *ApJ*, 732, L10

Moldón, J., Ribó, M., & Paredes, J. M. 2011b, *A&A*, 533, L7

Molkov, S., Lutovinov, A., & Grebenev, S. 2003, *A&A*, 411, L357

Molkov, S. V., Cherepashchuk, A. M., Lutovinov, A. A., et al. 2004a, *Astronomy Letters*, 30, 534

Molkov, S. V., Cherepashchuk, A. M., Revnivtsev, M. G., et al. 2004b, *The Astronomer's Telegram*, 274, 1

Monet, D. & et al. 1998, *VizieR Online Data Catalog*, 1252, 0

Mook, D. E., Boley, F. I., Foltz, C. B., & Westpfahl, D. 1974, *PASP*, 86, 894

Morel, T. & Grosdidier, Y. 2005, *MNRAS*, 356, 665

Morgan, E., Remillard, R., & Swank, J. 2003, *The Astronomer's Telegram*, 199, 1

Mori, M., Kawachi, A., Nagataki, S., & Takata, J. 2011, *arXiv:1111.0367M*

- Morii, M., Kawai, N., Sugimori, K., et al. 2010, *The Astronomer's Telegram*, 2527, 1
- Moritani, Y., Nogami, D., Okazaki, A. T., et al. 2013, *PASJ*, 65, 83
- Morris, D. C., Smith, R. K., Markwardt, C. B., et al. 2009, *ApJ*, 699, 892
- Motch, C., Belloni, T., Buckley, D., et al. 1991a, *A&A*, 246, L24
- Motch, C., Guillout, P., Haberl, F., et al. 1998, *A&AS*, 132, 341
- Motch, C., Haberl, F., Dennerl, K., Pakull, M., & Janot-Pacheco, E. 1997, *A&A*, 323, 853
- Motch, C., Herent, O., & Guillout, P. 2003, *Astronomische Nachrichten*, 324, 61
- Motch, C. & Janot-Pacheco, E. 1987, *A&A*, 182, L55
- Motch, C., Lopes de Oliveira, R., Negueruela, I., Haberl, F., & Janot-Pacheco, E. 2007, in *Astronomical Society of the Pacific Conference Series*, Vol. 361, *Active OB-Stars: Laboratories for Stellar and Circumstellar Physics*, ed. A. T. Okazaki, S. P. Owocki, & S. Stefl, 117
- Motch, C., Pakull, M., Haberl, F., & Dennerl, K. 1996, *IAU Circ.*, 6285, 2
- Motch, C., Pakull, M. W., Janot-Pacheco, E., & Mouchet, M. 1988, *A&A*, 201, 63
- Motch, C., Stella, L., Janot-Pacheco, E., & Mouchet, M. 1991b, *ApJ*, 369, 490
- Motch, C., Warwick, R., Cropper, M. S., et al. 2010, *A&A*, 523, A92
- Mukherjee, U., Bapna, S., Raichur, H., Paul, B., & Jaaffrey, S. N. A. 2006, *Journal of Astrophysics and Astronomy*, 27, 25
- Müller, S., Ferrigno, C., Kühnel, M., et al. 2013, *A&A*, 551, A6
- Müller, S., Kühnel, M., Caballero, I., et al. 2012, *A&A*, 546, A125
- Müller, S., Kühnel, M., Pottschmidt, K., et al. 2010, *The Astronomer's Telegram*, 3077, 1
- Munar-Adrover, P., Paredes, J. M., Ribó, M., et al. 2014, *ApJ*, 786, L11
- Nagase, F., Dotani, T., Tanaka, Y., et al. 1991, *ApJ*, 375, L49

Nakahira, S., Yamaoka, K., Yoshida, A., et al. 2010, *The Astronomer's Telegram*, 2369, 1

Nakajima, M., Mihara, T., Makishima, K., & Niko, H. 2006, *ApJ*, 646, 1125

Nakajima, M., Mihara, T., Serino, M., et al. 2011, *The Astronomer's Telegram*, 3677, 1

Nakajima, M., Mihara, T., Sugizaki, M., et al. 2012, *The Astronomer's Telegram*, 4561, 1

Nakajima, M., Nakagawa, Y. E., Nakahira, S., et al. 2013, *The Astronomer's Telegram*, 5205, 1

Nakajima, M., Negoro, H., Kawagoe, A., et al. 2014, *The Astronomer's Telegram*, 6212, 1

Nakajima, M., Sugizaki, M., Matsuoka, M., et al. 2010, *The Astronomer's Telegram*, 2427, 1

Napoli, V. J., McSwain, M. V., Boyer, A. N. M., & Roettenbacher, R. M. 2011, *PASP*, 123, 1262

Negueruela, I., Casares, J., Verrecchia, F., et al. 2008, *The Astronomer's Telegram*, 1876, 1

Negueruela, I., Israel, G. L., Marco, A., Norton, A. J., & Speziali, R. 2003, *A&A*, 397, 739

Negueruela, I. & Okazaki, A. T. 2001, *A&A*, 369, 108

Negueruela, I., Okazaki, A. T., Fabregat, J., et al. 2001, *A&A*, 369, 117

Negueruela, I., Reig, P., Coe, M. J., & Fabregat, J. 1998, *A&A*, 336, 251

Negueruela, I., Reig, P., Finger, M. H., & Roche, P. 2000, *A&A*, 356, 1003

Negueruela, I., Ribó, M., Herrero, A., et al. 2011, *ApJ*, 732, L11

Negueruela, I., Roche, P., Buckley, D. A. H., et al. 1996, *A&A*, 315, 160

Negueruela, I., Roche, P., Fabregat, J., & Coe, M. J. 1999, *MNRAS*, 307, 695

- Negueruela, I. & Schurch, M. P. E. 2007, *A&A*, 461, 631
- Negueruela, I., Torrejón, J. M., & McBride, V. 2007, *The Astronomer's Telegram*, 1239, 1
- Neiner, C. & Hubert, A.-M. 2009, *Communications in Asteroseismology*, 158, 194
- Nespoli, E., Fabregat, J., & Mennickent, R. E. 2010, *A&A*, 516, A106
- Nespoli, E. & Reig, P. 2011, *A&A*, 526, A7
- Nespoli, E., Reig, P., & Zezas, A. 2012, *A&A*, 547, A103
- Nichelli, E., Israel, G. L., Moretti, A., et al. 2011, *The Astronomer's Telegram*, 3205, 1
- Oja, T. 1991, *A&AS*, 89, 415
- Okazaki, A. T. 1991, *PASJ*, 43, 75
- Okazaki, A. T. 1997, *A&A*, 318, 548
- Okazaki, A. T. 2000, in *Astronomical Society of the Pacific Conference Series*, Vol. 214, *IAU Colloq. 175: The Be Phenomenon in Early-Type Stars*, ed. M. A. Smith, H. F. Henrichs, & J. Fabregat, 409
- Okazaki, A. T. 2001, *PASJ*, 53, 119
- Okazaki, A. T. 2007, in *Astronomical Society of the Pacific Conference Series*, Vol. 361, *Active OB-Stars: Laboratories for Stellar and Circumstellar Physics*, ed. A. T. Okazaki, S. P. Owocki, & S. Stefl, 230
- Okazaki, A. T., Hayasaki, K., & Moritani, Y. 2013, *PASJ*, 65, 41
- Okazaki, A. T., Nagataki, S., Naito, T., et al. 2011, *PASJ*, 63, 893
- Okazaki, A. T. & Negueruela, I. 2001a, *A&A*, 377, 161
- Okazaki, A. T. & Negueruela, I. 2001b, in *Astronomical Society of the Pacific Conference Series*, Vol. 234, *X-ray Astronomy 2000*, ed. R. Giacconi, S. Serio, & L. Stella, 281
- Osaki, Y. 1986, *PASP*, 98, 30

- Ozbey-Arabaci, M., Camero-Arranz, A., Fabregat, J., Ozcan, H. B., & Peris, V. 2014, *The Astronomer's Telegram*, 6265, 1
- Pahari, M. & Pal, S. 2012, *MNRAS*, 423, 3352
- Pakull, M. W., Motch, C., & Negueruela, I. 2003, *The Astronomer's Telegram*, 202, 1
- Palmer, D., Barthelmy, S., Cummings, J., et al. 2005, *The Astronomer's Telegram*, 678, 1
- Pandey, M., Rao, A. P., Ishwara-Chandra, C. H., Durouchoux, P., & Manchanda, R. K. 2007, *A&A*, 463, 567
- Pandey, M., Rao, A. P., Manchanda, R., Durouchoux, P., & Ishwara-Chandra, C. H. 2006, *A&A*, 453, 83
- Papaloizou, J. C., Savonije, G. J., & Henrichs, H. F. 1992, *A&A*, 265, L45
- Papaloizou, J. C. B. & Savonije, G. J. 2006, *A&A*, 456, 1097
- Paredes, J. M. & Figueras, F. 1986, *A&A*, 154, L30
- Paredes, J. M., Marti, J., Peracaula, M., & Ribo, M. 1997, *A&A*, 320, L25
- Paredes, J. M., Martí, J., Ribó, M., & Massi, M. 2000, *Science*, 288, 2340
- Paredes, J. M., Marziani, P., Marti, J., et al. 1994, *A&A*, 288, 519
- Parkes, G. E., Murdin, P. G., & Mason, K. O. 1980, *MNRAS*, 190, 537
- Parmar, A. N., Stella, L., Ferri, P., & White, N. E. 1985, *IAU Circ.*, 4066, 1
- Parmar, A. N., White, N. E., & Stella, L. 1989a, *ApJ*, 338, 373
- Parmar, A. N., White, N. E., Stella, L., Izzo, C., & Ferri, P. 1989b, *ApJ*, 338, 359
- Paul, B. & Rao, A. R. 1998, *A&A*, 337, 815
- Pavlinisky, M. N., Grebenev, S. A., & Sunyaev, R. A. 1992, *Soviet Astronomy Letters*, 18, 88
- Pellizza, L. J., Chaty, S., & Negueruela, I. 2006, *A&A*, 455, 653

- Percy, J. R., Jakate, S. M., & Matthews, J. M. 1981, *AJ*, 86, 53
- Perryman, M. A. C., Lindegren, L., Kovalevsky, J., et al. 1997, *A&A*, 323, L49
- Piraino, S., Santangelo, A., Segreto, A., et al. 2000, *A&A*, 357, 501
- Portegies Zwart, S. F. 1995, *A&A*, 296, 691
- Porter, J. M. 1996, *MNRAS*, 280, L31
- Porter, J. M. 1998, *A&A*, 336, 966
- Porter, J. M. & Rivinius, T. 2003, *PASP*, 115, 1153
- Pottschmidt, K., Kreykenbohm, I., Wilms, J., et al. 2005, *ApJ*, 634, L97
- Pottschmidt, K., McBride, V. A., Suchy, S., et al. 2007, *The Astronomer's Telegram*, 1283, 1
- Pradhan, P., Maitra, C., Paul, B., & Paul, B. C. 2013, *MNRAS*, 436, 945
- Priedhorsky, W. C. & Holt, S. S. 1987, *SSRv*, 45, 291
- Priedhorsky, W. C. & Terrell, J. 1983, *ApJ*, 273, 709
- Pringle, J. E. 1981, *ARA&A*, 19, 137
- Pringle, J. E. & Rees, M. J. 1972, *A&A*, 21, 1
- Produit, N., Ballet, J., & Mowlavi, N. 2004, *The Astronomer's Telegram*, 278, 1
- Raguzova, N. V. & Popov, S. B. 2005, *A&AT*, 24, 151
- Rahoui, F. & Chaty, S. 2008, *A&A*, 492, 163
- Rahoui, F., Chaty, S., Lagage, P.-O., & Pantin, E. 2008, *A&A*, 484, 801
- Raichur, H. & Paul, B. 2010, *MNRAS*, 406, 2663
- Rakowski, C. E., Schulz, N. S., Wolk, S. J., & Testa, P. 2006, *ApJ*, 649, L111
- Rappaport, S., Clark, G. W., Cominsky, L., Li, F., & Joss, P. C. 1978, *ApJ*, 224, L1
- Rappaport, S. A. & Joss, P. C. 1983, in *Accretion-Driven Stellar X-ray Sources*, ed. W. H. G. Lewin & E. P. J. van den Heuvel, 13

Ray, P. S. & Chakrabarty, D. 2002, ApJ, 581, 1293

Reed, B. C. & Beatty, A. E. 1995, ApJS, 97, 189

Reig, P. 2007, MNRAS, 377, 867

Reig, P. 2008, A&A, 489, 725

Reig, P. 2011, Ap&SS, 332, 1

Reig, P., Belloni, T., Israel, G. L., et al. 2008, A&A, 485, 797

Reig, P., Fabregat, J., & Coe, M. J. 1997a, A&A, 322, 193

Reig, P., Fabregat, J., Coe, M. J., et al. 1997b, A&A, 322, 183

Reig, P., Kougentakis, T., & Papamastorakis, G. 2004a, The Astronomer's Telegram, 308, 1

Reig, P., Larionov, V., Negueruela, I., Arkharov, A. A., & Kudryavtseva, N. A. 2007, A&A, 462, 1081

Reig, P. & Mavromatakis, F. 2003, The Astronomer's Telegram, 173, 1

Reig, P., Negueruela, I., Buckley, D. A. H., et al. 2001, A&A, 367, 266

Reig, P., Negueruela, I., Coe, M. J., et al. 2000, MNRAS, 317, 205

Reig, P., Negueruela, I., Fabregat, J., et al. 2004b, A&A, 421, 673

Reig, P., Negueruela, I., Fabregat, J., Chato, R., & Coe, M. J. 2005a, A&A, 440, 1079

Reig, P., Negueruela, I., Papamastorakis, G., Manousakis, A., & Kougentakis, T. 2005b, A&A, 440, 637

Reig, P., Nespoli, E., Fabregat, J., & Mennickent, R. E. 2011, A&A, 533, A23

Reig, P. & Roche, P. 1999a, MNRAS, 306, 100

Reig, P. & Roche, P. 1999b, MNRAS, 306, 95

Reig, P., Słowikowska, A., Zezas, A., & Blay, P. 2010a, MNRAS, 401, 55

Reig, P., Stevens, J. B., Coe, M. J., & Fabregat, J. 1998, MNRAS, 301, 42

Reig, P., Torrejón, J. M., Negueruela, I., et al. 2009, *A&A*, 494, 1073

Reig, P. & Zezas, A. 2014a, *A&A*, 561, A137

Reig, P. & Zezas, A. 2014b, *MNRAS*, 442, 472

Reig, P., Zezas, A., & Gkouvelis, L. 2010b, *A&A*, 522, A107

Remillard, R., Levine, A., Takeshima, T., et al. 1998, *IAU Circ.*, 6826, 2

Remillard, R. & Marshall, F. 2003, *The Astronomer's Telegram*, 197, 1

Revnivtsev, M., Molkov, S., & Grebenev, S. 2005, *The Astronomer's Telegram*, 531, 1

Revnivtsev, M., Sunyaev, R., Lutovinov, A., & Sazonov, S. 2007, *The Astronomer's Telegram*, 1253, 1

Revnivtsev, M. G., Sunyaev, R. A., Varshalovich, D. A., et al. 2004, *Astronomy Letters*, 30, 382

Reynolds, A. P., Bell, S. A., & Hilditch, R. W. 1992, *MNRAS*, 256, 631

Reynolds, A. P., Parmar, A. N., Hakala, P. J., et al. 1999, *A&AS*, 134, 287

Reynolds, A. P., Parmar, A. N., & White, N. E. 1993, *ApJ*, 414, 302

Ricker, G. R., McClintock, J. E., Gerassimenko, M., & Lewin, W. H. G. 1973, *ApJ*, 184, 237

Riquelme, M. S., Torrejón, J. M., & Negueruela, I. 2012, *A&A*, 539, A114

Rivinius, T., Baade, D., Stefl, S., et al. 1998, *A&A*, 336, 177

Rivinius, T., Carciofi, A. C., & Martayan, C. 2013, *A&ARv*, 21, 69

Roberts, D. H., Lehar, J., & Dreher, J. W. 1987, *AJ*, 93, 968

Roche, P., Coe, M. J., Fabregat, J., et al. 1993, *A&A*, 270, 122

Roche, P., Larionov, V., Tarasov, A. E., et al. 1997, *A&A*, 322, 139

Rodriguez, J., Bodaghee, A., Kaaret, P., et al. 2006, *MNRAS*, 366, 274

- Rodriguez, J., Tomsick, J. A., & Bodaghee, A. 2010, *A&A*, 517, A14
- Rodriguez, J., Tomsick, J. A., Bodaghee, A., et al. 2009a, *A&A*, 508, 889
- Rodriguez, J., Tomsick, J. A., & Chaty, S. 2009b, *A&A*, 494, 417
- Rodriguez, J., Tuerler, M., Chaty, S., & Tomsick, J. A. 2009c, *The Astronomer's Telegram*, 1998, 1
- Romano, P., Sidoli, L., Cusumano, G., et al. 2009, *ApJ*, 696, 2068
- Romano, P., Sidoli, L., Mangano, V., & Mereghetti, S. 2007, *The Astronomer's Telegram*, 1287, 1
- Rosenberg, F. D., Eyles, C. J., Skinner, G. K., & Willmore, A. P. 1975, *Nat*, 256, 628
- Rutledge, R. E., Bildsten, L., Brown, E. F., et al. 2007, *ApJ*, 658, 514
- Safi-Harb, S., Ribó, M., Butt, Y., et al. 2007, *ApJ*, 659, 407
- Sakano, M., Koyama, K., Murakami, H., Maeda, Y., & Yamauchi, S. 2002, *ApJS*, 138, 19
- Sanduleak, N. 1978, *IAU Circ.*, 3170, 3
- Sarty, G. E., Kiss, L. L., Huziak, R., et al. 2009, *MNRAS*, 392, 1242
- Sarty, G. E., Pilecki, B., Reichart, D. E., et al. 2011, *Research in Astronomy and Astrophysics*, 11, 947
- Sato, N., Nagase, F., Kawai, N., et al. 1986, *ApJ*, 304, 241
- Sazonov, S., Krivonos, R., Revnivtsev, M., Churazov, E., & Sunyaev, R. 2008, *A&A*, 482, 517
- Scargle, J. D. 1982, *ApJ*, 263, 835
- Scargle, J. D. 1989, *ApJ*, 343, 874
- Schmidtke, P. C. & Cowley, A. P. 2005, *AJ*, 130, 2220
- Schreier, E., Levinson, R., Gursky, H., et al. 1972, *ApJ*, 172, L79
- Scott, D. M., Finger, M. H., Wilson, R. B., et al. 1997, *ApJ*, 488, 831

- Secchi, A. 1866, *Astronomische Nachrichten*, 68, 63
- Segreto, A., La Parola, V., Cusumano, G., et al. 2013, *A&A*, 558, A99
- Seifina, E. V. 2007, in *ESA Special Publication*, Vol. 622, *ESA Special Publication*, 499
- Semaan, T., Hubert, A. M., Zorec, J., et al. 2013, *A&A*, 551, A130
- Sguera, V., Bazzano, A., Bird, A. J., et al. 2006, *ApJ*, 646, 452
- Sguera, V., Drave, S., Goossens, M., et al. 2012, *The Astronomer's Telegram*, 4168, 1
- Sguera, V., Hill, A. B., Bird, A. J., et al. 2007, *A&A*, 467, 249
- Shakura, N. I. & Sunyaev, R. A. 1973, *A&A*, 24, 337
- Shapiro, S. L. & Teukolsky, S. A. 1983, *Black holes, white dwarfs, and neutron stars: The physics of compact objects*
- Shaw, S. E., Hill, A. B., Kuulkers, E., et al. 2009, *MNRAS*, 393, 419
- Sidoli, L., Drave, S. P., Fiacchi, M., et al. 2012a, *The Astronomer's Telegram*, 4136, 1
- Sidoli, L., Mereghetti, S., Sguera, V., & Pizzolato, F. 2012b, *MNRAS*, 420, 554
- Silaj, J., Jones, C. E., Tycner, C., Sigut, T. A. A., & Smith, A. D. 2010, *ApJS*, 187, 228
- Slettebak, A. 1982, *ApJS*, 50, 55
- Smith, D. A. & Takeshima, T. 1998, *The Astronomer's Telegram*, 36, 1
- Smith, M. A., Cohen, D. H., Gu, M. F., et al. 2004, *ApJ*, 600, 972
- Soffitta, P., Tomsick, J. A., Harmon, B. A., et al. 1998, *ApJ*, 494, L203
- Sootome, T., Mihara, T., Matsuoka, M., et al. 2011a, *The Astronomer's Telegram*, 3766, 1
- Sootome, T., Nakajima, M., Mihara, T., et al. 2011b, *The Astronomer's Telegram*, 3829, 1

Stairs, I. H., Manchester, R. N., Lyne, A. G., et al. 2001, MNRAS, 325, 979

Staubert, R., Pottschmidt, K., Doroshenko, V., et al. 2011, A&A, 527, A7

Steele, I. A., Negueruela, I., Coe, M. J., & Roche, P. 1998, MNRAS, 297, L5

Steiner, C., Eckert, D., Mowlavi, N., Decourchelle, A., & Vink, J. 2005, The Astronomer's Telegram, 672, 1

Steiner, J. E., Ferrara, A., Garcia, M., et al. 1984, ApJ, 280, 688

Stella, L. & White, N. E. 1983, IAU Circ., 3902, 1

Stella, L., White, N. E., Davelaar, J., et al. 1985, ApJ, 288, L45

Stevens, J. B., Reig, P., Coe, M. J., et al. 1997, MNRAS, 288, 988

Stollberg, M. T., Finger, M. H., Wilson, R. B., et al. 1993, IAU Circ., 5836, 1

Strohmayer, T., Rodriguez, J., Markwardt, C., et al. 2009, The Astronomer's Telegram, 2002, 1

Suchkov, A. A. & Hanisch, R. J. 2004, ApJ, 612, 437

Suchy, S., Pottschmidt, K., Rothschild, R. E., et al. 2011, ApJ, 733, 15

Sugizaki, M., Mitsuda, K., Kaneda, H., et al. 2001, ApJS, 134, 77

Sunyaev, R. 1990a, IAU Circ., 5123, 2

Sunyaev, R. 1990b, IAU Circ., 5122, 2

Suzuki, M., Mihara, T., Nakagawa, Y. E., et al. 2010, The Astronomer's Telegram, 2769, 1

Swank, J. 2005, The Astronomer's Telegram, 413, 1

Swank, J. & Morgan, E. 2000, IAU Circ., 7531, 4

Swank, J., Remillard, R., & Smith, E. 2004, The Astronomer's Telegram, 349, 1

Swank, J. H., Smith, D. M., & Markwardt, C. B. 2007, The Astronomer's Telegram, 999, 1

- Takagi, T., Mihara, T., Nakajima, M., et al. 2014, *The Astronomer's Telegram*, 5931, 1
- Takeshima, T., Corbet, R. H. D., Marshall, F. E., Swank, J., & Chakrabarty, D. 1998, *IAU Circ.*, 6826, 1
- Takeshima, T., Dotani, T., Mitsuda, K., & Nagase, F. 1994, *ApJ*, 436, 871
- Tam, P. H. T., Huang, R. H. H., Takata, J., et al. 2011, *ApJ*, 736, L10
- Tarana, A., Bazzano, A., Chenevez, J., et al. 2006, *The Astronomer's Telegram*, 962, 1
- Taylor, A. R. & Gregory, P. C. 1982, *ApJ*, 255, 210
- Telting, J. H., Heemskerk, M. H. M., Henrichs, H. F., & Savonije, G. J. 1994, *A&A*, 288, 558
- Telting, J. H., Waters, L. B. F. M., Roche, P., et al. 1998, *MNRAS*, 296, 785
- Terrell, J. & Priedhorsky, W. C. 1984, *ApJ*, 285, L15
- Terrell, J., Priedhorsky, W. C., Davelaar, J., et al. 1983, *IAU Circ.*, 3893, 1
- Thompson, R. J., Shelton, R. G., & Arning, C. A. 1998, *AJ*, 115, 2587
- Thompson, T. W. J., Tomsick, J. A., in 't Zand, J. J. M., Rothschild, R. E., & Walter, R. 2007, *ApJ*, 661, 447
- Tomsick, J. A., Chaty, S., Rodriguez, J., Walter, R., & Kaaret, P. 2006, *The Astronomer's Telegram*, 959, 1
- Tomsick, J. A., Chaty, S., Rodriguez, J., Walter, R., & Kaaret, P. 2007, *The Astronomer's Telegram*, 1231, 1
- Tomsick, J. A., Chaty, S., Rodriguez, J., Walter, R., & Kaaret, P. 2008, *ApJ*, 685, 1143
- Tomsick, J. A., Chaty, S., Rodriguez, J., Walter, R., & Kaaret, P. 2009, *ApJ*, 701, 811
- Tomsick, J. A., Heinke, C., Halpern, J., et al. 2011, *ApJ*, 728, 86
- Torii, K., Kinugasa, K., Katayama, K., et al. 1998, *ApJ*, 508, 854

- Torrejón, J. M., Negueruela, I., Smith, D. M., & Harrison, T. E. 2010, *A&A*, 510, A61
- Torrejón, J. M. & Orr, A. 2001, *A&A*, 377, 148
- Torrejón, J. M., Schulz, N. S., & Nowak, M. A. 2012, *ApJ*, 750, 75
- Tsygankov, S., Lutovinov, A., & Krivonos, R. 2011, *The Astronomer's Telegram*, 3137, 1
- Tsygankov, S. S., Krivonos, R. A., & Lutovinov, A. A. 2012, *MNRAS*, 421, 2407
- Tsygankov, S. S., Lutovinov, A. A., Churazov, E. M., & Sunyaev, R. A. 2006, *MNRAS*, 371, 19
- Tsygankov, S. S., Lutovinov, A. A., Churazov, E. M., & Sunyaev, R. A. 2007, *Astronomy Letters*, 33, 368
- Tueller, J., Barthelmy, S., Burrows, D., et al. 2005, *The Astronomer's Telegram*, 669, 1
- Tuohy, I. R., Buckley, D. A. H., Remillard, R. A., Bradt, H. V., & Schwartz, D. A. 1988, in *Physics of Neutron Stars and Black Holes*, ed. Y. Tanaka, 93–96
- Turler, M., Rodriguez, J., & Ferrigno, C. 2009, *The Astronomer's Telegram*, 1997, 1
- Ulmer, M. P., Baity, W. A., Wheaton, W. A., & Peterson, L. E. 1973, *ApJ*, 184, L117
- Unger, S. J., Norton, A. J., Coe, M. J., & Lehto, H. J. 1992, *MNRAS*, 256, 725
- Vakili, F., Mourard, D., Stee, P., et al. 1998, *A&A*, 335, 261
- van Bever, J. & Vanbeveren, D. 1997, *A&A*, 322, 116
- van den Bergh, S. 1972, *Nat*, 235, 273
- van den Heuvel, E. P. J. 2001, in *The Neutron Star - Black Hole Connection*, ed. C. Kouveliotou, J. Ventura, & E. van den Heuvel, 173
- Verrecchia, F., Israel, G. L., Negueruela, I., et al. 2002, *A&A*, 393, 983
- Villa, G., Page, C. G., Turner, M. J. L., et al. 1976, *MNRAS*, 176, 609

- Villada, M., Giovannelli, F., & Polcaro, V. F. 1992, *A&A*, 259, L1
- Villada, M., Rossi, C., Polcaro, V. F., & Giovannelli, F. 1999, *A&A*, 344, 277
- Voges, W., Aschenbach, B., Boller, T., et al. 1996, *IAU Circ.*, 6420, 1
- Wackerling, L. R. 1970, *Mem. R. Astron. Soc.*, 73, 153
- Walter, R., Zurita Heras, J., Bassani, L., et al. 2006, *A&A*, 453, 133
- Wang, N., Johnston, S., & Manchester, R. N. 2004, *MNRAS*, 351, 599
- Wang, W. 2010, *A&A*, 516, A15
- Warwick, R. S., Watson, M. G., & Sims, M. R. 1981, *SSRv*, 30, 461
- Waters, L. B. F. M. & van Kerkwijk, M. H. 1989, *A&A*, 223, 196
- Watson, M. G., Warwick, R. S., & Ricketts, M. J. 1981, *MNRAS*, 195, 197
- Wegner, W. 1994, *MNRAS*, 270, 229
- Wegner, W. 2006, *MNRAS*, 371, 185
- Wen, L., Remillard, R. A., & Bradt, H. V. 2000, *ApJ*, 532, 1119
- Wheaton, W. A., Doty, J. P., Primini, F. A., et al. 1979, *Nat*, 282, 240
- White, N. E. 2002, *High-mass X-ray binaries* (Kluwer Academic Publishers), 823
- White, N. E., Mason, K. O., Giommi, P., et al. 1987, *MNRAS*, 226, 645
- White, N. E., Mason, K. O., Sanford, P. W., & Murdin, P. 1976, *MNRAS*, 176, 201
- White, N. E., Parkes, G. E., Sanford, P. W., Mason, K. O., & Murdin, P. G. 1978, *Nat*, 274, 664
- White, N. E., Swank, J. H., & Holt, S. S. 1983, *ApJ*, 270, 711
- Whitlock, L. 1989, *ApJ*, 344, 371
- Whitlock, L., Roussel-Dupre, D., & Priedhorsky, W. 1989, *ApJ*, 338, 381
- Wilson, C. A. & Finger, M. H. 2006, *The Astronomer's Telegram*, 877, 1

- Wilson, C. A., Finger, M. H., Coe, M. J., Laycock, S., & Fabregat, J. 2002, *ApJ*, 570, 287
- Wilson, C. A., Finger, M. H., Coe, M. J., & Negueruela, I. 2003a, *ApJ*, 584, 996
- Wilson, C. A., Finger, M. H., Harmon, B. A., Chakrabarty, D., & Strohmayer, T. 1998a, *ApJ*, 499, 820
- Wilson, C. A., Finger, M. H., Harmon, B. A., et al. 1997, *ApJ*, 479, 388
- Wilson, C. A., Finger, M. H., Wilson, R. B., & Scott, D. M. 1998b, *IAU Circ.*, 7014, 2
- Wilson, C. A., Patel, S. K., Kouveliotou, C., et al. 2003b, *ApJ*, 596, 1220
- Wilson, C. A., Weisskopf, M. C., Finger, M. H., et al. 2005, *ApJ*, 622, 1024
- Wilson, C. A., Zhang, S. N., Finger, M. H., et al. 1995a, *IAU Circ.*, 6238, 1
- Wilson, R. B., Finger, M. H., Stollberg, M., et al. 1994a, *IAU Circ.*, 5955, 1
- Wilson, R. B., Harmon, B. A., Fishman, G. J., & Finger, M. H. 1994b, *IAU Circ.*, 5945, 2
- Wilson, R. B., Zhang, S. N., Scott, M., et al. 1995b, *IAU Circ.*, 6207, 3
- Wood, K. S., Meekins, J. F., Yentis, D. J., et al. 1984, *ApJS*, 56, 507
- Yamamoto, T., Mihara, T., Sugizaki, M., et al. 2014, *PASJ*
- Yamamoto, T., Mihara, T., Sugizaki, M., et al. 2011a, *The Astronomer's Telegram*, 3309, 1
- Yamamoto, T., Mihara, T., Sugizaki, M., et al. 2013, *The Astronomer's Telegram*, 4759, 1
- Yamamoto, T., Nakahira, S., Kawai, N., et al. 2009, *The Astronomer's Telegram*, 2297, 1
- Yamamoto, T., Sugizaki, M., Mihara, T., et al. 2011b, *PASJ*, 63, 751
- Yamamoto, T., Tomida, H., Mihara, T., et al. 2012, *The Astronomer's Telegram*, 3856, 1

- Yan, J., Zurita Heras, J. A., Chaty, S., Li, H., & Liu, Q. 2012, *ApJ*, 753, 73
- Zamanov, R. & Martí, J. 2000, *A&A*, 358, L55
- Zamanov, R., Martí, J., Stoyanov, K., Borissova, A., & Tomov, N. A. 2014, *A&A*, 561, L2
- Zamanov, R. K., Martí, J., Paredes, J. M., et al. 1999, *A&A*, 351, 543
- Zhang, S., Qu, J.-L., Song, L.-M., & Torres, D. F. 2005, *ApJ*, 630, L65
- Zhang, S. N., Harmon, B. A., Paciesas, W. S., et al. 1996, *A&AS*, 120, C227
- Ziolkowski, J. 2002, *Mem. Soc. Astron. Ital.*, 73, 1038
- Zurita Heras, J. A. & Chaty, S. 2008, *A&A*, 489, 657

CURRICULUM VITAE

PERSONAL INFORMATION

Surname, Name: Özbey Arabacı, Mehtap

Nationality: Turkish (TC)

Date and Place of Birth: 05.12.1981, İzmir

Marital Status: Married

Phone: 0 312 2107637/4307

Fax: 0 312 2105099

EDUCATION

2008–2014	Ph.D., Middle East Technical University (METU), The Graduate School of Natural and Applied Sciences, Physics Department, Ankara
2006–2008	M.S., Middle East Technical University (METU), The Graduate School of Natural and Applied Sciences, Physics Department, Ankara
2005–2006	Conditional Program, Middle East Technical University (METU), Physics Department, Ankara
1999–2004	B.S., Ankara University, Department of Astronomy and Space Sciences, Ankara
1995–1999	High School, Selma Yiğitalp Anatolian High School, İzmir

PROFESSIONAL EXPERIENCE

Mar 2013–Oct 2013	Project Assistant, Analysis and interpretation of optical/X-ray astrophysical data for a research project supported by TÜBİTAK (Timing properties galactic black hole transients as the compact jets turn-on; P.N. 111T222, Assoc. Prof. Emrah Kalemci), Sabancı University & Middle East Technical University
2009–2013	Analysis and interpretation of optical/X-ray astrophysical data for a research project supported by TÜBİTAK (Investigating the distribution of pulsars and star forming regions (SFR) in the galaxy; P.N. 109T736, P.I Assoc. Prof. Dr. S. Kaan Yerli), Middle East Technical University
Jun 2010–Aug 2010	Visiting Researcher (Marie Curie Host Fellowship), Investigating the IR properties of the milli-second pulsar SAX J1808.4–3658 in VLT/X-Shooter data (P.I. Prof. Dr. Lex Kaper), University of Amsterdam, Astronomical Institute of Anton Pannekoek
2006–2009	Project Assistant, Analysis and interpretation of optical/X-ray astrophysical data for a research project supported by TÜBİTAK (Studying accretion disks in compact X-ray binaries; P.N. 106T040, P.I Prof. Dr. Ümit Kızılođlu), Middle East Technical University

PUBLICATIONS

1. E. Kalemci, M. Özbey Arabacı, T. Güver, , D. M. Russell, J. A. Tomsick, J. Wilms, G. Weidenspointner, E. Kuulkers, M. Falanga, T. Dinçer, S. Drave, T. Belloni, M. Coriat, M. Lewis, T. Muños Darias, "Multiwavelength Observations of the Black Hole Transient Swift J1745–26 During the Outburst Decay", MNRAS, Accepted for publication, 2014, 2014arXiv1409.1932K.
2. M. Özbey Arabacı, A. Camero-Arranz, J. Fabregat, H. Bilal Ozcan, V. Peris, Evidence of the Presence of a Be Circumstellar Disk in the Be/X-ray Binaries

KS 1947+ 300 and Cep X-4", ATel, 6265, 2014.

3. A. Camero, C. Zurita, J. Gutierrez Soto, M. Özbey Arabacı, E. Nespoli, F. Kjaerød, E. Bekken, J. Garcia-Rojas, M. Caballero-Garcia, "Recent Activity of the Be/X-ray Binary System SAX J2103.5+4545", A&A, Accepted for publication, 2014, 2014arXiv1405.4216C.
4. A. Camero-Arranz, M. Özbey Arabacı, J. Fabregat, J. Gutierrez-Soto, Mark H. Finger, V. Peris, O. Brevia, "Detection of a Large Increase of the Size of the Be Disk From the X-ray Binary A 0535+262", ATel, 6043, 2014.
5. M. Özbey Arabacı, E. Kalemci, J. A. Tomsick, J. Halpern, A. Bodaghee, S. Chaty, J. Rodriguez, F. Rahoui, " Investigating the Optical Counterpart Candidates of Four INTEGRAL Sources Localized with Chandra", ApJ, 761, 4, 2012.
6. J. A. Tomsick, A. Bodaghee, S. Chaty, J. Rodriguez, F. Rahoui, J. Halpern, E. Kalemci, M. Özbey Arabacı, "Localizing INTEGRAL Sources with Chandra: X-Ray and Multi-wavelength Identifications and Energy Spectra", ApJ, 754, 145, 2012.
7. S. C. Butler, J. A. Tomsick, S. Chaty, J. A. Z. Heras, J. Rodriguez, R. Walter, P. Kaaret, E. Kalemci, M. Özbey Arabacı, "Identifications of Five INTEGRAL Sources via Optical Spectroscopy", ApJ, 698, 502, 2009.
8. Ü. Kızıloğlu, N. Kızıloğlu, A. Baykal, S. K. Yerli, M. Özbey, "Long-term optical observations of the Be/X-Ray binary system V0332+53", IBVS, 5865, 2008.
9. Ü. Kızıloğlu, N. Kızıloğlu, A. Baykal, S. K. Yerli, M. Özbey, "On the Optical Activity of GRO J2058+42 (CXOU J205847.5+414637) Prior X-ray to outburst", ATel, 1517, 2008.
10. Ü. Kızıloğlu, N. Kızıloğlu, A. Baykal, S. K. Yerli, M. Özbey, "Detection of Increase in the Optical Light of Be/X-Ray Binary System GRO J2058+42", IBVS, 5821, 2008.

11. A. Baykal, Ü. Kızılođlu, N. Kızılođlu, E. Beklen, M. Özbey, "Recent RX-TE/ASM and ROTSEIII observations of EXO 2030+375 (V2246 Cygni)", *A&A*, 479, 301, 2008.
12. Ü. Kızılođlu, N. Kızılođlu, A. Baykal, S. K. Yerli, M. Özbey, "Optical variabilities in the Be/X-ray binary system. GRO J2058+42 (CXOU J205847.5+414637)", *A&A*, 470, 1023, 2008.